2017

Characterization of the In Vivo Consequences of Salicylate Co-Administration on the Efficacy of Topoisomerase II Poison-Based Chemotherapy in a Model of Human Breast Cancer

Crovetto, Gina Marie Alexandra

UNIVERSITY OF CALGARY

Characterization of the *In Vivo* Consequences of Salicylate Co-Administration on the Efficacy of Topoisomerase II Poison-Based Chemotherapy in a Model of Human Breast Cancer

by

Gina Marie Alexandra Crovetto

A THESIS

SUBMITTED TO THE FACULTY OF GRADUATE STUDIES

IN PARTIAL FULFILMENT OF THE REQUIREMENTS FOR THE

DEGREE OF MASTER OF SCIENCE

GRADUATE PROGRAM IN MEDICAL SCIENCE

CALGARY, ALBERTA

JANUARY, 2017

Abstract

Human DNA topoisomerase IIα (TOP2A) is an essential enzyme that resolves the topological complexities of DNA, via transient DNA double-strand breaks (DSBs), during replication, transcription, and mitosis. Several gold-standard chemotherapeutics used for treating breast cancer are TOP2 poisons, which act by covalently trapping TOP2-DNA complexes leading to an accumulation of cytotoxic DNA DSBs. Salicylate, the primary metabolite of aspirin, catalytically inhibits DNA cleavage by TOP2A and is known to attenuate TOP2 poison cytotoxicity in MCF-7 breast cancer cells. Given, the widespread use of aspirin and other salicylate derivatives, determining their effects on chemotherapeutic efficacy could have far-reaching implications. To address this, a panel breast cancer cell lines was compiled to further characterize the effect of salicylate on TOP2 poison cytotoxicity. Following the *in cyto* work, a murine xenograft model of human breast cancer was used to evaluate the *in vivo* consequences of salicylate co-administration on TOP2 poison-based chemotherapy.

Acknowledgements

First and foremost, I would like to thank my supervisor, Dr. Ebba Kurz, for her insight, wisdom and constant support. Ebba's enthusiasm for research, belief in a solution and unwavering encouragement was essential for getting me through the more challenging moments of my research. I am truly grateful for her guidance and thankful for the excellent example she has provided as a successful researcher, professor, and mentor.

I would also like to thank the past and present members of the Kurz Lab whose friendship, good advice and collaboration contributed immensely to my research experience. I am especially indebted to Jason Bau, whose research laid the foundation upon which mine was built, and Zhili Kang, whose technical prowess and patience proved invaluable. For the animal work in this thesis, I would like to thank the Morris Lab for their collaboration. I am particularly grateful to Qiao Shi for her assistance and for imparting her knowledge and technical skill.

Furthermore, I would like to thank my committee members, Dr. Don Morris and Dr. Susan Lees-Miller, for their contribution of time and scientific expertise to my graduate studies.

I gratefully acknowledge the funding source that made my M.Sc. possible. My work was supported by an operating grant from the Canadian Breast Cancer Foundation (Prairies/NWT) held by Dr. Ebba Kurz.

Lastly, I would like to thank my family and friends for all their love and support throughout this journey.

Dedication

To my parents, Phoebe and Preben,

for nurturing my curiosity and encouraging my love of science.

Table of Contents

List of Tables

List of Figures

List of Symbols, Abbreviations and Nomenclature

Symbol	Definition
Units of Measurement	
µg	microgram
mg	milligram
g	gram
kg	kilogram
µL	microliter
mL	milliliter
mm^2	square millimeter
cm^2	square centimeter
m^2	square meter
nm	nanometer
mm	millimeter
m	meter
µM	micromolar
mM	millimolar
M	molar
sec	second
min	minute
h	hour
°C	degrees Celsius
%	percent
FU	fluorescence units
x g	gravitational acceleration
kDa	kilo Dalton
V	volt
v/v	mL solute per 100 mL solution
w/v	g solute per 100 mL solution
General	
5-IDNR	5-iminodaunorubicin
ADP	adenosine diphosphate
AKT	protein kinase B
AMPK	5' adenosine monophosphate-activated protein kinase
APS	ammonium persulfate

ASA	acetylsalicylic acid
ATM	ataxia telangiectasia mutated
ATM pS1981	ataxia telangiectasia mutated phospho-serine 1981
ATP	adenosine triphosphate
ATPase	adenosine triphosphatase
BCE	before common era
BChE	butyrylcholinesterase
BSA	bovine serum albumin
C-terminal	carboxy-terminal
Ca^{2+}	calcium
CCL2	chemokine (C-C motif) ligand 2
CES-1	carboxylesterase 1
CES-2	carboxylesterase 2
Chk2	checkpoint kinase 2
Chk2 pT68	checkpoint kinase 2 phospho-tyrosine 68
cIAPs	cellular inhibitor of apoptosis proteins
CO_2	carbon dioxide
COX	cyclooxygenase
COX-1	cyclooxygenase-1
COX-2	cyclooxygenase-2
CT	chemotherapy
DMEM	Dulbecco's modified Eagle's media
DMSO	dimethyl sulfoxide
DNA	deoxyribonucleic acid
DNA-PK	DNA-dependent protein kinase
DNA-PKcs	DNA-PK catalytic subunit
Dox	doxorubicin
DSB	double-strand break
ECL	enhanced chemiluminescence reagent; 0.1 M Tris-HCL pH 8.5, 12.5 mM luminol, 0.2 mM coumaric acid, 10% [v/v] H_2O_2
EDTA	ethylenediaminetetraacetic acid
EMT-6	murine EMT-6 breast cancer cells
ER	estrogen receptor
ERK	extracellular signal–regulated kinase
Etop	etoposide
FBS	fetal bovine serum
G-segment	gate-segment
H_2O	water
H_2O_2	hydrogen peroxide
HCL	hydrogen chloride

HER2	human epidermal growth factor receptor 2
HER2+	HER2-positive breast cancer subtype
HT	hormone therapy
$IC50_{Dox}$	IC_{50} of doxorubicin
$IC50_{Dox+Sal}$	IC_{50} of doxorubicin + salicylate
$IC50_{Etop}$	IC_{50} of etoposide
$IC50_{Etop+Sal}$	IC_{50} of etoposide + salicylate
ICAM-1	intercellular cell adhesion molecule-1
ICRF-187	dexrazoxane
ICRF-193	4-[2-(3,5-dioxo-1-piperazinyl)-1-methylpropyl]piperazine- 2,6-dione
IgG	immunoglobulin G
IKK	IκB kinase complex
IKKα	IκB kinase α
IKKβ	IκB kinase β
IKKγ	IκB kinase γ
IL	interleukin
IL-1	interleukin-1
IL-6	interleukin-6
IL-8	interleukin-8
IP	intraperitoneal injection
IκB	inhibitor of NFκB
KCl	potassium chloride
KH_2PO_4	monopotassium phosphate
Ki67	Ki67 marker of proliferation
LPS	lipopolysaccharide
M	mutant protein
MAPK	mitogen-activated protein kinase
MCF-7	human MCF-7 breast cancer cells
MDA-MB-231	human MDA-MB-231 breast cancer cells
MDA-MB-231-LUC	luciferase expressing MDA-MB-231 human breast cancer cells
MDA-MB-468	human MDA-MB-468 breast cancer cells
Mg^{2+}	magnesium
mTOR	mechanistic target of rapamycin
MTX	mitoxantrone
N-terminal	amino-terminal
Na_2HPO_4	disodium phosphate
NaCl	sodium chloride
NaN_3	sodium azide
Nbs1	Nijmegen breakage syndrome protein 1

NET-N	150 mM NaCl, 1 mM EDTA, 20 mM Tris, 1% [v/v] Nonidet-P40 lysis buffer
NFκB	nuclear factor κB
P	phosphate
P-Y	phosphotyrosyl linkage
p38 MAPK	p38 mitogen-activated protein kinase
p53	p53 tumor suppressor
p53 pS15	p53 phospho-serine 15
PBS	phosphate-buffered saline; 137 mM NaCl, 2.7 mM KCl, 10 mM Na_2HPO_4, 1.8 mM KH_2PO_4, pH 7.4
PDT	population doubling time
PG	prostaglandin
PGE_2	prostaglandin E2
PGI_2	prostacyclin
P_i	inorganic phosphate
PI3K	phosphatidylinositol-3 kinase
PMSF	phenylmethylsulfonyl fluoride
PON	paraoxonase
PP2A	protein phosphatase 2A
PR	progesterone receptor
$Prkdc^{scid}$	loss-of-function mutation in the mouse homologue of the human PRKDC gene
RNA	ribonucleic acid
Sal	salicylate
SCID	severe combined immunodeficient
SCID C.B.-17	Fox Chase SCID C.B-17 mice
SDS	sodium dodecyl sulfate
SDS-PAGE	sodium dodecyl sulfate-polyacrylamide gel electrophoresis
SK-BR-3	human SK-BR-3 breast cancer cells
SMC1	structural maintenance of chromosomes protein 1
SMC1 pS957	SMC1 phospho-serine 957
SRC tyrosine kinase	proto-oncogene tyrosine-protein kinase
SS	sodium salicylate
SSB	single-strand break
STAT	signal transducer and activator of transcription
T-segment	transfer-segment
TBS	Tris-buffered saline
TBS-T	Tris-buffered saline with Tween-20
TEMED	tetramethylethylenediamine
TLRs	toll-like receptors
TNF	tumour necrosis factor

TNFR	TNF receptor
TOP	DNA topoisomerase
TOP1	topoisomerase I
TOP1mt	mitochondrial topoisomerase I
Top2	murine topoisomerase II
TOP2	topoisomerase II
TOP2-DNAcc	topoisomerase II-DNA covalent complex
TOP2A	topoisomerase IIα
Top2a	murine topoisomerase IIα
TOP2B	topoisomerase IIβ
TOP3A	topoisomerase (DNA) IIIα
TOP3B	topoisomerase (DNA) IIIβ
TP53	gene encoding tumour suppressor protein p53
TPD2	tyrosyl-DNA-phosphodiesterase 2
TRAFs	tumor necrosis factor receptor-associated factors
Tris	tris(hydroxymethyl)aminomethane
TXA2	thromboxane A5
Tyr805	human topoisomerase IIα tyrosine active site residue 805
WT	wild-type protein
ZR-75-30	human ZR-75-30 breast cancer cells
λ	wavelength
(-)	negative
(+)	positive

Chapter One: Introduction

1.1 Breast Cancer

Globally, breast cancer is the most common cancer in women, accounting for 25.2% of all new cancer diagnoses (Ferlay *et al.*, 2015). In 2012, breast cancer was responsible for 14.7% of the more than 3.5 million cancer-related deaths in women worldwide. In Canada, breast cancer is the second most common cause of cancer-related death in women (Canadian Cancer Society's Advisory Committee on Cancer Statistics, 2015). Furthermore, it is estimated that 1 in 9 Canadian women will develop breast cancer at some point in her lifetime.

A combination of clinical examinations and imaging, supplemented by pathological assessments, are used to diagnose primary breast cancer (Senkus *et al.*, 2015). Treatment strategy is based on multiple factors, including the location, molecular profile and size of the primary tumour, the number and extent of lymph nodes involved, and the age, health and menopausal status of the patient. Standard treatment for breast cancer most often involves local surgery and radiation therapy followed by adjuvant chemotherapy to reduce the risk of recurrence (Gandhi *et al.*, 2014; Coates *et al.*, 2015; Senkus *et al.*, 2015).

1.1.1 Intrinsic Molecular Subtypes of Breast Cancer

Disease heterogeneity, due to complex genotypic and phenotypic variation, has long been recognized in breast cancer. Variation in the expression of growth factor and hormone receptors, proto-oncogenes, and mutations in tumour suppressor genes can have

significant consequences on treatment response and patient outcome (Vollenweider-Zerargui *et al.*, 1986; Slamon *et al.*, 1989; Elston & Ellis, 1991; Fisher *et al.*, 1993; Børresen *et al.*, 1995; Torregrosa *et al.*, 1997; Bergh *et al.*, 1995; Coates *et al.*, 2015). Recent advancements in molecular profiling have made it possible to define breast cancer subtypes at the molecular level and enable a more refined approach for selecting the appropriate treatment strategy.

Clinically, breast cancers are classified into four intrinsic subtypes. These molecular subtypes are luminal A, luminal B, human epidermal receptor 2-positive (HER2+), and basal-like breast cancers (Table 1.1) (Perou *et al.*, 2000; Sørlie *et al.*, 2001). Tumours are classified based on the expression of estrogen receptor (ER) and progesterone receptor (PR), human epidermal receptor 2 (HER2) overexpression, and, more recently, the expression of the proliferation marker Ki67 (Cheang *et al.*, 2009). Luminal A tumours are ER(+) and/or PR(+), and HER2(-). With the best prognosis of all the subtypes, approximately 73% of invasive breast cancer cases are identified as luminal A (Howlader *et al.*, 2014; Kohler *et al.*, 2015). Luminal B tumours are ER(+) and/or PR(+), and HER2(+) with high Ki67. Prognosis is good but not as good as luminal A; only 10% of invasive breast cancer cases are of the luminal B subtype (Howlader *et al.*, 2014; Kohler *et al.*, 2015). HER2+ tumours are ER(-) and PR(-), and HER2(+) (typically due to gene amplification) with high Ki67. The prognosis is worse than the luminal subtypes but better than basal-like cancer (Kohler *et al.*, 2015). HER2+ is the least common subtype making up only 5% of all invasive breast cancer cases (Howlader *et al.*, 2014). Basal-like tumours, also called triple-negative tumours, do not express ER, PR, or

Table 1.1 Molecular subtypes of human breast cancer and treatment recommendations

Subtype	ER	PR	HER2	Ki67	Prognosis	Recommended therapy
Luminal A	+	+/-	-	Low	Good	HT alone*
Luminal B	+	+/-	+	High	Intermediate	CT + anti-HER2 + HT
HER2+	-	-	+	High	Poor	CT + anti-HER2
Basal-like	-	-	-	High	Very Poor	CT
Claudin-low	-	-	-	Low	Very poor	CT

*Consider CT if: high tumour burden (positive lymph nodes ≥ 4 or tumour size ≥ 50 mm), grade 3

Chemotherapy (CT); estrogen receptor (ER); hormone therapy (HT); human epidermal growth factor receptor 2 (HER2); progesterone receptor (PR).

HER2 gene products. Triple-negative cancer is identified in 12% of invasive breast cancer cases and carries the worst prognosis of all the subtypes (Howlader *et al.*, 2014; Kohler *et al.*, 2015). Other molecular subtypes continue to be described, for example claudin-low was recently identified as a distinct subset of triple-negative breast cancer (Herschkowitz *et al.*, 2007). This type of tumour is ER(-), PR(-), and HER2(-), with low Ki67, and low expression of the tight junction proteins claudin-3, claudin-4 and claudin-7 (Herschkowitz *et al.*, 2007; Prat *et al.*, 2010).

Several studies have demonstrated a correlation between tumour subtype and chemotherapy response, disease relapse, site of metastasis and survival (Perou *et al.*, 2000; Sørlie *et al.*, 2001; Hugh *et al.*, 2009; Kennecke *et al.*, 2010; Cheang *et al.*, 2012; Drukker *et al.*, 2013). Because ER is a therapeutic target, breast cancer subtypes expressing ER (*i.e.* luminal A and luminal B) are responsive to hormone therapy (*e.g.* tamoxifen). Similarly, HER2 is a therapeutic target and subtypes expressing HER2 (*i.e.* HER2+ and luminal B) are responsive to anti-HER2 therapy (*e.g.* trastuzumab). However, ER and HER2 are absent in triple negative subtypes (*i.e.* basal-like and claudin-low), making these tumours considerably more challenging to treat. International guidelines, specifically those recommended by the 2015 St Gallen Consensus Conference and the European Society for Medical Oncology, agree that molecular subtype should define the choice of systemic adjuvant therapies (Table 1.1) (Coates *et al.*, 2015; Senkus *et al.*, 2015). Their strategic treatment recommendations follow as such: hormone therapy alone for luminal A tumours (except for high-risk cases, such as heavy tumour burden, where the addition of cytotoxic chemotherapy is recommended); a combination of cytotoxic chemotherapy, anti-HER2 therapy, and endocrine therapy for luminal B

tumours; a combination of cytotoxic chemotherapy, and anti-HER2 therapy for HER2+ tumours; and cytotoxic chemotherapy alone for triple negative cases. Canadian treatment guidelines use ER, PR, and HER2 status for clinical decision making; however, the use of intrinsic subtypes (beyond the capacity ER, PR, and HER2 status) is not recommended outside of clinical trials (Eisen *et al.*, 2015).

1.1.2 Chemotherapy in the Treatment of Breast Cancer

The standard treatment for breast cancer involves one or more of surgery, radiation therapy, and systemic therapy (*i.e.* chemotherapy, hormone therapy, and/or targeted therapy) (Senkus *et al.*, 2015). Surgery, the most common treatment for breast cancer, involves removing the tumour and surrounding affected tissue. In some cases of low-risk early-stage breast cancer, surgery alone can be sufficient to clear the disease (Eisen *et al.*, 2015). However, it is more common for surgical management to be followed by adjuvant radiation therapy to ensure any residual cancer cells are eradicated, thus reducing the risk of local recurrence (Eisen *et al.*, 2015; Coates *et al.*, 2015; Senkus *et al.*, 2015). Systemic therapy involves the delivery of anti-cancer agents to disseminated cancer cells throughout the body. In high-risk breast cancer (*i.e.* ER(+), ER(-) tumours greater than 5 mm in size, HER2+, triple-negative, or lymph node–positive disease) and metastatic disease, systemic therapy is administered either before surgery, to shrink tumour size, or after surgery to reduce the risk of metastases and minimize the risk of recurrence. Of these systemic approaches, adjuvant chemotherapy has proven to be beneficial in reducing the risk of metastatic recurrence and increasing overall survival in

essentially all types and stages of breast cancer (Eisen *et al.*, 2015; Coates *et al.*, 2015; Senkus *et al.*, 2015).

Chemotherapeutic compounds are diverse in structure and anticancer mechanism of action; these include alkylating agents, antimetabolites, anti-tumour antibiotics, topoisomerase poisons, and tubulin-binding drugs. These cytotoxic agents kill cancer cells by interfering with the process of cell division through various mechanisms including, but not limited to, impeding DNA synthesis, inducing DNA damage, preventing microtubule formation or dissolution, and producing reactive oxygen species (Lind, 2008). The therapeutic effectiveness of cytotoxic agents arises from the ability to generate a greater cytotoxic effect in cancer cells than healthy cells. This sensitivity differential, between malignant and healthy cells, is a consequence of the chronic uncontrolled proliferation of cancer cells, a fundamental characteristic of malignant disease (Hanahan & Weinberg, 2000). However, cytotoxic chemotherapeutics cannot differentiate cancer cells from rapidly dividing healthy cells (*e.g.* hair follicles, intestinal mucosa, and bone marrow). As such, common side-effects of chemotherapy include hair loss, inflammation of the intestinal lining, and bone marrow suppression.

Combination therapy, where treatment regimens consist of a combination of cytotoxic agents, hormone therapy, and/or targeted therapy, is considered superior to single agent regimens (Coates *et al.*, 2015). Of these, anthracycline-based regimens are superior to non-anthracycline-based regimens in the treatment of breast cancer, and anthracycline-taxane-based combination therapy confers the greatest therapeutic effect on patient outcome (Early Breast Cancer Trialists' Collaborative Group, 2005; Gandhi *et al.*,

2014). Hormonal and targeted therapies (*e.g.* anti-ER and anti-HER2) can further increase therapeutic efficacy if targets are present in tumour cells.

1.2 DNA Topoisomerases – Molecular Scissors

All cells require the ability to replicate their genetic material accurately and efficiently to pass the genetic information from generation to generation. This information is stored as DNA, which must be meticulously organized through an array of processes orchestrated by specialized enzymes, each of which has a specific role. The length and double helical structure of DNA pose a unique challenge for living cells. The haploid human genome contains approximately 3.2×10^9 base pairs of DNA. However, with the exception of the germline, most cells in the human body are diploid. This means that 6.4×10^9 base pairs of DNA are packaged into each cell. Given that each base pair is approximately 0.34 nm long, each diploid cell contains roughly 2 m of DNA. The challenge for living cells is that genetic material not only needs to be packaged efficiently, but also needs to be readily accessible for DNA damage repair, replication, and transcription. These essential processes require access to the information encoded by the nucleotide sequence, necessitating strand separation, which creates flanking supercoiled DNA segments. If left unresolved, supercoiled DNA can interfere with gene expression during transcription and generate chromosomal entanglements during DNA repair and replication, which could potentially result in mutagenic or cytotoxic DNA strand breaks. Thus, chromosomal topology must maintain a controlled yet highly dynamic balance between the accessing and the packaging of genetic materials.

Topoisomerases are a unique family of enzymes that resolve topological challenges through coordinated regulation of DNA topology. Highly conserved, DNA topoisomerases are ubiquitous and essential for the survival of all living organisms. Through an elegant mechanism involving the controlled cleavage and religation of DNA, these enzymes can untangle seemingly complex aberrations of DNA topology (Wang, 2002). Through a nucleophilic attack utilizing a conserved tyrosine residue, these molecular scissors form a covalent phosphotyrosyl bond with the phosphodiester backbone in DNA, consequently generating a transient DNA strand break through which topological manipulation can be accomplished (Deweese & Osheroff, 2009; Ashour *et al.*, 2015).

The topoisomerases are divided into two core classifications: type I and type II (Forterre & Gadelle, 2009). Type I enzymes introduce transient single-strand DNA breaks (SSBs) (Depew *et al.*, 1978; Liu & Wang, 1979; Tse *et al.*, 1980; Champoux, 1981), while type II introduce double-strand DNA breaks (DSBs) (Brown *et al.*, 1979; Liu & Wang, 1979; Morrison & Cozzarelli, 1979; Sander & Hsieh, 1983). Each class can be further divided into subclasses based on the ability to allow secondary strand passage and the mechanism by which strand passage occurs.

Type I topoisomerases expressed in humans are subdivided into Type IA and Type IB (Table 1.2). The type IA topoisomerases, TOP3A and TOP3B, catalyze strand passage whereby a single DNA strand is transiently cleaved and a 5′-phosphotyrosine TOP3-DNA covalent cleavage-complex intermediate is formed (Tse *et al.*, 1980; Hanai *et al.*, 1996; Perry & Mondragón, 2003). A second single DNA strand can then pass through the stabilized opening after which the cleaved strand is religated and released

Table 1.2 Classification of human topoisomerase enzymes

Class	Enzyme	P-Y	kDa	Composition	DNA Break	Supercoil Affinity	Clinical Target
IA	TOP3A	5′	113	Monomer	SSB	-	No
	TOP3B	5′	97	Monomer	SSB	-	No
IB	TOP1	3′	100	Monomer	SSB	+/-	Yes
	TOP1mt	3′	70	Monomer	SSB	+/-	No
IIA	TOP2A	5′	170	Homodimer	DSB	+/-	Yes
	TOP2B	5′	180	Homodimer	DSB	+/-	Yes

Double-strand break (DSB); Orientation of TOP-phosphotyrosyl linkage (P-Y); Single-strand break (SSB).

(Feinberg *et al.*, 1999). This controlled strand passage allows type IA enzymes to relieve torsional stress due to DNA supercoiling, and catalyze DNA untangling and decatenation. In contrast, the type IB topoisomerases, TOP1 and mitochondrial TOP1mt, catalyze DNA relaxation by cleaving one DNA strand, forming a 3′-phosphotyrosine-linked TOP1-DNA covalent cleavage-complex intermediate, and allowing the rotation of the complementary DNA strand to relieve torsional stress resulting from DNA supercoiling (Redinbo *et al.*, 1999; Forterre & Gadelle, 2009). TOP1 is essential for cell growth and division in vertebrates; mouse embryos lacking TOP1 fail between the 4- and 16-cell stage (Morham *et al.*, 1996). Compounds that interfere with TOP1 activity, such as camptothecin, are effective anticancer agents. Topoetecan, a water soluble derivative of camptothecin and commonly used anti-cancer chemotherapeutic, intercalates between the base pairs at the DNA cleavage site, stabilizing the TOP1-DNA covalent cleavage-complex and preventing religation (Pommier, 2006). This interference leads to the accumulation of DNA SSBs, which, following replication, are converted into one-ended DSBs (Saleh-Gohari *et al.*, 2005). If left unresolved, further disruptions to DNA replication and transcription occur, ultimately resulting in cell death.

Type II topoisomerases are divided into IIA or IIB subclasses based on amino acid sequence and protein structure. Regardless of subclass, all type II topoisomerases manage DNA topology by inducing a transient enzyme-bridged DSB through which a second DNA duplex passes. The C-terminal and N-terminal domains serve as a two-gate mechanism containing the T (transfer)-segment DNA before, during, and after its transit through the G (gate)-segment break point. This DNA cleavage mechanism enables the

efficient resolution of DNA tangles and catenanes essential for successful replication, transcription, and chromosome segregation.

Humans express two genetically and biochemically distinct type IIA topoisomerases: topoisomerase IIα (TOP2A) and topoisomerase IIβ (TOP2B) (Gadelle *et al.*, 2003). The protein sequences of the two isoforms share 68% identity and 77% homology overall; however, these similarities increase to 78% identity and 86% homology in the catalytic portions of the enzymes (Austin *et al.*, 1993). Both isoforms require Mg^{2+} and the energy cofactor ATP. Two separate genes encode the isoforms, yet the enzymes share nearly identical catalytic mechanisms. Although the ATPase and catalytic core domains are highly conserved, the C-termini of the isozymes diverge. Furthermore, regulation of TOP2A and TOPB differs considerably during cell growth and differentiation (Capranico *et al.*, 1992; Tsutsui *et al.*, 1993; Turley *et al.*, 1997). TOP2A is expressed exclusively in proliferating cells, where it manages DNA tangles and supercoiling and is essential for DNA replication and chromosome segregation at mitosis. (Goto & Wang, 1982; Heck *et al.*, 1988; Downes *et al.*, 1991; Akimitsu *et al.*, 2003). Conversely, TOP2B, expressed in all cell types, is involved in the expression of developmentally- and hormonally-regulated genes and neuronal differentiation (Yang *et al.*, 2000; Ju *et al.*, 2006; Tiwari *et al.*, 2012). Together, these two isoforms, with distinct roles in genome topology maintenance, are necessary for correct cellular function.

1.2.1 TOP2A – Essential Nuclear Enzyme

TOP2A is an essential nuclear enzyme that manages and untangles DNA topology during DNA replication, transcription, and sister chromatid separation (Figure 1.1).

A)

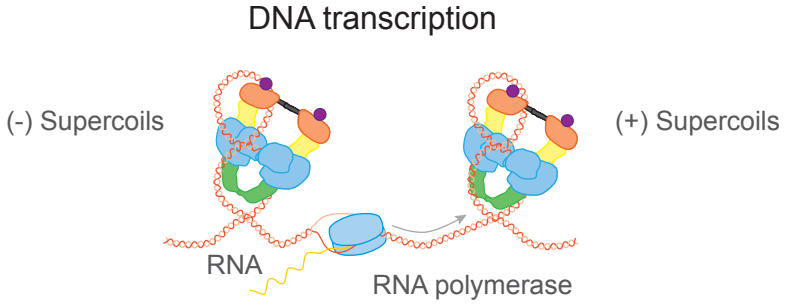
DNA transcription
(-) Supercoils
(+) Supercoils
RNA
RNA polymerase

B)

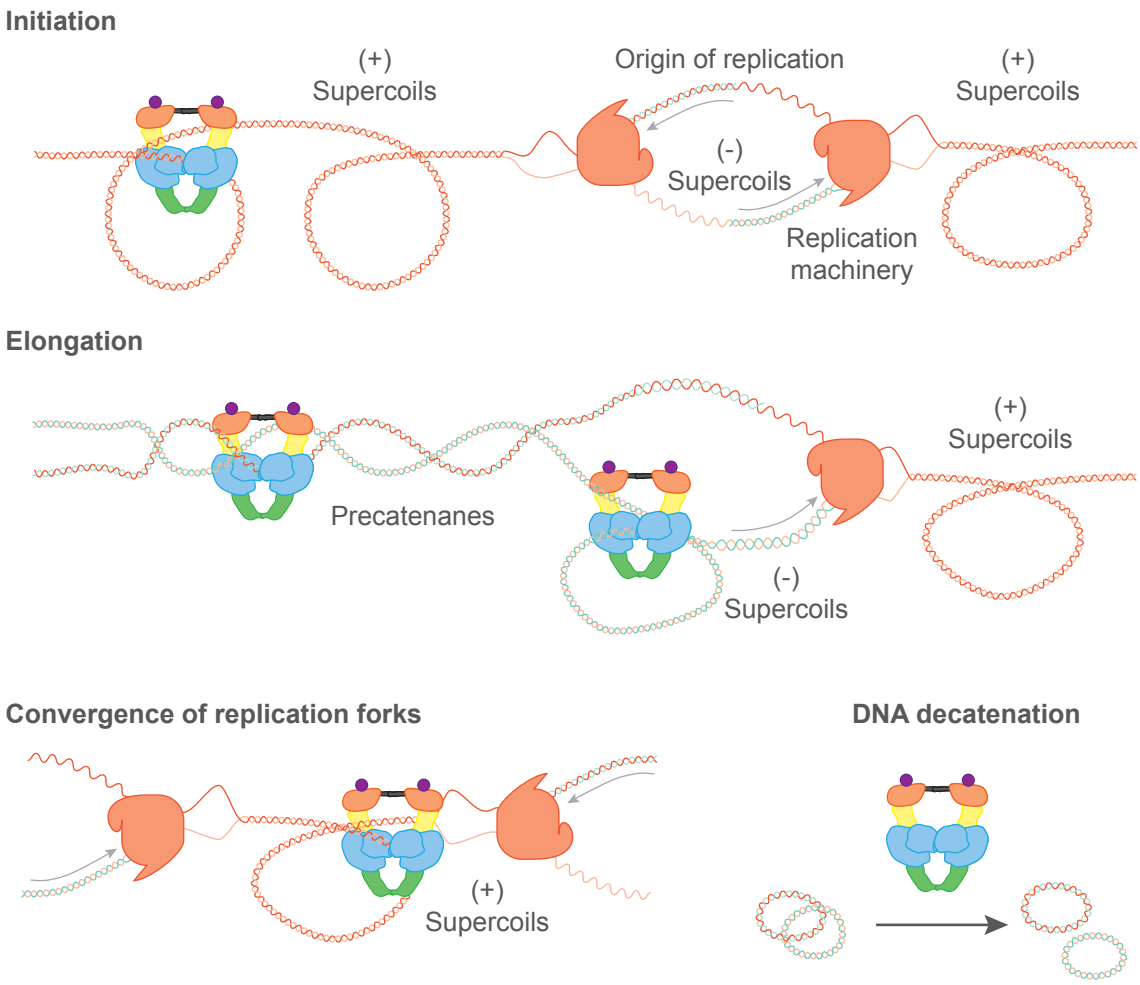
DNA replication
Initiation
(+)
Supercoils
Origin of replication
(+)
Supercoils
(-)
Supercoils
Replication
machinery
Elongation
Precatenanes
(+)
Supercoils
(-)
Supercoils
Convergence of replication forks
(+)
Supercoils
DNA decatenation

C)

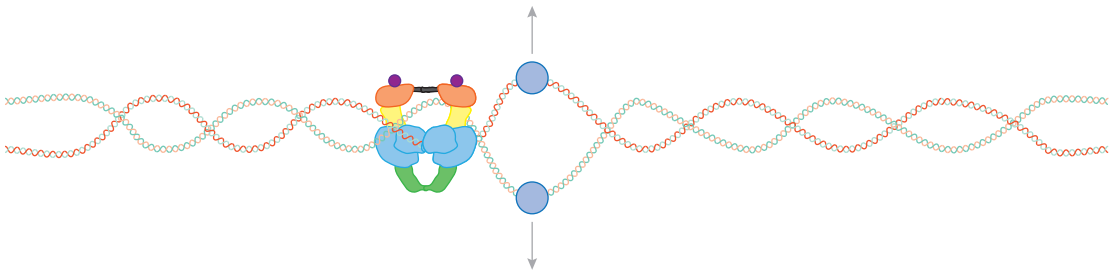
Sister chromatid separation

Figure 1.1 Biological functions of TOP2A.

TOP2A is involved in the management of DNA catenanes, tangles, and supercoiling associated with transcription, replication, and sister chromatid separation. A) During transcription, DNA in front of the advancing transcription bubble becomes overwound generating positive supercoils and DNA trailing behind the transcription machinery becomes underwound generating negative supercoils. B) During replication, the separation of parental DNA strands generates negative supercoils at the origin of replication and positive supercoils ahead of the replication machinery due to topological barriers that prevent compensatory rotation of the replication fork. As replication proceeds, positive supercoils accumulate ahead of the fork and negative supercoils accumulate behind it. Rotation of the replication fork during elongation can intertwine nascent daughter DNA strands forming precatenanes. High degrees of topological and torsional stress during replication can result in the generation of catenated DNA. C) If these topological issues go unresolved, tangled sister chromatids cannot accurately segregate during mitosis leading to chromosome shattering and cell death.

During transcription, TOP2A manages DNA supercoiling that results from the progression of the transcription bubble. During replication, TOP2A regulates DNA supercoils that arise from the separation of complementary DNA strands and the progression of the replication fork. Furthermore, TOP2A removes precatenanes and catenanes generated by the helical rotation of nascent daughter DNA strands and high degrees of topological and torsional stress. Lastly, TOP2A untangles intertwined sister chromatids at anaphase onset allowing accurate segregation during mitosis.

TOP2A is a homodimer comprised of two 170 kDa protomers, each containing an ATPase domain, a transducer domain, a catalytic DNA cleavage domain, an N-terminal gate, and a C-terminal gate (Figure 1.2A) (Berger *et al.*, 1996; Champoux, 2001). TOP2A expression is cell cycle-dependent with gradual rise in expression during S-phase and peak expression in G_2/M (Heck *et al.*, 1988; Woessner *et al.*, 1991; Kaufmann *et al.*, 1991; Sugimoto *et al.*, 1998). Expression of TOP2A protein varies in different cancer cells; however, when compared to normal cells, expression levels of TOP2A are generally higher (Turley *et al.*, 1997). More recently, TOP2A expression in breast cancer patients has been suggested to serve as a marker for high proliferation and aggressive tumour subtypes (Romero *et al.*, 2011).

In mouse cells, down regulation of Top2a (the murine homologue of TOP2A) expression prevents the untangling of sister chromatids resulting in mitotic catastrophe (Akimitsu *et al.*, 2003). Mouse embryos lacking Top2a due to gene deletion do not survive past the 4- to 8-cell stage due to mitotic failure (Akimitsu *et al.*, 2003). In yeast, which express only one Top2 isoform, the phenotype of cells lacking Top2 differs from that of cells expressing a catalytically inactive Top2 mutant (Baxter & Diffley, 2008).

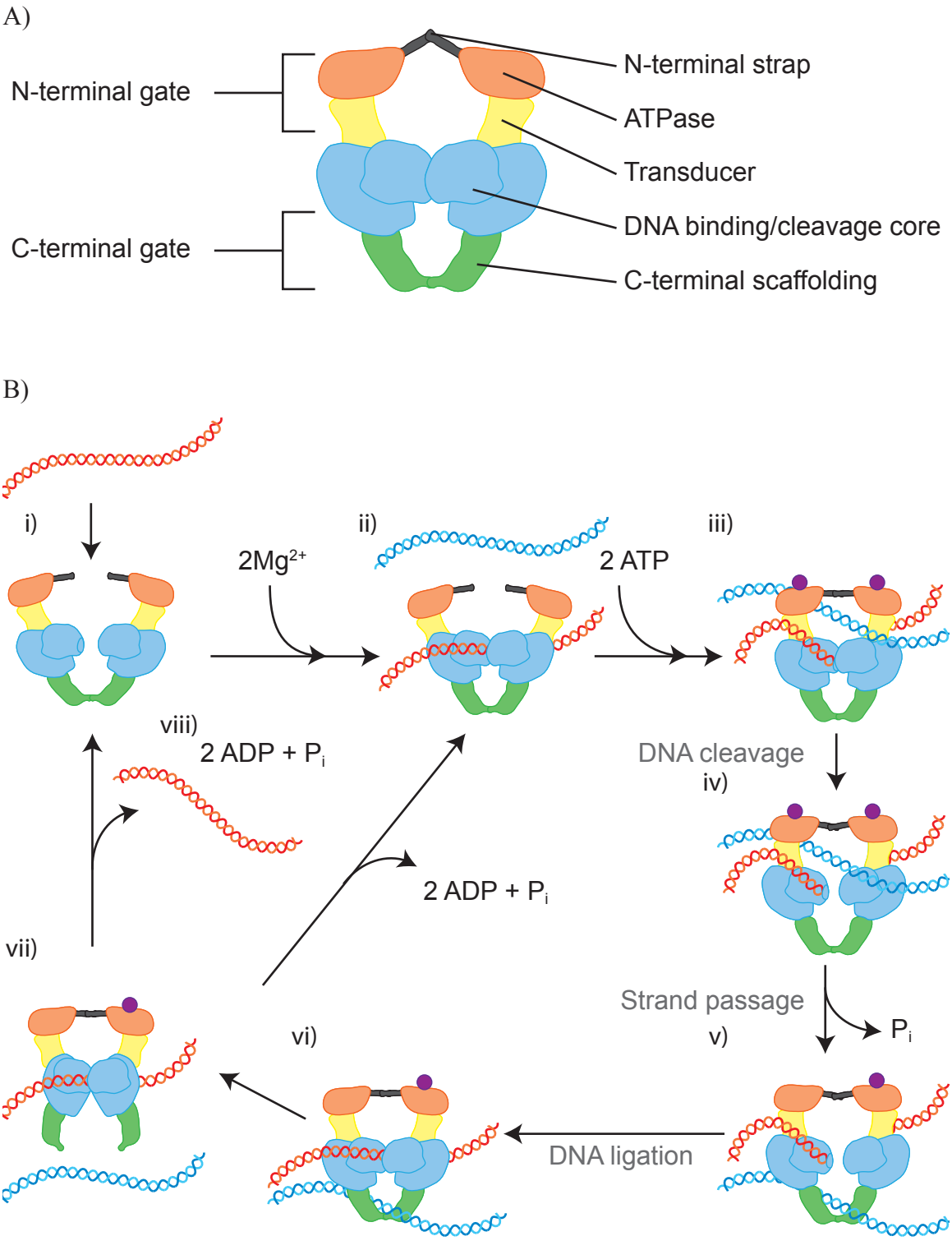
A)
N-terminal gate
C-terminal gate
N-terminal strap
ATPase
Transducer
DNA binding/cleavage core
C-terminal scaffolding
B)
i)
ii)
iii)
2Mg2+
2 ATP
DNA cleavage
iv)
Strand passage
v)
Pi
DNA ligation
vi)
vii)
viii)
2 ADP + Pi
2 ADP + Pi

Figure 1.2 TOP2A and its strand passage mechanism.

A) TOP2A is a homodimer, each subunit is comprised of an ATPase domain (orange), a transducer domain (yellow), DNA cleavage domains (blue), N-terminal gate, and C-terminal gate. B) A TOP2A dimer interacts with two double stranded DNA segments, the gate (G)-segment (red) and the transfer (T)-segment (blue), to facilitate DNA untangling. i) The G-segment is bound by the DNA binding core; ii) the T-segment enters the N-terminal gate; iii) two ATP molecules bind the ATPase domains, inducing the N-terminal gate to close and capturing the T-segment; iv) the catalytic DNA cleavage domain induces a DSB in the G-segment via nucleophilic attack of a catalytic tyrosine residue (Tyr805 in human TOP2A) on the DNA sugar-phosphate backbone; v) hydrolysis of one ATP molecule drives the T-segment through the DNA DSB in the G-segment; vi) the G-segment is ligated; vii) the T-segment exits the enzyme-DNA complex via the C-terminal gate; and viii) hydrolysis of the second ATP molecule allows the release the G-segment from the enzyme. Alternately, the enzyme may initiate another catalytic cycle without releasing the G-segment.

Yeast knockouts of Top2 complete mitosis; however, the extensive chromosome mis-segregation results in mitotic failure. Conversely, a catalytically inactive Top2 mutant disrupts the termination of DNA replication at sites where replication forks meet, resulting in hypercatenated daughter DNA molecules and stable G_2 arrest (Baxter & Diffley, 2008). Thus, decatenation by Top2 may be required for the resolution of replication-induced supercoils before replication can terminate.

1.2.2 Topoisomerase 2A – Catalytic Mechanism

The mechanism by which TOP2A induces transient DNA DSBs is highly coordinated (Figure 1.2B). The 5` ends of the cleaved DNA strands are held in a covalent complex with TOP2A (TOP2-DNAcc), thereby protecting the site from the DNA damage response machinery (Berger *et al.*, 1996). TOP2A interacts with two double-stranded DNA segments, the G-segment and the T-segment, to facilitate DNA untangling (Figure 1.2). The catalytic DNA cleavage domain binds the G-segment. Following G-segment binding, the T-segment enters the N-terminal gate. Two ATP molecules bind the ATPase domains, inducing the N-terminal gate to close, thereby capturing the T-segment. The catalytic DNA cleavage domain induces a DSB in the G-segment through the nucleophilic attack of the DNA phosphodiester backbone by a catalytic tyrosine residue in each protomer (Tyr805 in human TOP2A). Hydrolysis of one ATP molecule drives the T-segment through the break in the G-segment. The T-segment exits the enzyme-DNA complex via the C-terminal coiled-coil domain, while the G-segment is religated. Hydrolysis of the second ATP molecule allows release of the G-segment from the

enzyme. Alternately, the enzyme may initiate another catalytic cycle without releasing the G-segment.

1.3 TOP2A – Chemotherapeutic Target

TOP2A has been identified as the target of several long-standing chemotherapeutics used to treat a broad range of cancer types (Nitiss, 2009). Interestingly, several early adopted cancer chemotherapeutics were determined to be TOP2 poisons decades after their initial implementation in the clinic. The effectiveness of targeting TOP2A for cancer treatment is multifaceted. TOP2A is a ubiquitously expressed and essential enzyme required for successfully proliferation; no viable cell can survive in the absence of its activity. Additionally, disruption of TOP2 activity leads to either the generation of cytotoxic DNA DSBs, or mitotic failure due to an inability to resolve catenated sister chromatids. Compounds that target TOP2 can be broadly classified into one of two groups: TOP2 catalytic inhibitors or TOP2 poisons (Figure 1.3) (Pommier *et al.*, 2010). TOP2 poisons increase the number of TOP2-DNAcc by covalently trapping the enzyme-DNA complex. These compounds exploit canonical TOP2 DNA cleavage, effectively turning the enzyme into a cellular poison that generates cytotoxic DNA DSBs. In contrast, TOP2 catalytic inhibitors inhibit the catalytic activity of TOP2 but do not increase the number of TOP2-DNAcc. Unlike poisons, the cytotoxicity of the majority of compounds in this second class is due to the elimination of TOP2 essential enzymatic activity (Nitiss, 2009).

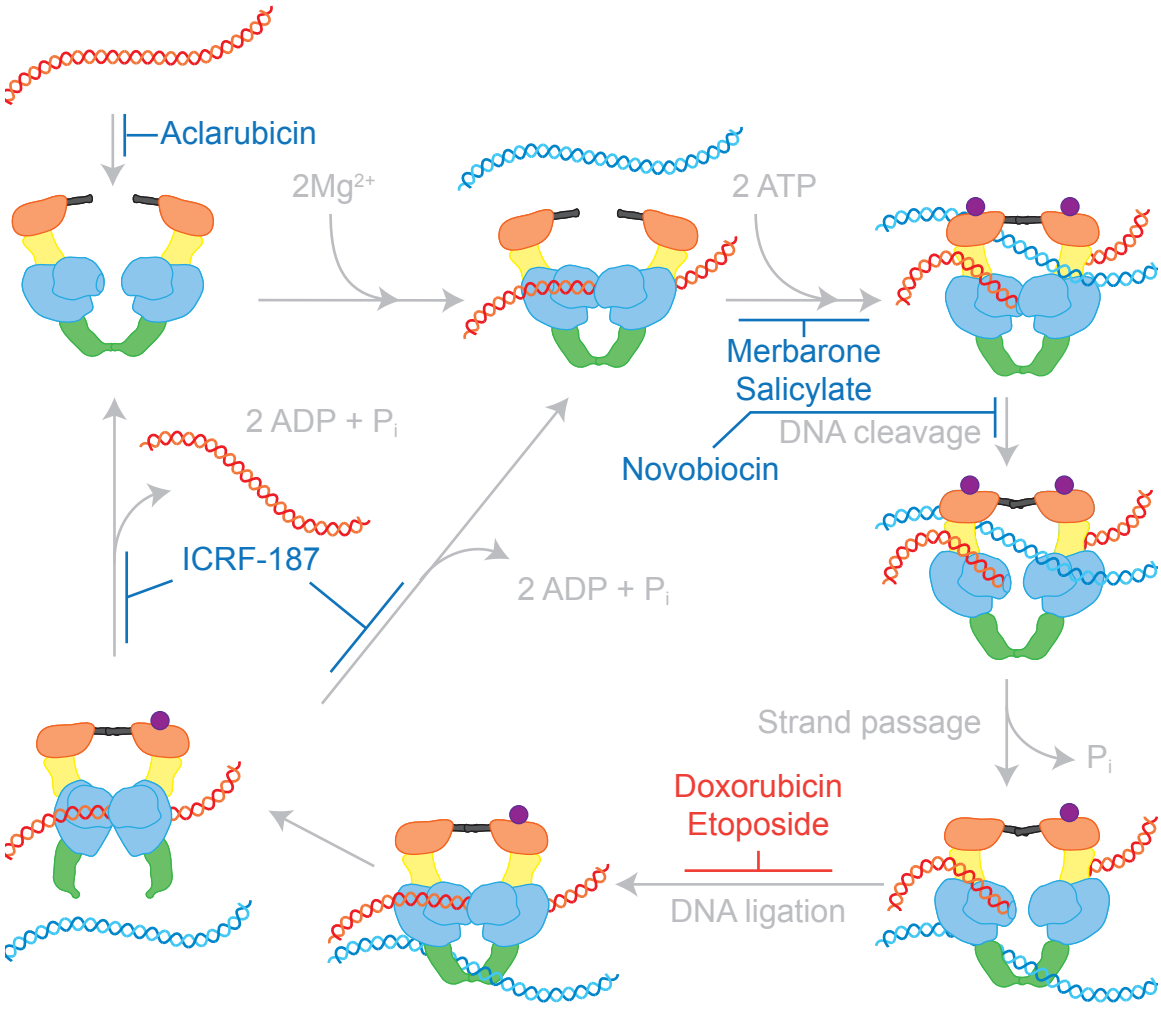
Aclarubicin
2Mg2+
2 ATP
Merbarone
Salicylate
DNA cleavage
Novobiocin
2 ADP + Pi
ICRF-187
2 ADP + Pi
Strand passage
Pi
Doxorubicin
Etoposide
DNA ligation

Figure 1.3 Catalytic inhibition and poisoning of TOP2

Drugs that target TOP2 can be broadly classified into one of two groups: TOP2 catalytic inhibitors and TOP2 poisons. TOP2 catalytic inhibitors act by inhibiting any part of the TOP2 catalytic cycle except stabilization of the TOP2-DNAcc. Numerous TOP2 catalytic inhibitors have been identified including aclarubicin (a DNA intercalator), ICRF-187 (a closed-clamp stabilizer), novobiocin (an ATPase inhibitor), merbarone (an inhibitor of TOP2-mediated DNA cleavage), and salicylate (an inhibitor of TOP2-mediated DNA cleavage). In contrast, TOP2 poisons, which include some of the most commonly used chemotherapeutics (*i.e.* doxorubicin and etoposide), exploit the enzyme's ability to induce DNA DSBs, trapping TOP2 in a covalent complex with DNA, resulting in the accumulation of cytotoxic DNA DSBs. As a result, DNA damage response pathways are induced and cell cycle progression is arrested to allow for repair of the damage if possible. If the damage incurred is excessive, cells undergo apoptosis.

1.3.1 TOP2 Poisons

Several clinically active anticancer agents are categorized as TOP2 poisons (Pommier *et al.*, 2010). These agents act by either preventing enzyme-mediated DNA religation or enhancing the rate of the forward DNA cleavage reaction (Tewey *et al.*, 1984). Because of the strong association between TOP2 subunits, the complexes must be removed to generate cytotoxic DNA DSBs. Collision with replication or transcription machinery stimulates proteasomal degradation of TOP2 subunits, and tyrosyl-DNA phosphodiesterase 2 (TPD2) eliminates the residual DNA adducts (Gao *et al.*, 2014). The proteasomal degradation of TOP2 prevents it from re-entering the catalytic cycle. The resulting DNA DSB activates DNA damage response pathways (*i.e.* ATM autophosphorylation and subsequent activation of downstream effectors: p53, Chk2, SMC1, and Nbs1) (Rossi *et al.*, 2006; Huelsenbeck *et al.*, 2012). Cell cycle progression is arrested for damage repair processing; however, if the damage is excessive, affected cells undergo apoptosis (Roninson, 2003).

The anthracycline doxorubicin, a derivative of daunorubicin (originally isolated from *Streptomyces peucetius var. Canisius*), is one of the most active chemotherapeutic agents in use today (Arcamone et al., 1969; Gewirtz, 1999; Carvalho et al., 2009). Several different mechanisms are responsible for the powerful anticancer activity of doxorubicin. First, doxorubicin acts as a TOP2 poison by preventing the enzyme-mediated DNA religation reaction (Tewey *et al.*, 1984; Box, 2007; Pommier *et al.*, 2010). Second, the planar structure of doxorubicin allows it to intercalate into the DNA helix (Box, 2007). The resulting distortion of the polynucleotide structure inhibits the binding

and passage of machinery required for DNA and RNA synthesis (Cutts *et al.*, 1996). Third, doxorubicin accumulates in mitochondria where it undergoes single-electron reduction forming a semiquinone radical (Thorn *et al.*, 2011). Redox cycling of the semiquinone form of doxorubicin, a short-lived toxic metabolite, leads to the production of reactive oxygen species. Reactive oxygen species can then react with lipids, proteins, and nucleic acids leading to substantial interference with mitochondrial function, protein expression and lipid oxidation (Goodman & Hochstein, 1977; Halligan *et al.*, 1984; Cutts *et al.*, 1996, 2005; Gewirtz, 1999; Box, 2007). Because of its broad anti-tumour activity, compatibility with other anticancer agents, and flexibility in dose and treatment schedule, doxorubicin is a component of many polychemotherapy regimens and is considered the gold standard in the treatment of breast cancer (Table 1.3).

1.3.2 TOP2 Catalytic Inhibitors

Unlike poisons, catalytic inhibitors of TOP2 do not stabilize the TOP2-DNAcc. Instead, this class of drugs acts by impairing essential TOP2 enzymatic activity (Pommier, 2013). The complex mechanism of TOP2 catalytic activity provides several instances where inhibitors can interfere with TOP2 function. As a class, catalytic inhibitors do not act at a single step, but can act at multiple steps in in the TOP2 catalytic cycle. The anthracycline aclarubicin intercalates DNA, changing the shape of the helical structure, thus preventing TOP2 from recognizing and binding DNA (Sørensen *et al.*, 1992). Merbarone, a drug used for mechanistic and cellular research, non-covalently inhibits TOP2-mediated DNA cleavage (Fortune & Osheroff, 1998). Dexrazoxane (ICRF-187), used in the clinic to mitigate anthracycline-related cardiotoxicity, interferes

Table 1.3 Adjuvant chemotherapy regimens containing doxorubicin for patients with breast cancer.

Anthracycline–taxane regimen is considered the optimal strategy for adjuvant chemotherapy, particularly in patients with high risk breast cancer.
– Doxorubicin and cyclophosphamide
– Doxorubicin and cyclophosphamide followed by paclitaxel
– Doxorubicin and cyclophosphamide followed by paclitaxel and trastuzumab
– Doxorubicin and cyclophosphamide followed by docetaxel
– Doxorubicin and cyclophosphamide followed by docetaxel and trastuzumab
– Cyclophosphamide, doxorubicin, and fluorouracil

with ATPase activity and prevents DNA dissociation by locking the N-terminal gate (Speyer *et al.*, 1992; Classen *et al.*, 2003). Of specific relevance to the work presented herein, salicylate, the primary metabolite of aspirin (acetylsalicylic acid; ASA), interferes with the DNA cleavage reaction preventing the formation of the TOP2A-DNAcc as well as non-competitively inhibiting TOP2A ATPase activity (Bau & Kurz, 2011; Bau *et al.*, 2014).

1.4 Salicylates

The medicinal use of salicylates, originally derived from extracts of plants such as willow and myrtle, can be traced back through antiquity (Lévesque & Lafont, 2000). Sumerian stone tablets (*c*. 3500–2000 BCE) describe how Assyrian physicians would use extracts of white willow bark as analgesic and anti-inflammatory agents. The Ancient Egyptians, documented by the Ebers Papyrus (*c*. 1500 BCE), used willow bark leaves to treat inflammation, and pain associated with wounds (Riddle, 1999; Mahdi *et al.*, 2006). Centuries later, Hippocrates (*c*. 400 BCE) recommended using concoctions of willow bark and myrtle leaves for the treatment of eye diseases, and pain associated with childbirth (Rainsford, 2004).

In the early 19th century, salicylic acid, salicin (a β-glucoside alcohol that is metabolized into salicylic acid), and methyl salicylate were isolated and identified as the therapeutic agents active in willow bark (Leroux, 1930; Miner & Hoffhines, 2007). Then in 1897, Arthur Eichengrün, at Friedrich Bayer & Company, was the first to synthesize acetylsalicylic acid (ASA), a more stable form of salicylic acid (Sneader, 2000). By 1899, Friedrich Bayer & Company registered ASA under the trademark Aspirin and

began mass-production of the drug, marketing it as an analgesic, anti-inflammatory, and antipyretic. Subsequent research established its efficacy as an antiplatelet agent, and for the prevention of acute myocardial infarction and stroke (Hass *et al.*, 1989; Collaboration, 1994; Baigent *et al.*, 1998). ASA is included on the World Health Organization's Model List of Essential Medicines and is one of the most widely used drugs in the world, with annual global consumption of over 40,000 tonnes (Fuster & Sweeny, 2011). Approximately 36% of patients over the age of 35 and 40% of patients over the age of 55 report using ASA on a regular basis (Ajani *et al.*, 2006; Kolber *et al.*, 2013). Although ASA has many therapeutic uses, 87% of patients using ASA do so for cardiovascular prevention and at present it is most commonly used as daily low-dose therapy for the prevention of secondary major occlusive vascular events, including myocardial infarction and stroke (Antithrombotic Trialists' Collaboration, 2002; Kolber *et al.*, 2013).

1.4.1 Salicylate – Mechanism of Action

Following oral administration, ASA is rapidly absorbed from the stomach and small intestine. ASA rapidly undergoes first-pass metabolism to salicylate via esterases in the gastrointestinal wall, liver, lung, plasma, and red blood cells (Figure 1.4) (Williams, 1985). ASA, and its primary metabolite salicylate, act through multiple common mechanisms that affect cellular pathways involved in cell cycle progression, proliferation, inflammation and apoptosis (Figure 1.5). The therapeutic properties of ASA and salicylate can be directly linked to their involvement in these cellular pathways.

A)

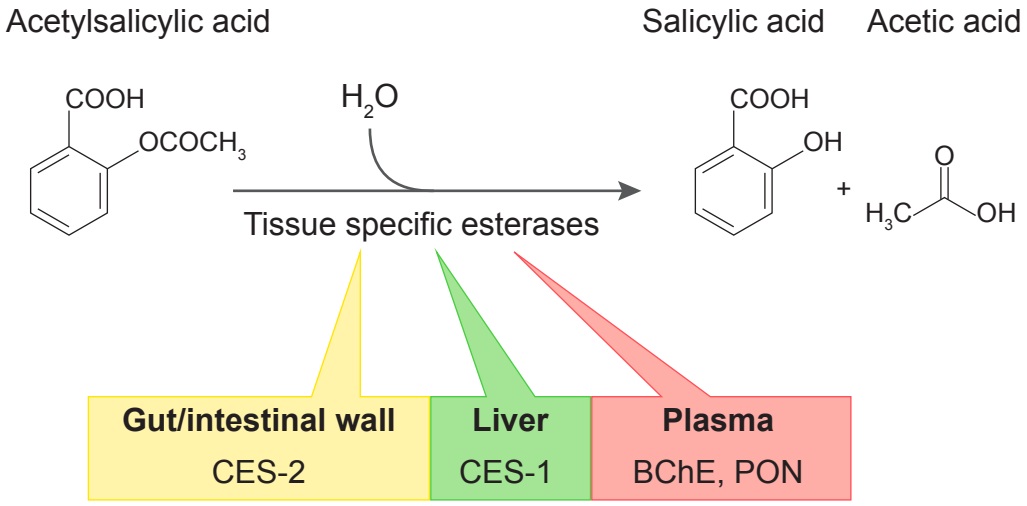
Acetylsalicylic acid
Salicylic acid
Acetic acid
COOH
OCOCH3
H2O
Tissue specific esterases
COOH
OH
+
O
H3C
OH
Gut/intestinal wall
CES-2
Liver
CES-1
Plasma
BChE, PON

B)

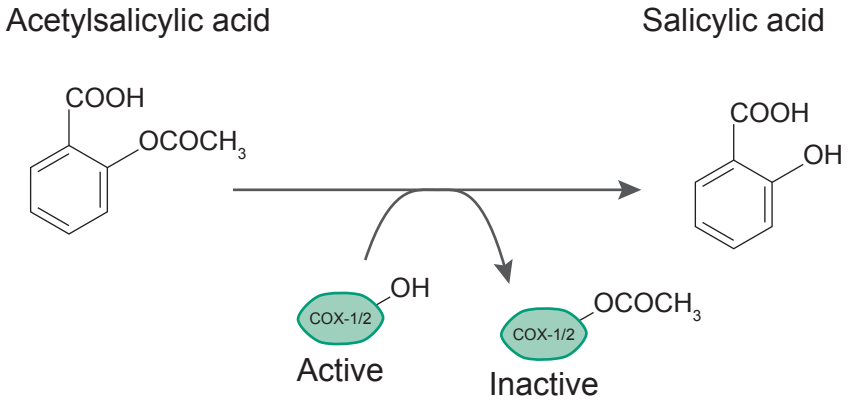
Acetylsalicylic acid
Salicylic acid
COOH
OCOCH3
COOH
OH
OH
COX-1/2
Active
OCOCH3
COX-1/2
Inactive

Figure 1.4 ASA metabolism.

ASA is rapidly absorbed from the gastrointestinal tract through passive diffusion. A) Spontaneous metabolism of ASA into salicylic acid and acetic acid by tissue-specific esterases begins in the wall of the stomach and small intestine. Then, as the drug enters the hepatic portal system, metabolism continues in the plasma and liver. Furthermore, ASA is capable of acetylating various proteins in different tissues including the cyclooxygenase (COX) family of enzymes, which act as mediators of inflammation. ASA acetylation of COX-1 or COX-2 irreversibly deactivates the enzymes, releasing salicylic acid. The antiplatelet effect of ASA is attributed to its deactivation of COX-1, while the drug's anti-inflammatory and antipyretic effects are mainly due to COX-2 deactivation and the effects of free salicylic acid. BChE, butyrylcholinesterase; CES-2, carboxylesterase 2; CES-2, carboxylesterase 1; PON, paraoxonase.

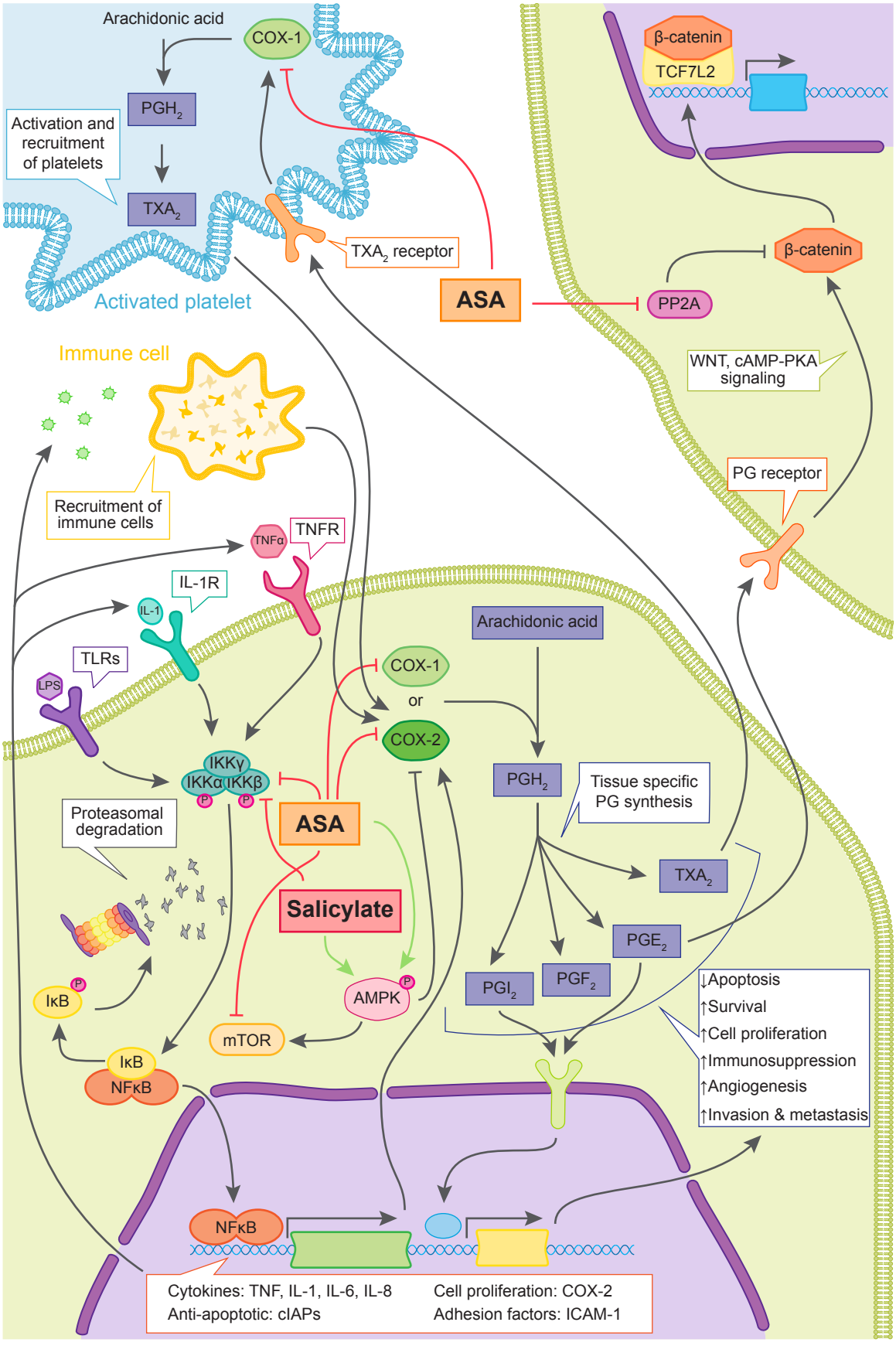
Arachidonic acid
COX-1
PGH2
Activation and recruitment of platelets
TXA2
TXA2 receptor
Activated platelet
ASA
β-catenin
TCF7L2
β-catenin
PP2A
WNT, cAMP-PKA signaling
PG receptor
Immune cell
Recruitment of immune cells
TNFα
TNFR
IL-1
IL-1R
TLRs
LPS
Arachidonic acid
COX-1
or
COX-2
IKKγ
IKKα
IKKβ
P
ASA
Proteasomal degradation
Salicylate
PGH2
Tissue specific PG synthesis
TXA2
PGE2
PGI2
PGF2
AMPK
mTOR
IκB
NFκB
↓Apoptosis
↑Survival
↑Cell proliferation
↑Immunosuppression
↑Angiogenesis
↑Invasion & metastasis
NFκB
Cytokines: TNF, IL-1, IL-6, IL-8
Anti-apoptotic: cIAPs
Cell proliferation: COX-2
Adhesion factors: ICAM-1

Figure 1.5 Cellular signalling pathways affected by ASA and salicylate.

ASA and its primary metabolite salicylate affect several interconnected cellular pathways. Acetylation of COX-1 and COX-2 by ASA irreversibly blocks prostaglandin synthesis from free arachidonic acid preventing the production of PGH_2. Tissue-specific isomerases convert PGH_2 into a range of prostanoids involved in processes like cell proliferation and survival, inflammation response and platelet activation. Therefore, inhibition of COX enzymes by ASA attenuates the downstream activation of these signalling pathways. ASA and salicylate inhibit NFκB signalling by competitively inhibiting ATP activation of IKKβ. IKKβ activation releases NFκB from IκB allowing for the nuclear localisation of NFκB and subsequent transcription of related inflammatory response factors. Several other pathways are also affected by ASA or salicylate both directly, like AMPK and PP2A signalling, or indirectly, like WNT–β-catenin and immune cell recruitment signalling. ASA, acetylsalicylic acid; AMPK, 5' adenosine monophosphate-activated protein kinase; cIAPs, cellular inhibitor of apoptosis proteins; COX, cyclooxygenase; ICAM-1, intercellular cell adhesion molecule-1; IκB, inhibitor of NFκB; IKK, IκB kinase; IL, interleukin; LPS, lipopolysaccharide; mTOR, mechanistic target of rapamycin; NFκB, nuclear factor κB; P, phosphate; PG, prostaglandin; PGI_2, prostacyclin; PP2A Protein phosphatase 2A; TCF7L2, transcription factor 7 like 2; TLRs, toll-like receptors; TNF, tumour necrosis factor; TNFR, TNF receptor; TXA_2, thromboxane A_2.

ASA acts primarily by inhibiting the biosynthesis of prostanoids, such as prostaglandins and thromboxane, from arachidonic acid via prostaglandin H-synthases (COX-1 and COX-2) (Vane & Botting, 2003). Prostanoids activate specific G-protein coupled receptors in response to diverse stimuli. Tissue-specific synthases metabolize the products of COX-1 and COX-2 activity into different prostanoids, prostaglandins (PG) (specifically PGE_2 and PGI_2) and thromboxane (TX)A_2 (Dubois *et al.*, 1998). COX-1, expressed in many but not all tissue and cell types, promotes platelet activation via TXA_2 generation and gastroprotection in gastric epithelial cells via PGE_2 generation (Dubois *et al.*, 1998). In contrast, COX-2 expression in most cells is low; however, expression levels increase dramatically in response to inflammation (Eckmann *et al.*, 1997). COX-2 promotes anti-thrombotic, and vasoprotective signalling in endothelial cells via PGI_2 generation, and promotes inflammation progression via PGE_2 generation. In colorectal cancer, elevated expression of COX-2 is linked to increased cell proliferation, resistance to apoptosis, cell migration, and angiogenesis (Chan *et al.*, 2007). ASA irreversibly inactivates COX-1 and COX-2 through acetylation, generating salicylate in the process (Roth *et al.*, 1975; Roth & Majerus, 1975). At therapeutic concentrations, ASA and salicylate suppress COX-2 gene expression by modulating protein kinase C and protein tyrosine phosphatase (Xu *et al.*, 1999; Duan *et al.*, 2014). Daily low-dose ASA has been shown to inhibit COX-1; this effect inhibits platelet activation by TXA_2, resulting in an anti-thrombotic effect, and gastric protection by PGE_2 resulting in gastrointestinal side-effects, such as ulcers (Patrono *et al.*, 2004). High doses of ASA over a short period are capable of inhibiting COX-2; this effect inhibits inflammation progression (including

inflammatory hyperalgesia and pyrexia) through PGE_2, resulting in anti-inflammatory, analgesic, and antipyretic effects.

ASA and salicylate-mediated inhibition of the nuclear factor κB (NFκB) pathway has also been extensively characterized (Kopp & Ghosh, 1994; Yin *et al.*, 1998; Yuan *et al.*, 2001; Dikshit *et al.*, 2006; Stark *et al.*, 2007). The NFκB pathway is considered a critical component in both the promotion and resolution of the inflammatory response (Barnes & Karin, 1997; Tak & Firestein, 2001; Lawrence & Fong, 2010). Furthermore, aberrant activity of NFκB promoting malignancy and survival through the upregulation of anti-apoptotic genes has been observed in a range of cancers (Staudt, 2010; DiDonato *et al.*, 2012). NFκB is a transcription factor that is sequestered in the cytoplasm by inhibitor of κB (IκB). In response to inflammatory signals, IκB is phosphorylated by IκB kinase complex (IKK; consisting of the catalytically active kinases IKKα, IKKβ, and the regulatory unit IKKγ). Phosphorylated IκB is then degraded by the proteasome, consequently releasing activated NFκB. NFκB, now free to translocate to the nucleus, regulates the expression of inflammatory cytokines such as interleukin(IL)-1, IL-6, IL-8 and chemokine (C-C motif) ligand 2 (CCL2), anti-apoptotic genes, such as the cellular inhibitor of apoptosis proteins (cIAPs) and the TNFR-associated factors (TRAFs), and adhesion molecules, including the intercellular cell adhesion molecule-1 (ICAM-1) and the vascular cell adhesion molecule-1 (DiDonato *et al.*, 2012; Hoesel & Schmid, 2013). ASA and salicylate competitively inhibit the binding of ATP to IKKβ, preventing the activation of NFκB mediated inflammatory response (Kopp & Ghosh, 1994; Yin *et al.*, 1998). Inhibition of the NFκB pathway has also been suggested as mechanism for ASA and salicylate-mediated anticancer effects (McCarty & Block, 2006; Stark *et al.*, 2007).

Salicylate and ASA affect several additional signalling pathways, including those mediated by AMPK, AKT, ERK, and p38 MAPK (Schwenger *et al.*, 1998; Ricchi *et al.*, 2003; Chae *et al.*, 2004; Serizawa *et al.*, 2014). Salicylate has also been shown to inhibit histone deacetylase in embryonic mice, suggesting salicylate-mediated epigenetic activity that could influence gene expression (Di Renzo *et al.*, 2008). Furthermore, the complexity of the NFκB pathway, and the increasing number of proposed NFκB-independent signals arising from the IKK complex, highlight the complex and extensive influence salicylate may have on biological systems (Scheidereit, 2006; Chariot, 2009; Oeckinghaus *et al.*, 2011).

1.4.2 Salicylate – Chemopreventative Agent

In recent years, ASA has garnered substantial attention regarding its use as a chemopreventative agent. The association of ASA with anticancer activity was first suggested when rats with thrombocytopenia, a platelet deficiency that results in slow blood clotting, demonstrated a decrease in tumour metastasis following treatment with ASA (Gasic *et al.*, 1968, 1972). Further support for this hypothesis came when elevated COX-mediated prostaglandin levels were observed in colorectal tumours of rats (Jaffe, 1974; Bennett & Del Tacca, 1975). The most compelling support for the use of ASA for the prevention of cancer is provided by epidemiological evidence of its effect on colorectal cancer (Kune *et al.*, 1988; Vainio *et al.*, 1997; Flossmann & Rothwell, 2007; Cuzick *et al.*, 2009; Chan *et al.*, 2012; Rothwell *et al.*, 2012*a*). A recent case-control study, using pooled data of 8634 colorectal cancer cases and 8553 controls from ten cohort and case control studies, reported that regular use of ASA, other nonsteroidal anti-

inflammatory drugs, or both, when compared to non-regular use, (prevalence, 38% vs 28%, odds ratio = 0.69 95% CI, 0.64−0.74) was associated with a lower risk of colorectal cancer (Nan *et al.*, 2015). Similarly, a 24% reduction (hazard ratio = 0.75; 95% CI 0.56–0.97) in the long-term risk of colorectal cancer in individuals regularly taking ASA (87-300 mg/day) for more than five years was reported by a meta-analysis of three randomized controlled trials conducted to examine the efficacy of ASA in the prevention of cardiovascular disease (Rothwell *et al.*, 2010). Reduced incidence of other cancers, including breast, bladder, lung, mouth, ovary, and skin, have also been associated with the use of ASA; however, the benefits are less consistently observed (Rothwell *et al.*, 2012*b*, 2012*a*; Algra & Rothwell, 2012).

The processes involved in the development of malignant disease are highly complex and, despite substantial research, the mechanisms through which ASA and salicylates impact carcinogenesis have yet to be determined and are likely many-fold and interconnected (Figure 1.5). Several cellular processes that regulate proliferation and differentiation are of particular interest. ASA can irreversibly bind and acetylate COX-1 and COX-2, thus inhibiting the propagation of pro-inflammatory signalling and associated promotion of angiogenesis, apoptotic resistance, and cellular proliferation. Given the significance of WNT deregulation seen in colorectal cancer, PGE_2 modulation of the WNT–β-catenin signalling pathway and the cross-regulation of NFκB and WNT signalling provide further mechanistic avenues for exploring chemoprevention (Du & Geller, 2010; Gala & Chan, 2015).

1.4.3 Salicylate – A Novel Catalytic Inhibitor of Human TOP2A

Salicylate was recently identified as a novel catalytic inhibitor of TOP2 and is selective for the TOP2A isoform (Bau & Kurz, 2011; Bau *et al.*, 2014). While conducting a study on the effect of hydroxyl radical scavengers on doxorubicin-induced DNA damage signalling, Bau and Kurz found that a brief pretreatment of MCF-7 human breast cancer cells with salicylate significantly attenuates doxorubicin-mediated DNA damage signalling through the ATM (ataxia telangiectasia mutated) protein kinase (Kurz & Lees-Miller, 2004; Bau & Kurz, 2011). This effect is neither dependent on the actions of salicylate as an antioxidant, nor is it due to inhibition of cyclooxygenases (COX-2 and COX-1) or NFκB (Bau & Kurz, 2011). Attenuation of DNA damage signalling by salicylate is not limited to anthracycline-based TOP2 poisons, as it is observed with non-anthracycline-based TOP2 poisons; however, it is specific for TOP2 poisons, and not observed with other inducers of DNA damage (Bau & Kurz, 2011). Furthermore, salicylate pretreatment diminishes the formation of doxorubicin-induced TOP2-DNAcc. It was subsequently demonstrated that salicylate inhibits the formation of doxorubicin and etoposide-mediated DSBs by inhibiting TOP2-mediated DNA cleavage and, to a lesser degree, non-competitively inhibiting TOP2 ATPase activity (Bau *et al.*, 2014). Importantly, a brief pretreatment of MCF-7 human breast cancer cells with salicylate significantly diminishes both doxorubicin and etoposide cytotoxicity (Bau & Kurz, 2011). This occurs at salicylate concentrations similar to those found in the plasma of patients receiving ASA for long-term analgesic/anti-inflammatory treatment (Grosser *et al.*, 2011). Similar results were observed for other salicylate-based drugs, but not with

non-salicylate-based non-steroidal anti-inflammatory agents (Bau & Kurz, 2014). These findings suggest that salicylate-based drugs could have an adverse impact on the anti-tumour efficacy of TOP2 poison-based chemotherapy commonly used in the treatment of breast and other cancers. However, these early investigations focused on the effects of acute salicylate treatment and at reasonably high dose. Since ASA is most commonly used as a daily low-dose regimen for the prevention of secondary heart attack or stroke, an investigation of the long-term effect of low-dose salicylate is warranted. Furthermore, the effect of salicylate on TOP2 has not been studied in a whole organism, and, given the promiscuity of salicylate in the cell and the multiple affected pathways, the biological relevance of these observations has yet to be established.

1.5 Translational Research – Animal Models of Human Breast Cancer

For cancer researchers, the ultimate goal of their work is to establish scientific findings that hold clinical relevance. The process of translating scientific discoveries from basic research into clinical applications is complex and highly regulated. Because of this, the field of translational cancer research relies heavily on animal models to evaluate effectiveness, establish therapeutic windows, confirm biological relevance of novel drug targets, and identify biomarkers of tumour response (Doroshow & Kummar, 2014). The mouse is by far the most frequently used model due to its relatively similar physiology to that of humans, the variety of available models, the ease of genetic manipulation, and the relatively low cost of housing. There are four major preclinical mouse model systems used for *in vivo* tumour biology studies. In xenograft models, established human tumour cell lines are transplanted into immunodeficient mice. In patient-derived xenograft

models, patient-derived tumour cells are directly implanted into immunodeficient mice, or implanted after limited passage in culture. The most obvious downfall of immunodeficient models is that they cannot be used to evaluate immune-targeting therapies or to monitor the contribution of the immune system to the drug response. For such studies, a syngeneic model, where established murine tumour cell lines are transplanted into immunocompetent mice, is preferable. Advancements in genetic manipulation have allowed the development of genetically engineered models that harbour mutations that can permit spontaneous or induced tumour development. Naturally, each model has its unique limitations, including those related to the fundamental differences between human and murine physiology. Each model system has its own set of benefits and caveats that must be carefully evaluated based on specific research needs. Moreover, no one model is universally best nor universally most appropriate.

The advantages of using cell line-based xenograft models, such as the one discussed in this thesis, are that the tumour cells are human-derived, there are a wide variety of well-established and well-documented cell lines and hosts available, and many of the models are easily controlled and reproducible (Sausville & Burger, 2006). The disadvantages of these models are the relatively high cost when compared to syngeneic models, that the stromal component of the tumours is not human, the prerequisite immunodeficient hosts (*e.g.* athymic nude or SCID mice), the artificially accelerated doubling time (most cell line tumours double every six days, whereas the doubling time for clinical human tumours is typically measured in months to years). Although distinct disease subtypes can be identified within collections of cultured cell lines, they do not

fully represent the genetic diversity observed in human tumours, and xenograft tumours lack the intratumoral heterogeneity seen in humans (Yap *et al.*, 2012; Gould *et al.*, 2015). Nevertheless, xenotransplantation of human cell lines is an exceedingly useful experimental paradigm given its relative convenience and versatility.

1.6 Hypothesis

Given the widespread use of low-dose ASA for the reduction of risk for secondary cardiovascular and cerebrovascular events combined with the observed effects of salicylate on TOP2A, this thesis addresses the hypothesis that salicylate, a newly described catalytic inhibitor of TOP2A, decreases the efficacy of co-administered TOP2 poison-based chemotherapy in a murine xenograft model of human breast cancer

The specific research aims for this work are:

Aim 1 – Characterization of the effects of salicylate on doxorubicin and etoposide cytotoxicity in a panel of cell lines representing the distinct subtypes of breast cancer.

Aim 2 – Evaluation of the impact of salicylate co-administration on TOP2 poison chemotherapeutic efficacy in murine models of breast cancer.

Determining the effects of salicylates on chemotherapeutic efficacy could have far-reaching implications. The results of these experiments will provide insight and information that may inform future clinical practice concerning salicylate co-

administration in women undergoing chemotherapy with TOP2-targeting drugs for the treatment of breast cancer.

Chapter Two: Methods and Materials

2.1 Cell Lines and Culture Conditions

MCF-7 and MDA-MB-231 cells were obtained from the American Type Culture Collection (Manassas, VA, USA). MDA-MB-231/GFP/Luc cells were purchased from (Cell Biolabs Inc., San Diego, CA, USA). SK-BR-3 cells were obtained from the Southern Alberta Cancer Research Institute Antibody Services Cell Bank (University of Calgary, Canada). EMT-6 and MDA-MB-468 were kindly provided by Dr Donald G Morris (Tom Baker Cancer Centre, Calgary, AB, Canada). MCF-7, MDA-MB-231, MDA-MB-231/GFP/Luc, MDA-MB-468, and SK-BR-3 cells were maintained in Dulbecco's modified Eagle's media (DMEM) (Sigma-Aldrich, Oakville, ON) supplemented with 10% [v/v] fetal bovine serum (FBS) (Sigma-Aldrich). EMT-6 cells were maintained in Waymouth MB 752/1 media (Sigma-Aldrich) supplemented with 10% FBS. All cells were maintained as sub-confluent monolayer cultures at 37°C in a humidified atmosphere containing 5% CO_2.

2.2 Antibodies

The rabbit monoclonal anti-TOP2A antibody was obtained from Abcam (Cambridge, MA; cat. no. ab52934). The primary antibody was diluted to 1:5000 in 1X Tris-buffered saline (50 mM Tris, 150 mM NaCl) containing 0.1% Tween-20 (TBS-T) with 0.1% [w/v] gelatin, 0.02% [w/v] NaN_3 prior to use in immunoblot analysis. Goat anti-rabbit IgG blotting-grade horseradish peroxidase secondary antibody conjugate (Bio-

Rad, Mississauga, ON) was used at a 1:3000 dilution in 5% [w/v] non-fat dry milk powder in 1X TBS-T.

2.3 Population Doubling Time of Breast Cancer Cell Lines

Changes in cell numbers were monitored by counting living cells using trypan blue exclusion assay. MCF-7, MDA-MB-231, MDA-MB-468, SK-BR-3, ZR-75-30, or EMT-6 cells were seeded in 60 mm cell culture plates at 1.0 x 10^5 cells per plate and were grown for 6 days at 37°C. Every 24 h, quadruplicate plates of cells were manually counted and then discarded. Cells were washed once with phosphate-buffered saline (PBS; 137 mM NaCl, 2.7 mM KCl, 10 mM Na_2HPO_4, 1.8 mM KH_2PO_4, pH 7.4) and incubated with 1 ml Trypsin-EDTA (0.05% [v/v] Trypsin, 0.53 mM EDTA; Invitrogen, Burlington ON) at 37°C for 5 min. Trypsinization was halted by the addition of 4 mL DMEM + 10% FBS. For the exclusion assay, 500 µL of cell suspension was diluted 1:1 with trypan blue stain (Sigma-Aldrich) and cells excluding the stain were counted using a haemocytometer. The population doubling time (PDT) was calculated as $\mathrm{PDT} = (t_i)\ln 2/\ln(x_f/x_i)$, where t is the duration of log phase growth, x_i is the cell number at the start of t, and x_f is the cell number at the end of t.

2.4 Assessment of Viability Using AlamarBlue®

2.4.1 Optimization of Seeding Density and AlamarBlue® Incubation Time

MCF-7, MDA-MB-231, MDA-MB-468, SK-BR-3, or EMT-6 cells were seeded at increasing densities in 96-well plates and incubated for 120 h. Following incubation,

cell confluency was assessed visually using a Zeiss Axiovert 25 inverted transmission light microscope (Carl Zeiss Canada Ltd., Toronto, ON). The medium was then aspirated from the plates and replaced with 100µl Opti-MEM Media (Invitrogen) containing 5% [v/v] AlamarBlue® (Invitrogen) and incubated for increasing time periods at 37°C in a humidified atmosphere containing 5% CO_2. Fluorescence of AlamarBlue® was measured $\lambda_{excitation}$ = 570 nm and $\lambda_{emission}$ = 585 nm using a SpectraMax M2^e plate reader (Molecular Devices, Sunnyvale, CA).

2.4.2 Drug Preparation and Treatment Conditions

Doxorubicin, etoposide, sodium salicylate and dimethyl sulfoxide (DMSO) were purchased from Sigma-Aldrich. Doxorubicin, and etoposide stock solutions were prepared in DMSO, protected from light and stored at -20°C. Sodium salicylate was prepared freshly in PBS prior to use.

2.4.3 AlamarBlue® Viability Assay

MCF-7, MDA-MB-231, MDA-MB-468, or SK-BR-3 cells were seeded at a density of 5 x 10^3 cells per well in a 96-well plate. EMT-6 cells were seeded at a density of 2 x 10^3 cells per well in a 96-well plate. Cells were allowed recover for 16 h prior to initiating treatment. Cells were treated with increasing concentrations of salicylate for 3 or 10 h, or pretreated with salicylate for 1 or 8 h prior to the addition of increasing concentrations of doxorubicin or etoposide and continued incubation for 2 h at 37°C. After 3 or 10 h of drug treatment, drug-containing medium was aspirated and replaced with fresh drug-free medium. MCF-7, MDA-MB-231, MDA-MB-468, and SK-BR-3

cells were grown for 96 h, while EMT-6 cells were grown for 72 h at 37°C in a humidified atmosphere containing 5% CO_2. Following incubation, the medium was aspirated and replaced with 100µL Opti-MEM (Invitrogen) containing 5% [v/v] AlamarBlue® (Invitrogen) and incubated for 3 h at 37°C. Fluorescence of AlamarBlue® was measured at $\lambda_{excitation}$ = 570 nm and $\lambda_{emission}$ = 585 nm using a SpectraMax M2^e plate reader (Molecular Devices).

2.5 Cell Harvest and Lysis

2.5.1 Cell Harvest

MCF-7, MDA-MB-231, MDA-MB-468, SK-BR-3, or EMT-6 cells at approximately 60-80% confluency were washed once with PBS and incubated with Trypsin-EDTA at 37°C for 5 min. Trypsinization was halted by the addition of 1 mL DMEM containing 10% FBS. Cells were collected in clean centrifuge tubes and pelleted by centrifugation at 1000 *x g* for 5 min at 4°C. Following centrifugation, the supernatant was removed and cell pellets were washed twice in PBS containing 0.2 mM phenylmethylsulfonyl fluoride (PMSF) (Sigma-Aldrich) with each wash followed by centrifugation at 1000 *x g* for 5 min at 4°C and removal of the PBS wash supernatant. Cell pellets were lysed as described below.

2.5.2 Preparation of NET-N Whole Cell Extracts

MCF-7, MDA-MB-231, MDA-MB-468, SK-BR-3, or EMT-6 cells were harvested as described in section 2.5.1. Cell pellets were resuspended in 250 µL of ice cold NET-N lysis buffer (150 mM NaCl, 1 mM EDTA, 20 mM Tris, 1% [v/v] Nonidet-

P40) supplemented with both protease inhibitors (0.2 mM PMSF, 0.2 μg/mL aprotinin, 0.2 μg/mL leupeptin, 0.1 μg/mL pepstatin A, dissolved in methanol) and phosphatase inhibitors (1 mM activated Na_3VO_4, 25 mM NaF). Samples were then incubated on ice for 10 min and sonicated using a microtip at 10% power for 6 sec on ice (repeated three times). Lysates were then centrifuged at 12,000 *x g* for 10 min at 4°C and the supernatant was transferred to clean microfuge tube. Protein concentrations of the samples were determined using a Bio-Rad *DC* Protein Assay kit (Bio-Rad) modified from the well-documented Lowry assay using bovine serum albumin (BSA; Sigma-Aldrich) as a protein standard (Lowry *et al.*, 1951). The absorbance of samples and standards was measured at λ = 750 nm on a SpectraMax M2^e plate reader.

2.6 Sodium Dodecyl Sulfate-Polyacrylamide Gel Electrophoresis (SDS-PAGE) and Immunoblot Analysis

2.6.1 SDS-PAGE

Whole cell extracts (50 μg) were prepared in 1X Laemmli's buffer (0.83 M Tris, pH 6.8, 2% [w/v] sodium dodecyl sulfate (SDS), 10% [v/v] glycerol, 0.002% [w/v] bromophenol blue, 3.3% [v/v] 2-mercaptoethanol) and heated for 5 min at 95°C. Proteins were resolved on an 8% [w/v] low bis-acrylamide gel (7.9% [w/v] acrylamide, 0.1% [w/v] bis-acrylamide, 375 mM Tris-HCl, pH 8.8, 0.1% [w/v] SDS, 0.06% [w/v] ammonium persulfate (APS), 0.001% [v/v] tetramethylethylenediamine (TEMED)) with a 4% stacking gel (3.8% [w/v] acrylamide, 0.2% [w/v] bis-acrylamide, 125 mM Tris-HCl, pH 6.8, 0.2% [w/v] SDS, 0.1% [w/v] APS, 0.002 % [v/v] TEMED). Samples were

stacked at 75 V for 20 mins then resolved at 150 V for approximately 1 h (until the dye front ran off the gel) in 1X SDS running buffer (25 mM Tris-HCl, pH 7.5, 192 mM glycine, 0.1% [w/v], 0.036% [w/v] SDS).

2.6.2 Immunoblot Analysis

Following resolution by SDS-PAGE, proteins were transferred to nitrocellulose membrane (Bio-Rad) in ice-cold transfer buffer (48 mM Tris-HCl, 192 mM glycine, 20% [v/v] methanol) for 1 h at 100 V. Membranes were stained with Ponceau S (0.1% [w/v] Ponceau S, 5% [v/v] acetic acid; Sigma-Aldrich) to confirm successful protein transfer then rinsed with 1X TBS-T and blocked in 1X TBS-T with 25% [w/v] non-fat dry milk powder for 1 h at room temperature with rocking. Blocked membranes were washed three times for 5-10 min in 1X TBS-T and incubated with primary antibody at 4°C overnight with rocking. The primary antibody was removed and the membranes were washed three times for 5-10 min each in 1X TBS-T and then incubated with affinity-purified goat anti-rabbit IgG horseradish peroxidase-conjugated secondary antibody (1:3000 dilution in 1X TBS-T with 5% [w/v] non-fat dry milk powder) for 1 h at room temperature. Membranes were then washed three times for 5-10 min in 1X TBS-T. Membranes were incubated in enhanced chemiluminescence (ECL) reagent (0.1 M Tris-HCL pH 8.5, 12.5 mM luminol, 0.2 mM coumaric acid, 10% [v/v] H_2O_2) for 1 min then covered in a plastic film and exposed to Fuji SuperRx medical X-ray film (Fuji, Mississauga, ON), and developed.

2.7 Animals and Housing Condition

Female 6 to 7-week-old Fox Chase severe combined immune deficient C.B-17/Icr-*Prkdc*^{scid}/IcrIcoCrl (SCID C.B.-17; strain code: 236) mice were purchased from Charles River Laboratories International Inc. (Wilmington, MA, USA). Animals were acclimatized to the local environment in the Biosafety II facility in the Animal Research Centre at the University of Calgary for one week prior to the start of each experiment. The animals were housed in standard polycarbonate shoebox cages with food and water *ad libitum* under a 12 h light/day cycle with lights on at 7:00 AM. All procedures were reviewed and approved by the University of Calgary Animal Care Committee under the animal ethics protocol AC12-0126.

2.8 *In Vivo* Studies in a Murine Xenograft Model of Human Breast Cancer

2.8.1 Establishment of Orthotopic Human Breast Cancer Xenografts in Immunodeficient Mice

MDA-MB-231-LUC cells grown to approximately 60-80% confluency were washed once with PBS and incubated with Trypsin-EDTA at 37° C for 5 min. Trypsinization was halted by the addition of 2 mL DMEM containing 10% FBS. A 500 µL sample was stained with trypan blue (1:1) and counted using a haemocytometer. The remaining cells were collected in clean centrifuge tubes and pelleted by centrifugation at 1000 *x g* for 5 min at room temperature. Following centrifugation, the cleared supernatant was removed and cell pellets were washed twice in PBS with each wash followed by centrifugation at 1000 *x g* for 5 min. SCID C.B.-17 mice were injected with

4 x 10^6 cells in 50 μL PBS per mouse into the mammary fat pad. Tumour growth was monitored daily and treatment commenced once tumours were palpable (5 mm x 5 mm), 1 week after implantation.

2.8.2 Treatment regimens

2.8.2.1 Animal Study 1 – Salicylate Co-Administration with Doxorubicin or Etoposide

SCID mice were treated via intraperitoneal (IP) injection with vehicle control (PBS), or salicylate (100 mg/kg/day) for four consecutive days following tumour establishment. On day 4, either vehicle control (PBS), doxorubicin (8 mg/kg/week), or etoposide (12 mg/kg/week) was also administered IP. All drugs and controls were administered in 50 μL volumes. The treatment schedule was repeated weekly for five consecutive weeks.

2.8.2.2 Animal Study 2 – Salicylate Co-Administration with Etoposide (Dose Modification)

SCID mice were treated IP with vehicle control (PBS), or salicylate (100 mg/kg/day) for four consecutive days following tumour establishment. On day 4, either vehicle control (PBS), or etoposide (12 mg/kg, 18 mg/kg, or 24 mg/kg) was administered IP. All drugs and controls were administered in 50 μL volumes. The treatment schedule was repeated weekly for seven consecutive weeks.

2.8.2.3 Animal Study 3 – Salicylate Co-Administration with Etoposide (Dose Modification)

SCID mice were treated IP with vehicle control (PBS), or salicylate (200 mg/kg/day) for four consecutive days following tumour establishment. On day 4, either vehicle control (PBS), or etoposide (24 mg/kg/week, 36 mg/kg/week, or 48 mg/kg/week) was administered IP. All drugs and controls were administered in 50 µL volumes. The treatment schedule was repeated on a weekly basis for two consecutive weeks.

Etoposide was observed precipitating out of solution when suspended in PBS. After two rounds of treatment, the protocol was modified to a lower etoposide dose range (18, 24 or 36 mg/kg/week) and using corn oil (Sigma-Aldrich) as the solvent. Corn oil and etoposide in corn oil were administered in 150 µL volumes, while PBS and salicylate in PBS were administered in 50 µL volumes. The treatment schedule was repeated on a weekly basis for six consecutive weeks.

2.8.2.4 Animal Study 4 – Salicylate Co-Administration with Etoposide (Dose Modification)

SCID mice were treated IP with vehicle control (PBS), or salicylate (200 mg/kg/day) for four consecutive days following tumour establishment. On day 4, either vehicle control (corn oil), or etoposide (18 mg/kg/week, 24 mg/kg/week, or 36 mg/kg/week) was administered IP. Corn oil, and etoposide in corn oil were administered in 150 µL volumes, while PBS and salicylate in PBS were administered in 50 µL volumes. The treatment schedule was repeated weekly for seven consecutive weeks.

2.8.3 Tumour Growth Assessment with In Vivo Bioluminescence Imaging

In vivo bioluminescence imaging was carried out with a Xenogen IVIS-200 imaging platform (PerkinElmer Inc., Woodbridge, ON). A sterile stock solution of 15 mg/mL D-luciferin (Gold Biotechnology Inc., St. Louis, MO) in PBS was prepared and stored at -20°C. D-luciferin (150 mg/kg) was administered IP 10 min prior to imaging to allow for the maximum luciferase signal to develop. Mice were anesthetized with Forane (isoflurane; Baxter Corporation, Mississauga, ON) and imaged. The bioluminescence image emitted from tumours was recorded and data were analyzed as the total photon flux emission (photons/second) in the region of interest using Living Image software (PerkinElmer Inc.). Mice were imaged upon tumour establishment, and 1-week post-treatment commencement then on a weekly basis (animal studies 1 and 2) or once every four weeks post-treatment (animal studies 3 and 4).

2.8.4 Tumour Growth Assessment with External Calipers

An external caliper was used to measure the greatest longitudinal diameter (length) and the greatest transverse diameter (width) of each tumour. Tumour volume was calculated by the modified ellipsoidal formula $V = L \times W^2 / 2$, where V is the volume, L is the length, and W is the width of the tumour.

2.8.5 Tumour Collection

Necropsies were conducted to examine possible sites of metastasis and to collect tumour samples. Tumour samples were collected, flash frozen in liquid nitrogen, and stored at -80°C for future analysis.

2.8.6 Blood Collection

Blood samples were collected, via the saphenous vein, prior to tumour cell implantation, upon tumour establishment, 1-week post-treatment initiation, 3-weeks post-treatment initiation, and, via cardiac puncture, upon sacrifice. Whole blood samples were allowed to coagulate and then centrifuged at 1200 *x g* for 10 min at 4°C. Sera were then collected into clean microfuge tubes and stored at -80° C for future biochemical assays and/or cytokine analysis.

2.8.7 Euthanasia of Animals

Animals were euthanized via carbon dioxide gas in accordance with the animal care protocol. Immediate ethical euthanasia was conducted if any one of the following conditions was met: tumours reached a size greater than 20 mm in diameter or if tumours impeded normal behaviour, tumour necrosis over 50% of tumour surface area, loss of more than 20% body weight, or severe toxicity (*i.e.* dull fur combined with severe diarrhoea, lethargy and/or swollen/discoloured abdomen). In cases where animals did not meet any single ethical criterion for euthanasia but demonstrated a combination of the criteria to a lesser degree, they were monitored and assessed daily on a case-by-case

basis. Otherwise, all surviving animals were euthanized upon the completion of the experiment. A post-mortem laparotomy was performed to collect tumour and tissue samples. Blood samples at sacrifice were collected via cardiac puncture using a 23-gauge needle and a 3 mL syringe.

2.9 Statistical Analysis

GraphPad Prism (version 6; GraphPad Software, Inc.) was used for statistical analyses. Multiple unpaired Student's t-tests were used to assess statistical significance observed in the cytotoxicity assays and *in vivo* tumour growth. Survival data were used to generate Kaplan-Meier curves. Mantel-Cox log-rank tests were used to compare survival rate curves. All reported *p* values were two-sided and were considered to be statistically significant at 0.01.

Chapter Three: Salicylate Attenuates the Cytotoxicity of TOP2 Poisons in Human and Murine Breast Cancer Cell Lines

3.1 Identification of a Cell Line Panel Representative of the Subclasses of Human Breast Cancer

Foundational work identifying salicylate as a novel catalytic inhibitor of TOP2A and characterizing its effects on doxorubicin and etoposide cytotoxicity in cultured cells did so using the MCF-7 cell line (Bau & Kurz, 2011, 2014; Bau *et al.*, 2014). MCF-7 cells are a commonly used experimental breast cancer model (Lee *et al.*, 2015); however, they are not broadly representative of all forms of breast cancer.

Clinically, breast cancer is a heterogeneous disease. Identification of distinct molecular subtypes, characterized by the presence or absence of specific biological markers in the primary tumour, impacts prognosis and treatment recommendations (Stingl & Caldas, 2007; Polyak, 2011; Kessler *et al.*, 2014). The absence or presence of ER, PR, and/or HER2 in the primary tumour plays a significant role in classification. Based on these and other predictive biomarkers, five intrinsic breast cancer subtypes have been identified: luminal A, luminal B, HER2+, basal-like, and claudin-low (Table 1.1) (Kao *et al.*, 2009; Prat *et al.*, 2010, 2013). Given that the previous work identifying salicylate as a catalytic inhibitor of TOP2A was conducted using a single cell line, MCF-7 (Bau & Kurz, 2011), representative of the luminal A, ER(+) subtype of breast cancer, the next logical step was to determine if salicylate had the same effect in cell lines representative of all subtypes of breast cancer. This approach required the identification of a panel of breast cancer cell lines that represents the heterogeneity observed in the

clinic. Six cell lines were chosen to represent the five intrinsic subtypes of breast cancer: MCF-7 (luminal A), ZR-75-30 (luminal B), SK-BR-3 (HER2+), MDA-MB-468 (basal-like), and MDA-MB-231 (claudin-low) (Table 3.1). The murine EMT-6 (luminal A-like) breast cancer cell line was included in the panel for evaluation for future use in an immunocompetent syngeneic murine model of breast cancer.

3.2 Population Doubling Time of Human and Murine Breast Cancer Cell Lines

Changes in cell numbers were measured by trypan blue exclusion assay. MCF-7, MDA-MB-231, MDA-MB-468, SK-BR-3, ZR-75-30, or EMT-6 cells were seeded in 60 mm cell culture plates at 1.0×10^5 cells per plate and grown for 6 days. Every 24 h quadruplicate plates of cells were independently trypsinized and manually counted by trypan blue exclusion using a haemocytometer. Data were used to generate growth curves for each cell line and to calculate PDT (Figure 3.1). The PDTs were 39 h, 37 h, 47 h, 36 h, 111 h, and 13 h for MCF-7, MDA-MB-231, MDA-MB-468, SK-BR-3, ZR-75-30, and EMT-6 respectively.

3.3 Cytotoxicity Assays

Cytotoxicity assays, including the AlamarBlue® viability assay, are an efficient means to directly measure the phenotypic consequences of salicylate pretreatment on the efficacy of TOP2 poisons (Bau & Kurz, 2011; Rampersad, 2012). The AlamarBlue® viability assay involves the metabolic reduction of resazurin (blue and non-fluorescent) to resorufin (pink and highly fluorescent). The two most influential variables that affect the reduction of resazurin to resorufin are the length of incubation with the AlamarBlue®

Table 3.1 Subtype classification of human breast cancer cell lines chosen for study

Cell Line	Subtype	ER	PR	HER2	TP53
MCF-7	Luminal A	+	+	-	*WT*
ZR-75-30	Luminal B	+	-	+	*WT*
MDA-MB-468	Basal-like	-	-	-	*M*
MDA-MB-231	Claudin-low	-	-	-	*M*
SK-BR-3	HER2+	-	-	+	*M*

Estrogen receptor (ER), human epidermal growth factor receptor 2 (HER2), progesterone receptor (PR), and tumour protein p53 (TP53); ER/PR positivity, HER2 overexpression, and TP53 mutational status (obtained from the Sanger web site; *M*, mutant protein; *WT*, wild-type protein) are indicated.

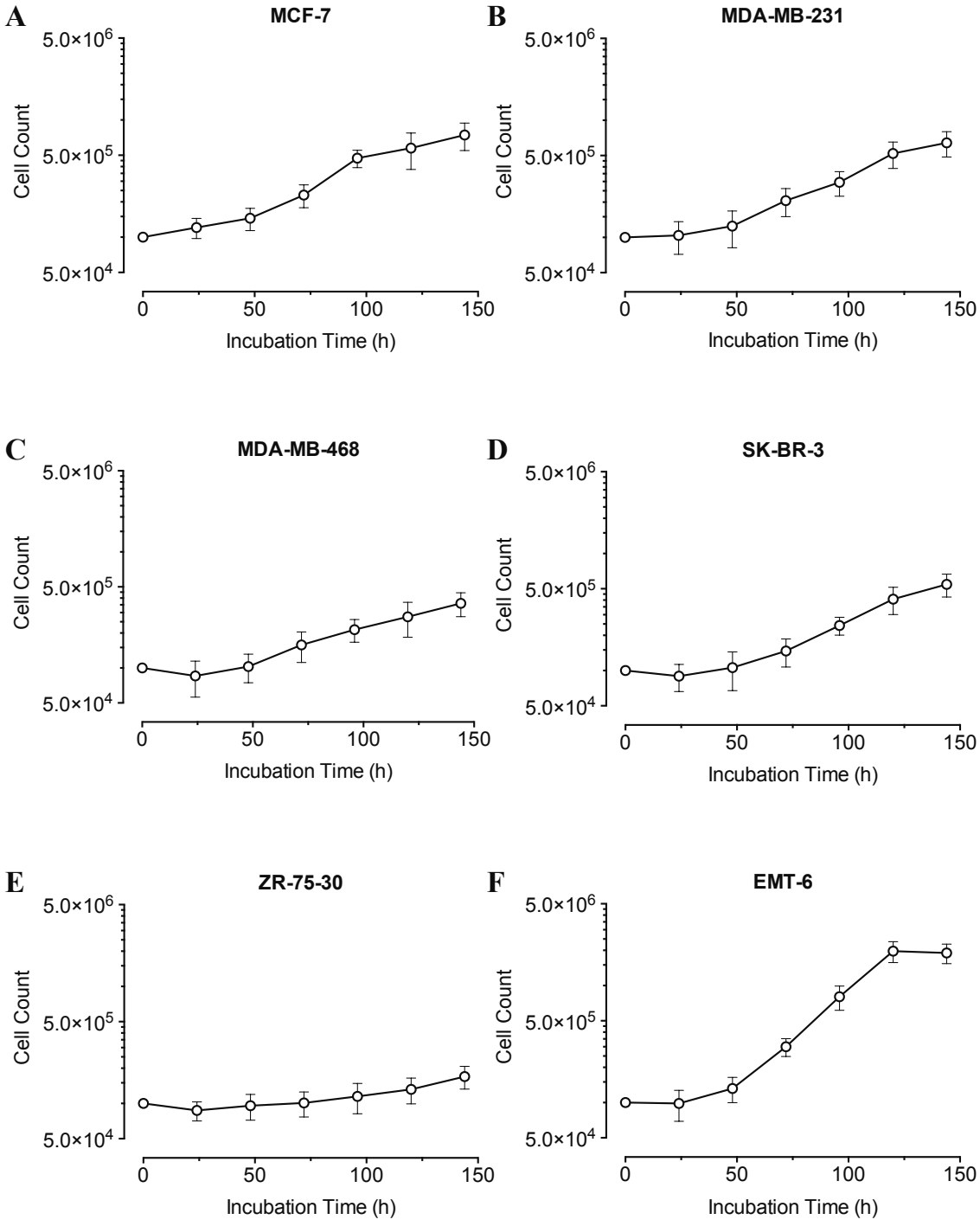
A
MCF-7
B
MDA-MB-231
C
MDA-MB-468
D
SK-BR-3
E
ZR-75-30
F
EMT-6
Cell Count
5.0×10^6
5.0×10^5
5.0×10^4
0
50
100
150
Incubation Time (h)

Figure 3.1 Growth curves of cell lines chosen for study.

A) MCF-7, B) MDA-MB-468, C) MDA-MB-231, D) SK-BR-3, E) ZR-75-30, and F) EMT-6 cells were seeded at 1 x 10^5 cells/cm^2 in 60 mm plates and grown at 37° C in a humidified atmosphere containing 5% CO_2. Changes in cell numbers were monitored by trypan blue exclusion and haemocytometer counting over 6 days. Data shown represent the means and standard deviations of the cell densities at a given time point (n=2; 4 internal replicates per experiment).

substrate and the number of cells plated (O'Brien *et al.*, 2000). AlamarBlue® is most accurate at measuring cell proliferation during the log phase of growth. Cells seeded at too low a density may not have entered the log growth phase and the slower growth rate could result in insufficient resazurin reduction. In contrast, if cells are seeded at too high a density and become over-confluent, proliferation may decrease, resulting in a lower rate of resazurin reduction than anticipated. Thus, optimization of AlamarBlue® incubation time and cell seeding density are essential to provide an accurate measure of viability for a given cell population.

3.3.1 Optimization of Seeding Density

To determine the optimal incubation time and seeding density for the cytotoxicity assays, cells were seeded at increasing densities (5×10^2 to 1×10^4 cells/well) in 96-well plates and allowed to grow for 120 h. Cells were then treated with AlamarBlue® and fluorescence was measured every 30 min for 6 h. MCF-7, MDA-MB-231, MDA-MB-468, and SK-BR-3 cells seeded at greater than $5x10^3$ cells/well, and EMT-6 cells seeded at or greater than $5x10^2$ cells/well resulted in high fluorescence intensity within 1 h of incubation (Figure 3.2). MCF-7, MDA-MB-231, MDA-MB-468, and SK-BR-3 cells seeded at or below $2x10^3$ cells/well required over 4 h to achieve a fluorescence intensity within the linear range. However, the growth rate of ZR-75-30 cells was too slow to reliably measure in this experimental set-up. Consequently, no discernible difference in fluorescence intensity from background was observed in ZR-75-30 cells over 12 h of incubation with AlamarBlue®. Further analysis of ZR-75-30 cells was halted because of the protocol modifications needed to compensate for the slow growth of these cells.

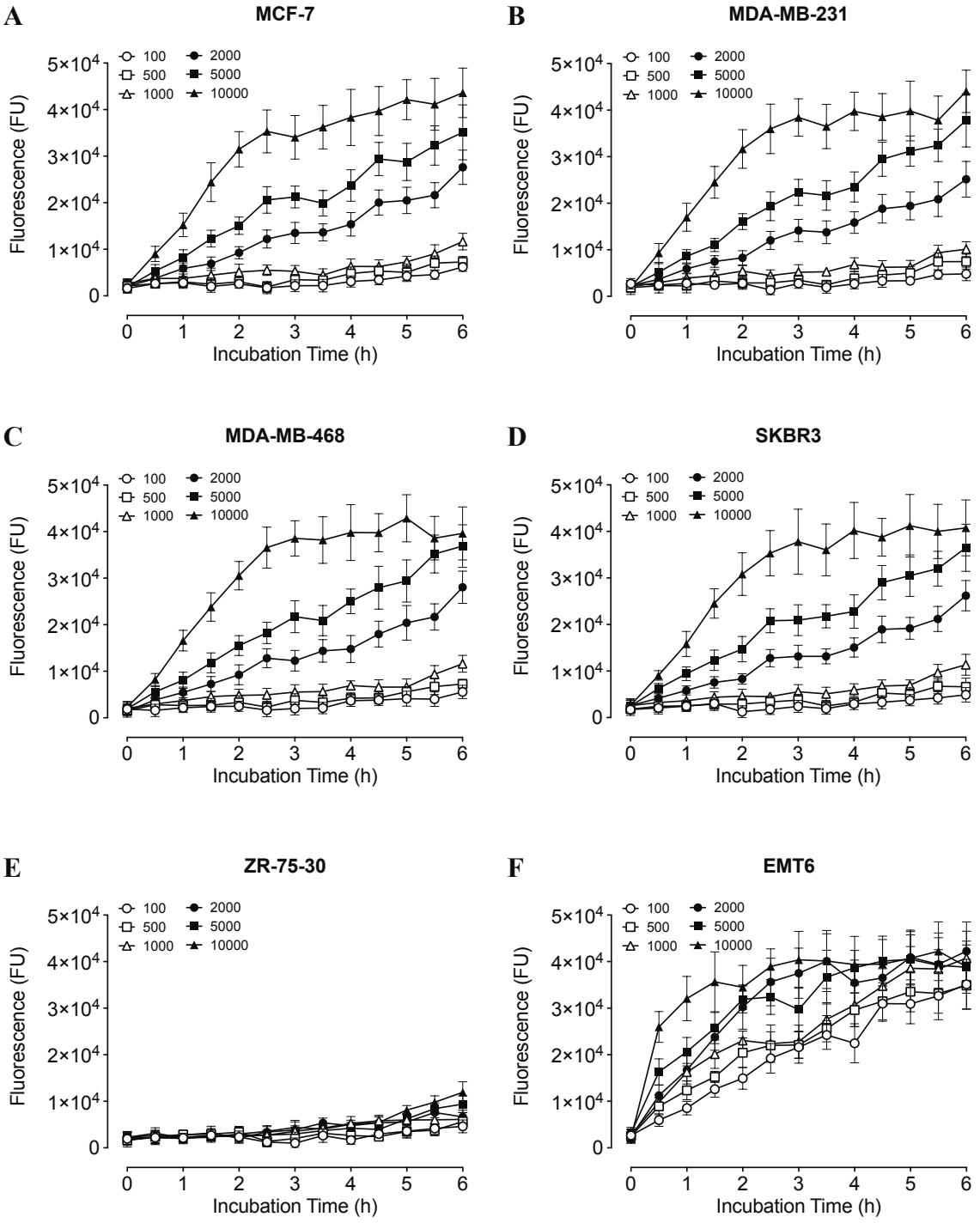
A
MCF-7
B
MDA-MB-231
C
MDA-MB-468
D
SKBR3
E
ZR-75-30
F
EMT6
100
500
1000
2000
5000
10000
Fluorescence (FU)
Incubation Time (h)
0
1×10^4
2×10^4
3×10^4
4×10^4
5×10^4
0
1
2
3
4
5
6

Figure 3.2 Optimization of seeding density for AlamarBlue assays.

96-well plates were seeded with A) MCF-7, B) MDA-MB-468, C) MDA-MB-231, D) SK-BR-3, E) ZR-75-30, or F) EMT-6 cells at increasing densities (5×10^2 to 1×10^4 cells/well). Cells were grown for 120 h (96 h for EMT-6) prior to the assessment of cell viability through the addition of AlamarBlue® and subsequent fluorescence measurement. Data shown represent the means and standard deviations of fluorescence intensity at a given incubation time (n=3; 8 internal replicates).

Given that EMT-6 cells were to be used in a later animal study, the cell line was screened a second time with modifications to compensate for rapid proliferation. EMT-6 cells were seeded as before, but grown for only 96 h to avoid reaching confluence and altering the cell growth rate. EMT-6 cells seeded at greater than $2x10^3$ cells/well produced high fluorescence intensity within 1-2 h of incubation. EMT-6 cells seeded at fewer than $5x10^2$ cells/well required over 6 h to achieve a fluorescence intensity within the linear range. Thus, the optimal seeding density for the 120 h proliferation assay in MCF-7, MDA-MB-231, MDA-MB-468, and SK-BR-3 cells was identified as $2x10^3$ cells/well and the optimal seeding density for the 96 h proliferation assay in EMT-6 cells was identified as $5x10^2$ cells/well.

3.3.2 Optimization of Salicylate Treatment

Previously, it was shown that the cytotoxicity of TOP2 poisons was attenuated in MCF-7 cells pretreated with 10 mM salicylate for 1 h (Bau & Kurz, 2011). In addition to examining the effect of the short duration, high dose salicylate pretreatment on TOP2 poison cytotoxicity, we also sought to examine the impact of a modestly lower dose (3 mM), but longer duration (8 h) pretreatment on the cytotoxicity of TOP2 poisons. First, a non-toxic salicylate treatment had to be identified for the cell lines in the panel. To establish if a longer duration of a lower dose of salicylate exposure recapitulated the effect of a short duration, high dose salicylate, cells were treated with increasing concentrations of salicylate for either 3 or 10 h and allowed to grow for an additional 96 h (72 h in the case of EMT-6) prior to cytotoxicity analysis. Salicylate concentrations up to 30 mM for 3 h or 10 h did not result in significant cytotoxicity in MCF-7, MDA-MB-

468, MDA-MB-231, SK-BR-3, or EMT-6 cells (Figures 3.3 and 3.4). Treatment with either 10 mM or 3 mM salicylate for a total exposure time of 3 h or 10 h, respectively, were chosen for further analysis on TOP2 poison cytotoxicity.

3.3.3 Salicylate Attenuates the Cytotoxicity of Doxorubicin and Etoposide in Human and Murine Breast Cancer Cell Lines

To determine if salicylate attenuates TOP2 poison cytotoxicity in the chosen panel of human breast cancer cell lines, MCF-7, MDA-MB-468, MDA-MB-231, SK-BR-3, or EMT-6 cells seeded in 96-well plates were pretreated for 1 h with 10 mM salicylate prior to the addition of increasing concentrations of doxorubicin or etoposide (in the range of what is observed in the plasma of patients undergoing cancer treatment) and incubated for an additional 2 h (Figure 3.5) (Hande *et al.*, 1984; Slevin, 1991; Twelves *et al.*, 1991; Barpe *et al.*, 2010).

Salicylate induced a modest yet statistically significant attenuation of doxorubicin cytotoxicity in all of the cell lines (Figure 3.6A-E). Maximum attenuation was observed at 0.03 μM doxorubicin in EMT-6 cells (17.0%), at 0.1 μM doxorubicin in MDA-MB-231 (18.3%), MDA-MB-468 (16.4%), and SK-BR-3 (10.4%) cells, and at 0.3 μM doxorubicin in MCF-7 cells (16.2%). Cytotoxicity data were used to calculate IC_{50} of doxorubicin alone ($IC50_{Dox}$) and in combination with salicylate ($IC50_{Dox+Sal}$) (Figure 3.6F). The magnitude of salicylate-mediated cytoprotection was dose-dependent on doxorubicin, with greater attenuation observed as the $IC50_{Dox}$ was approached. A significant shift was observed between $IC50_{Dox}$ and $IC50_{Dox+Sal}$ across all of the cell lines, with the exception of SK-BR-3, where no significant difference was measured.

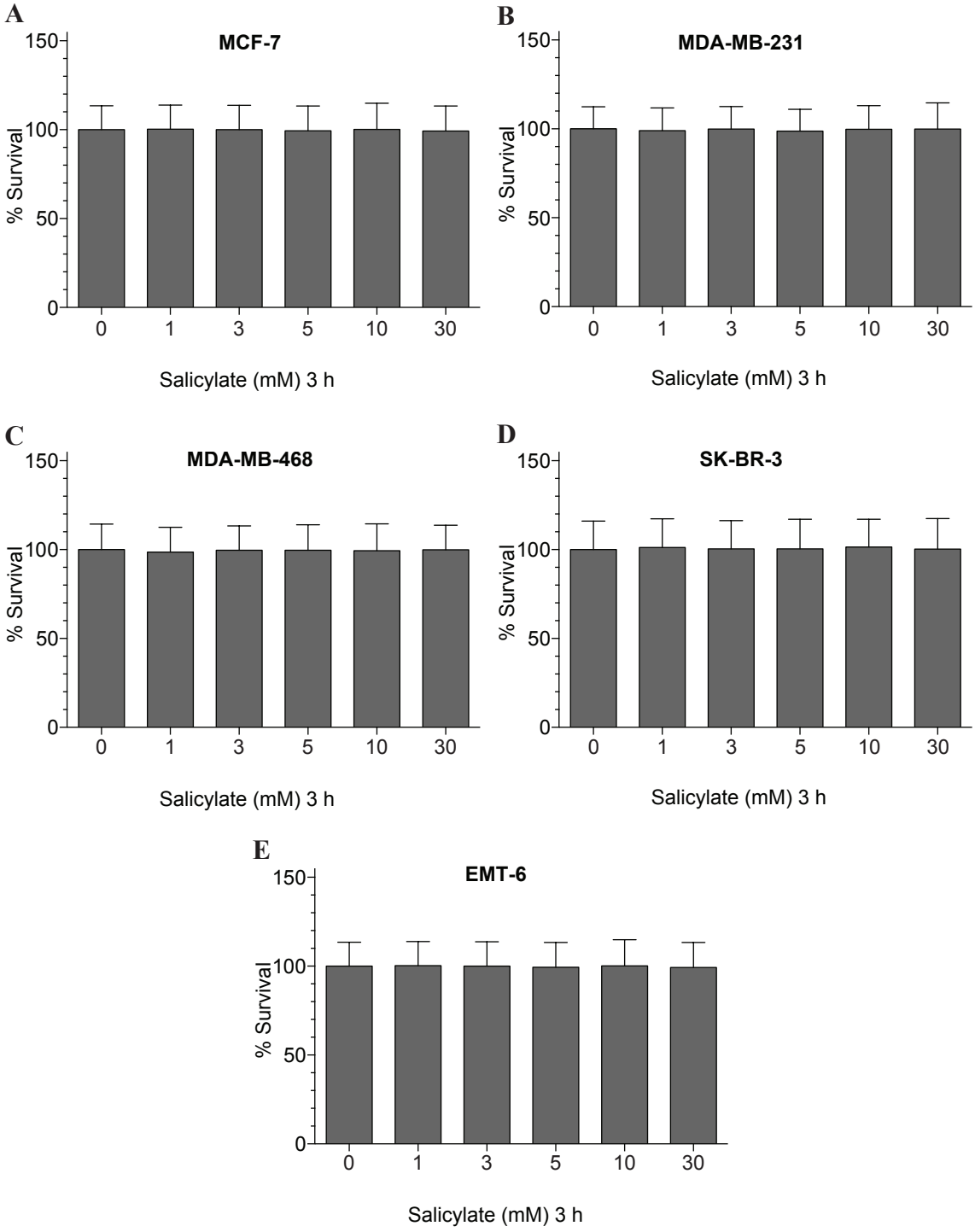
A
MCF-7
% Survival
150
100
50
0
0 1 3 5 10 30
Salicylate (mM) 3 h
B
MDA-MB-231
% Survival
150
100
50
0
0 1 3 5 10 30
Salicylate (mM) 3 h
C
MDA-MB-468
% Survival
150
100
50
0
0 1 3 5 10 30
Salicylate (mM) 3 h
D
SK-BR-3
% Survival
150
100
50
0
0 1 3 5 10 30
Salicylate (mM) 3 h
E
EMT-6
% Survival
150
100
50
0
0 1 3 5 10 30
Salicylate (mM) 3 h

Figure 3.3 Short-term exposure to salicylate is not cytotoxic to human or murine breast cancer cells in culture.

A) MCF-7, B) MDA-MB-468, C) MDA-MB-231, D) SK-BR-3, or E) EMT-6 cells were seeded in 96-well plates 16 h prior to drug treatment. In replicates of eight, cells were treated with increasing concentrations of salicylate for 3 h. Following treatment, the salicylate-containing medium was replaced with fresh medium. Cell were incubated for an additional 96 h (or 72 h for EMT-6) before an AlamarBlue® cell viability assay was performed. Data shown represent the means and standard deviations of the percent cell survival normalized to cells not treated with salicylate. Data were pooled from three independent experiments (each with eight internal replicates) and analyzed by unpaired Student's t-tests (df=46; $p < 0.01$). No statistically significant differences were observed.

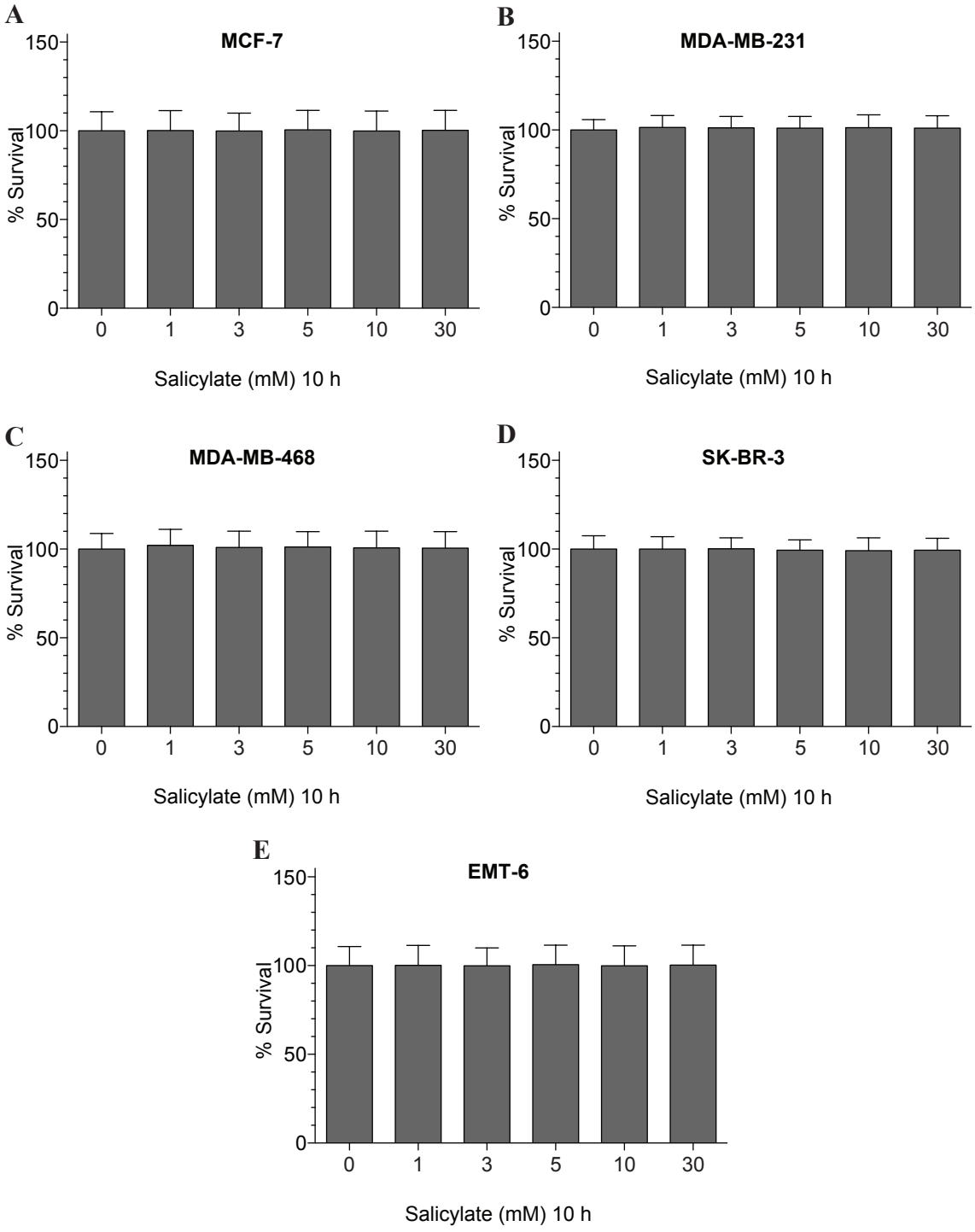
A
MCF-7
% Survival
150
100
50
0
0 1 3 5 10 30
Salicylate (mM) 10 h
B
MDA-MB-231
% Survival
150
100
50
0
0 1 3 5 10 30
Salicylate (mM) 10 h
C
MDA-MB-468
% Survival
150
100
50
0
0 1 3 5 10 30
Salicylate (mM) 10 h
D
SK-BR-3
% Survival
150
100
50
0
0 1 3 5 10 30
Salicylate (mM) 10 h
E
EMT-6
% Survival
150
100
50
0
0 1 3 5 10 30
Salicylate (mM) 10 h

Figure 3.4 Low-dose exposure to salicylate is not cytotoxic to human or murine breast cancer cells in culture.

A) MCF-7, B) MDA-MB-468, C) MDA-MB-231, D) SK-BR-3, or E) EMT-6 cells were seeded in 96-well plates 16 h prior to drug treatment. In replicates of eight, cells were treated with increasing concentrations of salicylate for 10 h. Following treatment, the salicylate-containing medium was replaced with fresh medium. Cells were incubated for an additional 96 h (or 72 h for EMT-6) after which an AlamarBlue® cell viability assay was performed. Data shown represent the means and standard deviations of the percent cell survival normalized to cells not treated with salicylate. Data were pooled from three independent experiments (each with eight internal replicates) and analyzed by unpaired Student's t-tests (df=46; $p < 0.01$). No statistically significant differences were observed.

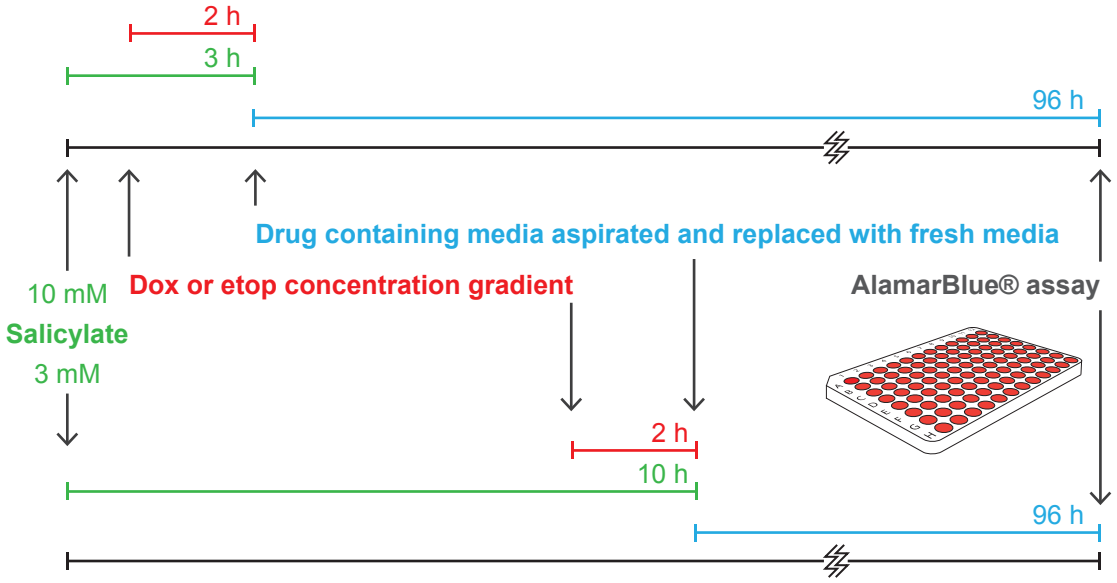

Figure 3.5 Schematic of timelines for cytotoxicity assays used to assess the effect of salicylate treatment on the cytotoxicity of TOP2 poisons *in vitro*.

Cells were pretreated with salicylate for either 1 h or 8 h followed by doxorubicin or etoposide treatment for two additional hours. Drug containing media was then aspirated and replaced with fresh media and cells were left to recover for 96 h before cell survival was analyzed with AlamarBlue®.

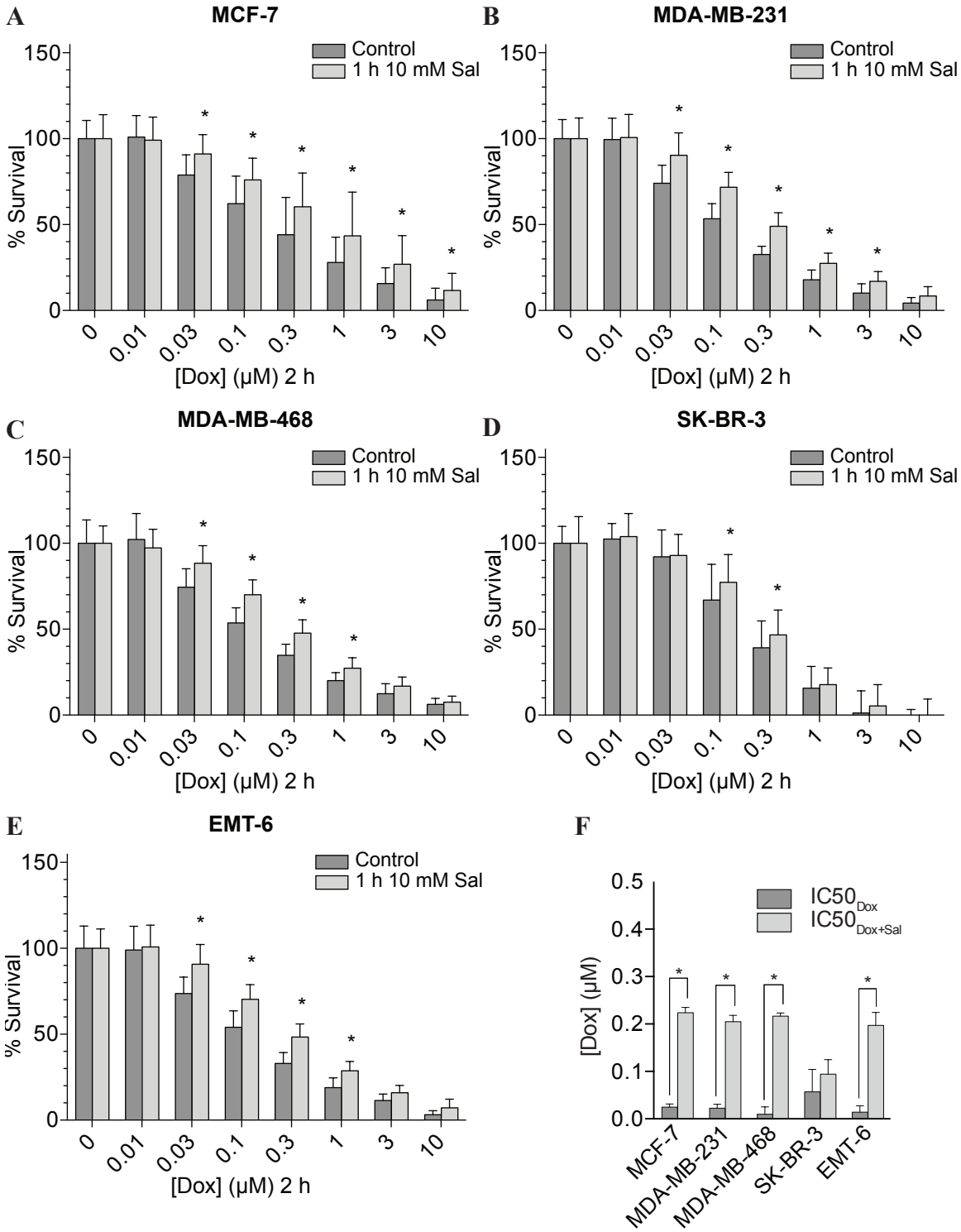
A
MCF-7
B
MDA-MB-231
C
MDA-MB-468
D
SK-BR-3
E
EMT-6
F
Control
1 h 10 mM Sal
% Survival
[Dox] (μM) 2 h
0
0.01
0.03
0.1
0.3
1
3
10
150
100
50
0
IC50Dox
IC50Dox+Sal
[Dox] (μM)
0.5
0.4
0.3
0.2
0.1
0.0
MCF-7
MDA-MB-231
MDA-MB-468
SK-BR-3
EMT-6

Figure 3.6 Brief pretreatment with salicylate attenuates doxorubicin-induced cytotoxicity in human and murine breast cancer cell lines.

A) MCF-7, B) MDA-MB-468, C) MDA-MB-231, D) SK-BR-3, or E) EMT-6 cells were seeded in 96-well plates 16 h prior to drug treatment. In replicates of eight, cells were treated (light grey bars) or not (dark grey bars) with 10 mM salicylate for 1 h prior to the addition of increasing concentrations of doxorubicin followed by a further 2 h incubation at 37°C. Subsequently, the drug-containing medium was replaced with fresh medium. Cells were incubated for an additional 96 h (or 72 h for EMT-6) after which an AlamarBlue® cell viability assay was performed. Data shown represent the means and standard deviations of the percent cell survival normalized to cells not receiving doxorubicin treatment. Data were pooled from three independent experiments and analyzed by unpaired Student's t-tests (df=46). Statistical significance between salicylate-treated and salicylate-untreated samples at a given doxorubicin concentration is denoted by an asterisk (*; $p < 0.01$). (F) Cytotoxicity data were used to calculate the IC_{50} of doxorubicin alone ($IC50_{Dox}$) and in combination with salicylate ($IC50_{Dox+Sal}$). Data shown represent the mean and standard deviation (n=3). Data were analyzed by unpaired Student's t-tests (df=4). Statistical significance between $IC50_{Dox}$ and $IC50_{Dox+Sal}$ in each cell line is denoted by an asterisk (*; $p < 0.01$).

Salicylate mediated-cytoprotection was also observed in cells treated with etoposide. (Figure 3.7). Like the observations in doxorubicin-treated cells, the degree of attenuation was dependent on etoposide dose. Salicylate-mediated cytoprotection peaked at 10 μM etoposide in MCF-7 (26.0%), MDA-MB-231 (24.2%), MDA-MB-468 (22.9%), and EMT-6 (29.5%) cells, and at 30 μM etoposide in SK-BR-3 cells (10.4%). IC_{50} of etoposide alone ($IC50_{Etop}$) and in combination with salicylate ($IC50_{Etop+Sal}$) were calculated with cytotoxicity data (Figure 3.7F). Again, apart from SK-BR-3, a statistically significant shift in $IC50_{Etop}$ was observed when cells were pretreated with salicylate.

To see if a lower dose of salicylate had the same effect, MCF-7, MDA-MB-468, MDA-MB-231, SK-BR-3, and EMT-6 cells were pretreated for 8 h with 3 mM salicylate prior to the addition of increasing concentrations of doxorubicin or etoposide for 2 h. Like the high dose salicylate pretreatment, 3 mM salicylate induced a cytoprotective effect in cells treated with doxorubicin (Figure 3.8A-E). Furthermore, the degree of salicylate attenuation of doxorubicin cytotoxicity was dependent on the dose of doxorubicin administered. Higher attenuation was observed at concentrations approaching the $IC50_{Dox}$. Maximum attenuation was observed at 0.1 μM doxorubicin in MDA-MB-231 (11.0%), MDA-MB-468 (18.9%), and EMT-6 (16.1%) cells, and at 0.3 μM doxorubicin in MCF-7 (17.2%) and SK-BR-3 (9.2%) cells. A statistically significant shift in $IC50_{Dox}$ was observed in MDA-MB-468 and EMT-6 (Figure 3.8F).

Low-dose salicylate pretreatment attenuated cytotoxicity in cells treated with etoposide (Figure 3.9). Attenuation increased as concentrations approached the $IC50_{Etop}$. Maximum salicylate attenuation of etoposide cytotoxicity was observed at 10 μM

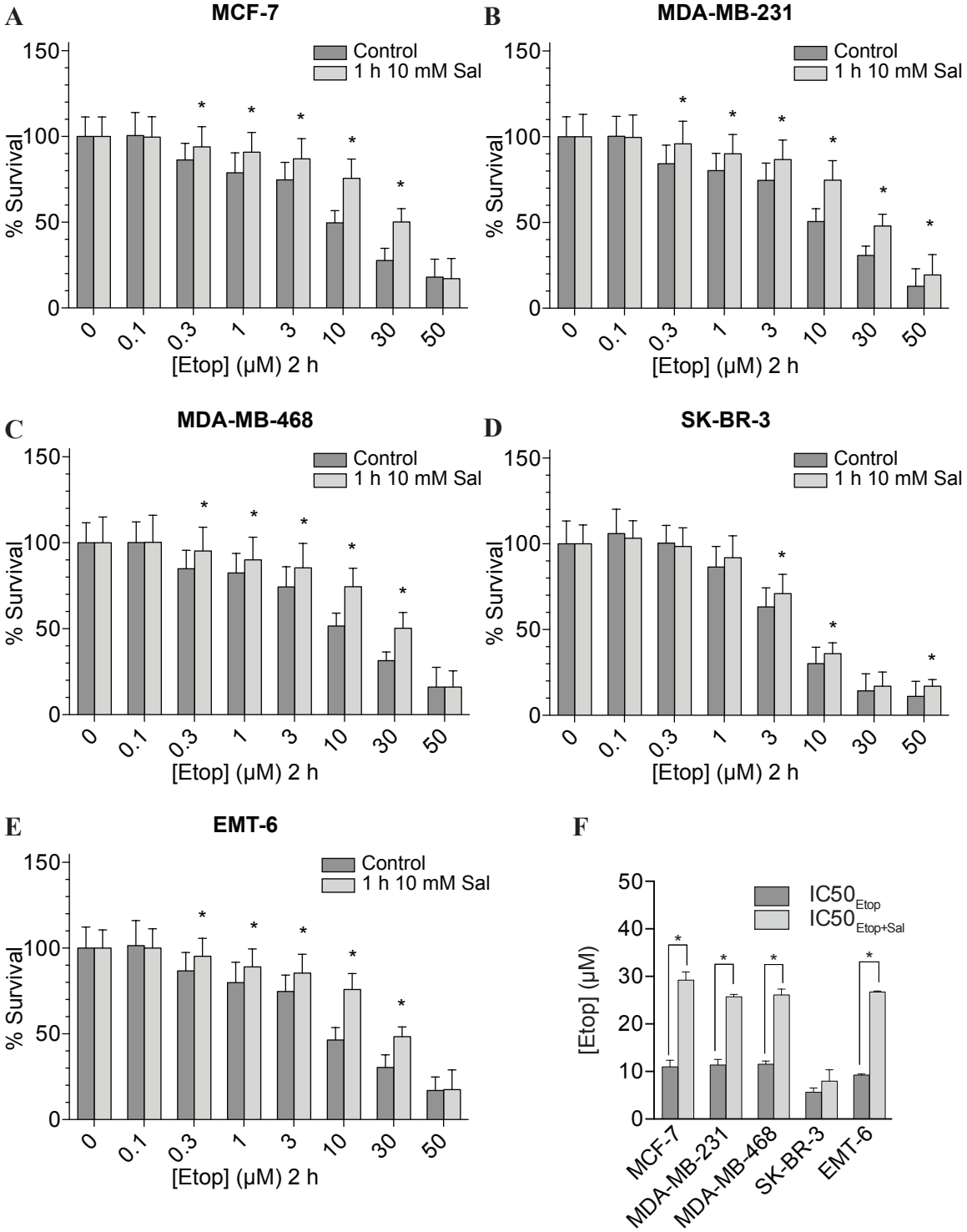
A
MCF-7
B
MDA-MB-231
C
MDA-MB-468
D
SK-BR-3
E
EMT-6
F
Control
1 h 10 mM Sal
% Survival
[Etop] (μM) 2 h
0
0.1
0.3
1
3
10
30
50
150
100
50
0
IC50Etop
IC50Etop+Sal
[Etop] (μM)
40
30
20
10
MCF-7
MDA-MB-231
MDA-MB-468
SK-BR-3
EMT-6

Figure 3.7 Brief pretreatment with salicylate attenuates etoposide-induced cytotoxicity in human and murine breast cancer cell lines.

A) MCF-7, B) MDA-MB-468, C) MDA-MB-231, D) SK-BR-3, or E) EMT-6 cells were seeded in 96-well plates 16 h prior to drug treatment. In replicates of eight, cells were treated (light grey bars) or not (dark grey bars) with salicylate (10 mM, 1 h) prior to the addition of increasing concentrations of etoposide followed by a further 2 h incubation at 37°C. Subsequently, the drug containing medium was replaced with fresh medium. Cells were incubated for an additional 96 h (or 72 h for EMT-6) after which an AlamarBlue® cell viability assay was performed. Data shown represent the means and standard deviations of the percent cell survival normalized to cells not receiving etoposide treatment. Data were pooled from three independent experiments and analyzed by unpaired Student's t-tests (df=46). Statistically significant differences between salicylate-treated and salicylate-untreated samples at a given etoposide concentration are denoted by asterisks (*; $p < 0.01$). (F) Cytotoxicity data were used to calculate the IC_{50} of etoposide alone ($IC50_{Etop}$) and in combination with salicylate ($IC50_{Etop+Sal}$). Data shown represent the mean and standard deviation (n=3). Data were analyzed by unpaired Student's t-tests (df=4). Statistical significance between $IC50_{Etop}$ and $IC50_{Etop+Sal}$ in each cell line is denoted by an asterisk (*; $p < 0.01$).

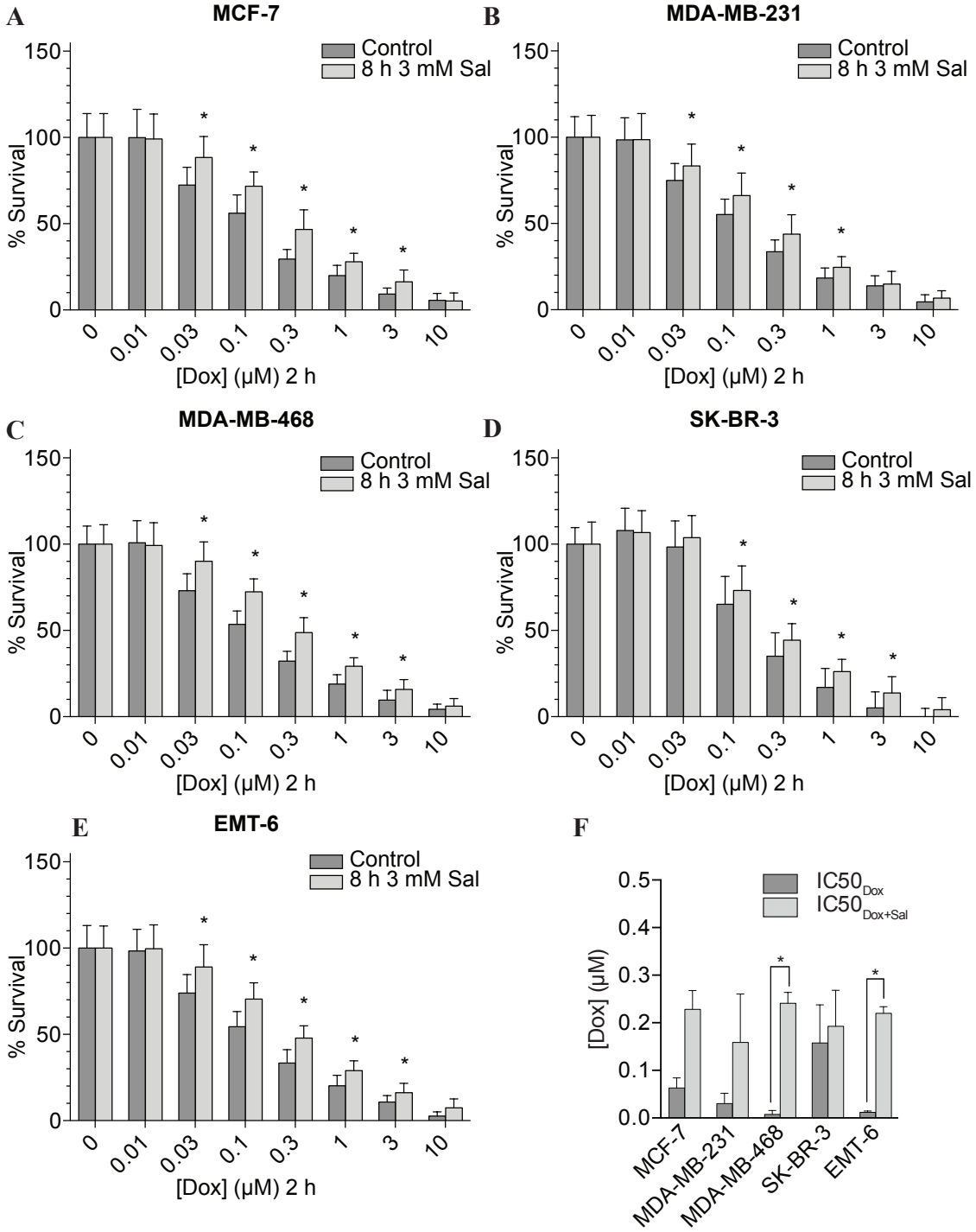
A
MCF-7
Control
8 h 3 mM Sal
% Survival
[Dox] (μM) 2 h
B
MDA-MB-231
C
MDA-MB-468
D
SK-BR-3
E
EMT-6
F
IC50Dox
IC50Dox+Sal
[Dox] (μM)
MCF-7
MDA-MB-231
MDA-MB-468
SK-BR-3
EMT-6

Figure 3.8 Extended low-dose pretreatment with salicylate attenuates doxorubicin-induced cytotoxicity in human and murine breast cancer cell lines.

A) MCF-7, B) MDA-MB-468, C) MDA-MB-231, D) SK-BR-3, or E) EMT-6 cells were seeded in 96-well plates 16 h prior to drug treatment. In replicates of eight, cells were treated (light grey bars) or not (dark grey bars) with 3 mM salicylate for 8 h prior to the addition of increasing concentrations of doxorubicin followed by a further 2 h incubation at 37°C. Following treatment, the drug-containing medium was replaced with fresh medium and cells were incubated for an additional 96 h (or 72 h for EMT-6) after which an AlamarBlue® assay was performed. Data shown represent the means and standard deviations of the percent cell survival normalized to cells not receiving doxorubicin treatment. Data were pooled from three independent experiments and analyzed by unpaired Student's t-tests (df=46). Statistically significant differences between salicylate-treated and salicylate-untreated samples at a given doxorubicin concentration are denoted by asterisks (*; $p < 0.01$). (F) Cytotoxicity data were used to calculate the IC_{50} of doxorubicin alone ($IC50_{Dox}$) and in combination with salicylate ($IC50_{Dox+Sal}$). Data shown represent the mean and standard deviation (n=3). Data were analyzed by unpaired Student's t-tests (df=4). Statistical significance between $IC50_{Dox}$ and $IC50_{Dox+Sal}$ in each cell line is denoted by an asterisk (*; $p < 0.01$).

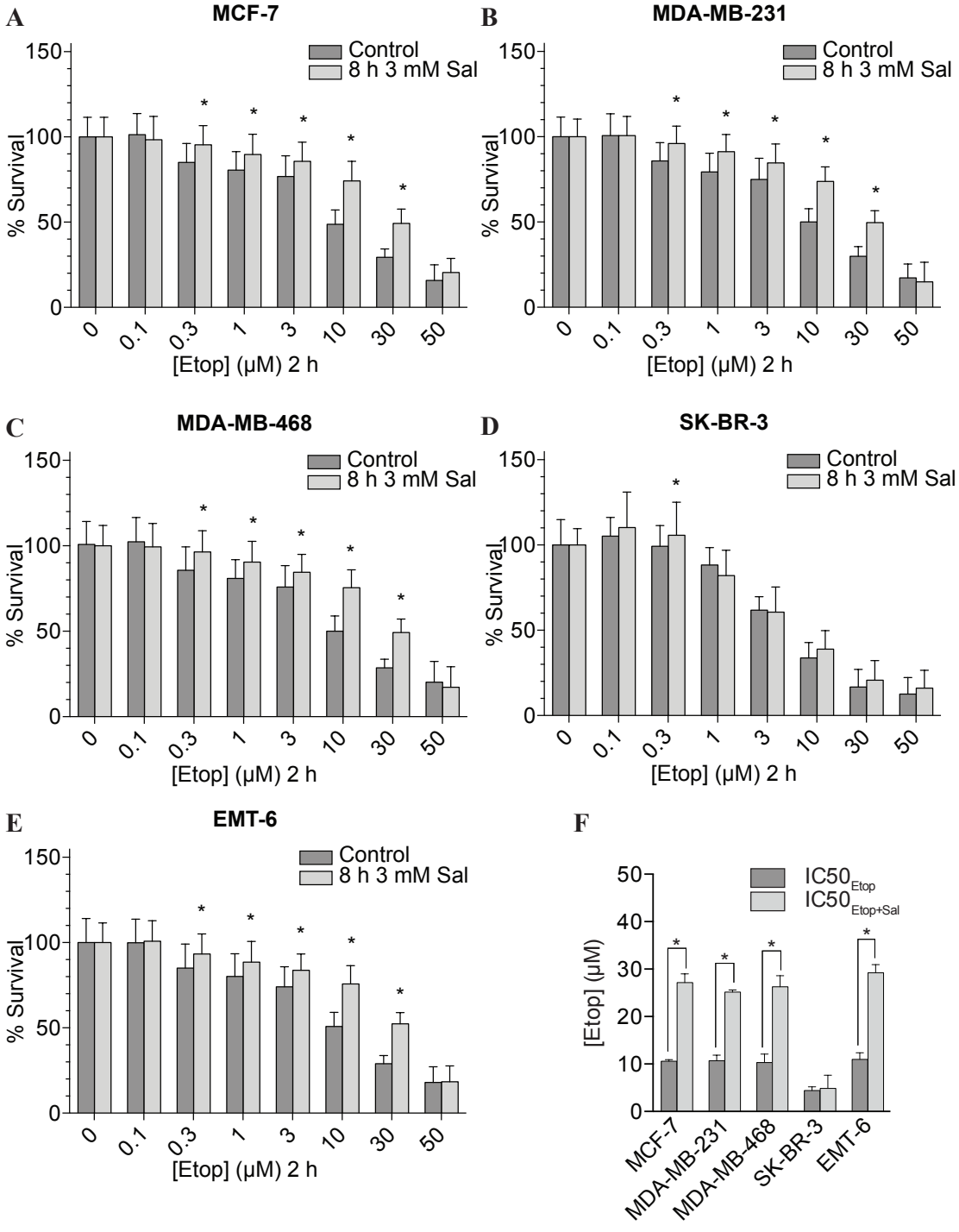
A
MCF-7
Control
8 h 3 mM Sal
% Survival
[Etop] (μM) 2 h
B
MDA-MB-231
C
MDA-MB-468
D
SK-BR-3
E
EMT-6
F
IC50Etop
IC50Etop+Sal
[Etop] (μM)
MCF-7
MDA-MB-231
MDA-MB-468
SK-BR-3
EMT-6

Figure 3.9 Extended low-dose pretreatment with salicylate attenuates etoposide-induced cytotoxicity in human and murine breast cancer cell lines.

A) MCF-7, B) MDA-MB-468, C) MDA-MB-231, D) SK-BR-3, or E) EMT-6 cells were seeded in 96-well plates 16 h prior to drug treatment. In replicates of eight, cells were treated (light grey bars) or not (dark grey bars) with 3 mM salicylate for 8 h prior to the addition of increasing concentrations of etoposide followed by a further 2 h incubation at 37°C. Following treatment, the drug containing medium was replaced with fresh medium and cells incubated for an additional 96 h (or 72 h for EMT-6) after which an AlamarBlue® assay was performed. Data shown represent the means and standard deviations of the percent cell survival normalized to cells not receiving etoposide. Data were pooled from three independent experiments and analyzed by unpaired Student's t-tests (df=46). Statistically significant differences between salicylate-treated and salicylate-untreated samples at a given etoposide concentration are denoted by asterisks (*; $p < 0.01$). (F) Cytotoxicity data were used to calculate the IC_{50} of etoposide alone ($IC50_{Etop}$) and in combination with salicylate ($IC50_{Etop+Sal}$). Data shown represent the mean and standard deviation (n=3). Data were analyzed by unpaired Student's t-tests (df=4). Statistical significance between $IC50_{Etop}$ and $IC50_{Etop+Sal}$ in each cell line is denoted by an asterisk (*; $p < 0.01$).

etoposide in MCF-7 (25.5%), MDA-MB-231 (23.8%), MDA-MB-468 (25.5%), and EMT-6 (25.0%), and at 0.3 μM etoposide in SK-BR-3 (6.6%). In addition, a statistically significant shift in $IC50_{Etop}$ was observed in cells pretreated with salicylate, with the exception of SK-BR-3 (Figure 3.9F).

3.4 TOP2A Expression in Human and Murine Breast Cancer Cell Lines.

Several studies have established TOP2A protein expression as a predictive factor of TOP2 poison sensitivity (Ferguson *et al.*, 1988; Fry *et al.*, 1991; Schneider *et al.*, 1994; Burgess *et al.*, 2008). Higher levels of TOP2A expression are associated with greater sensitivity to TOP2 poisons *in vitro*; cells expressing higher levels of TOP2 are more sensitive to treatment as more cleavage complexes can be stabilized by drug (Burgess *et al.*, 2008). Clinical data further support this hypothesis and support TOP2A expression as a possible determinant marker of response to TOP2 poison-based therapy in breast cancer patients (Knoop *et al.*, 2005; Oakman *et al.*, 2009; Brase *et al.*, 2010; Kawachi *et al.*, 2010; O'Malley *et al.*, 2011; Di Leo *et al.*, 2011; Du *et al.*, 2011).
To determine the relative expression levels of TOP2A/Top2a, cells extracts were subjected to immunoblotting and probed with an antibody cross-reactive for both human TOP2A and murine Top2A **(**Figure 3.10). Two biologically independent experiments were conducted using whole cell lysates of MCF-7, MDA-MB-231, MDA-MB-468, SK-BR-3, and EMT-6 cells. TOP2A/Top2a was detected as a single band of expected mass, approximately 170 kDa, in all five cell lines. TOP2A/Top2a were expressed across all relative cell lines. Cells were not synchronised prior to lysate collection; this may explain the slight variation in protein expression, given the fluctuation of TOP2A/Top2a

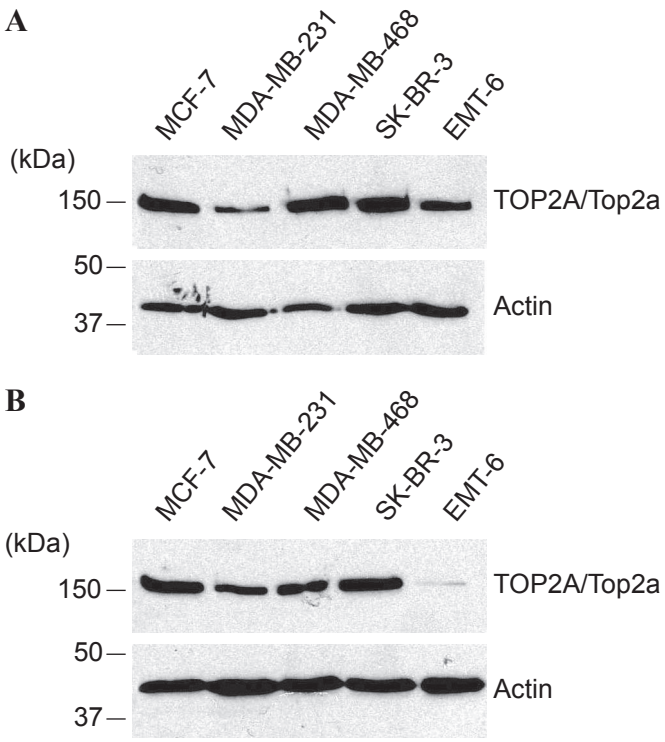

Figure 3.10 Expression of human TOP2A and murine Top2a in breast cancer cell lines.

The expression levels of TOP2A (in human MCF-7, MDA-MB-231, MDA-MB-468, and SK-BR-3 breast cancer cells), and Top2a (in murine EMT-6 breast cancer cells) were examined by immunoblotting. Whole cell NET-N lysates were collected from asynchronous cells in log–phase growth. Lysates were resolved by SDS-PAGE and immunoblotted for TOP2A/Top2a. Actin immunoblot analysis was performed as a loading control. Panels A and B represent biologically independent experiments.

expression during the cell cycle. Similarly, the apparent absence of Top2a expression in EMT-6 cells observed in Figure 3.10B was likely due to harvesting whole cell lysate from an over-confluent cell population.

3.5 Summary and Significance

At concentrations of doxorubicin and etoposide similar to those achieved in the plasma of patients undergoing treatment (Slevin, 1991; Twelves *et al.*, 1991; Barpe *et al.*, 2010), both short duration, high-dose and extended duration, low-dose pretreatment with salicylate induced a statistically significant attenuation of doxorubicin and etoposide cytotoxicity in a panel of cells representing the heterogeneity of human breast cancer. Furthermore, the cytoprotective effect of salicylate was observed in the murine EMT-6 breast cancer cell line confirming the effect is not species specific. These results lay the foundation for investigating the *in vivo* consequences of salicylate co-administration on TOP2 poison-based chemotherapy in a murine model of breast cancer.

Chapter Four: Co-administration of Salicylate Reduces the Efficacy of TOP2 Poison-Based Chemotherapy *In Vivo*.

4.1 Overview

While salicylate has been established as a catalytic inhibitor of TOP2A in cell culture and *in vitro* (Bau & Kurz, 2011; Bau *et al.*, 2014), the effect of salicylate on the efficacy of TOP2-targeting chemotherapeutics has not yet been studied *in vivo*. Given the widespread use of the TOP2 poisons for the treatment of breast cancer and the observations that salicylate inhibits the cytotoxicity of these drugs *in vitro* in multiple cell lines representing the molecular subtypes of human breast cancer, recapitulating this effect in an animal model could have significant clinical implications for women using ASA or other salicylate-based medications while undergoing TOP2 poison-based chemotherapy for the treatment of breast cancer.

Biological phenomena observed in simple experimental systems, such as cell culture, may have profound outcomes in a relatively controlled environment. However, biological relevance may disappear at the whole animal level due to the complexity and dynamic nature of such systems. Thus, translating scientific findings from basic research into relevant clinical applications is a multifaceted process. Translational medical research is the process by which *in vitro* observations, with intrinsic limitations in their application to clinical problems, are translated into a model that better represents what is observed in the clinic.

To extend the present study, an orthotopic murine xenograft model of human breast cancer was used. This chapter presents data gathered from a series of *in vivo*

experiments investigating the biological relevance of salicylate co-administration on the efficacy of TOP2 poison-based anticancer therapy.

4.2 Animal Study 1 – Salicylate Co-Administration with Doxorubicin or Etoposide

4.2.1 Experimental Approach

Salicylate concentrations can reach millimolar levels in the plasma of patients receiving ASA therapy (Grosser *et al.*, 2011). Similar plasma concentrations of salicylate are achievable in mice administered 50-400 mg/kg salicylate IP (Sturman *et al.*, 1968). Here, MDA-MB-231 cells expressing luciferase (MDA-MB-231-LUC) were injected (4 x 10^6 cells) into the mammary fat pad of 6 to 7-week-old female Fox Chase severe combined immune deficient C.B-17/Icr-*Prkdc*^{scid}/IcrIcoCrl (SCID C.B-17) mice (Figure 4.1). Tumour growth was monitored by bioluminescence imaging weekly and external caliper measurements semi-weekly. Palpable tumours were established one week post-implantation and mice were then randomly sorted into six groups, each bearing comparable tumour burdens. Group 1 (vehicle control) mice (n = 5) received IP injections of PBS (50 μL) for four consecutive days repeated weekly. Group 2 (salicylate) mice (n = 5) received IP injections of salicylate (100 mg/kg in 50 μL PBS) for four consecutive days repeated weekly. Group 3 (doxorubicin) mice (n = 5) received IP injections of PBS (50 μL) for four consecutive days plus an IP injection of doxorubicin (8 mg/kg in 50 μL PBS) on the fourth day, repeated weekly. Group 4 (etoposide) mice (n = 5) received IP injections of PBS (50 μL) for four consecutive days plus an IP injection of etoposide (12 mg/kg in 50 μL PBS) on the fourth day, repeated weekly. Group 5 (salicylate +

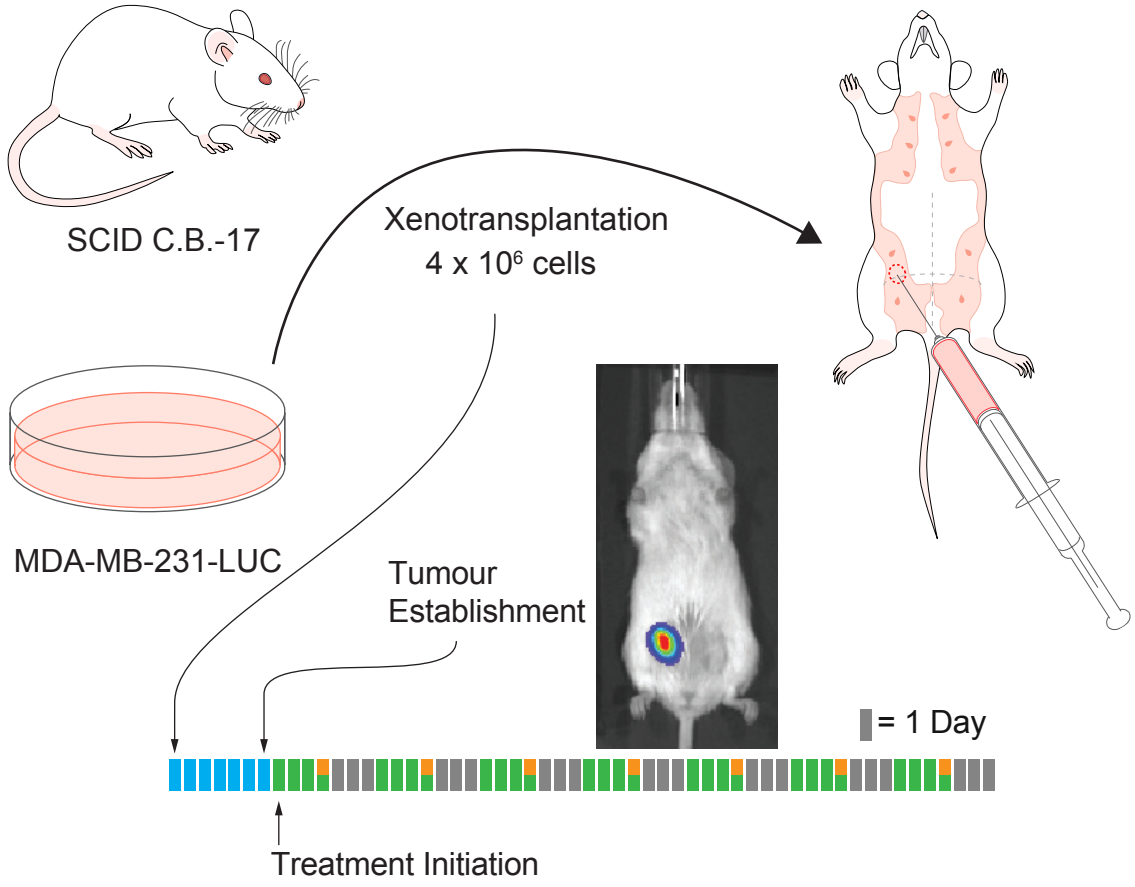
SCID C.B.-17
Xenotransplantation
4 x 10⁶ cells
MDA-MB-231-LUC
Tumour
Establishment
= 1 Day
Treatment Initiation

C

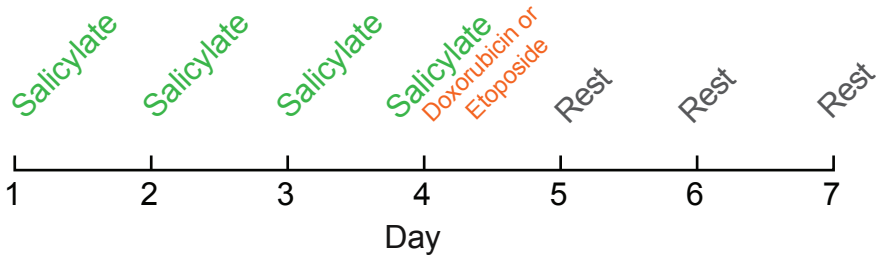
Salicylate
Salicylate
Salicylate
Salicylate
Doxorubicin or
Etoposide
Rest
Rest
Rest
1
2
3
4
5
6
7
Day

Figure 4.1 General schematic of orthotopic xenograft mouse model of breast cancer used to evaluate the impact of salicylate co-administration on TOP2 poison chemotherapeutic efficacy.

A) Human MDA-MB-231 tumour cells expressing luciferase were implanted into the mammary fat pad of 6 to 7-week-old female SCID C.B.-17 mice. B) Within 1 week of xenotransplantation, palpable tumours (5 mm x 5 mm) were established. Mice were then re-sorted into treatment groups bearing equal tumour burdens. C) Treatment groups received vehicle (PBS) control, salicylate alone, TOP2 poison alone (doxorubicin or etoposide), or salicylate co-administered with TOP2 poison. The treatment regimens were repeated weekly for a minimum of 5 weeks. Tumour growth was monitored via external caliper measurements and bioluminescence imaging.

doxorubicin) mice (n = 5) received IP injections of salicylate (100 mg/kg in 50 μL) for four consecutive days plus an IP injection of doxorubicin (8 mg/kg in 50 μL PBS) on the fourth day, repeated weekly. Group 6 (salicylate + etoposide) mice (n = 5) received IP injections of salicylate (100 mg/kg in 50 μL) for four consecutive days plus an IP injection of etoposide (12 mg/kg in 50 μL PBS) on the fourth day, repeated weekly. The doxorubicin and etoposide regimens used here were based on respective therapeutic regimens in murine cancer models reported in the literature (Wheeler *et al.*, 1982; Reichman *et al.*, 1989; Rahman *et al.*, 1990; Bellamy *et al.*, 1993, 1995; Remichkova *et al.*, 2008; Barpe *et al.*, 2010).

4.2.2 Doxorubicin Treatment at 8mg/kg is Toxic in SCID C.B-17 Mice Bearing MDA-MB-231-LUC Tumours.

Within days of the first treatment, mice treated with either doxorubicin alone or doxorubicin in combination with salicylate demonstrated signs of severe toxicity, including diarrhea, a dull coat, lethargy, and substantial weight loss. By Day 20 (9 days after the first treatment with doxorubicin), 80% (4/5) of mice treated with doxorubicin alone, and 100% (5/5) of mice co-treated with doxorubicin and salicylate had been euthanized for humane reasons as per the requirements of the animal care protocol. Although tumour measurements were taken prior to sacrifice, further interpretation of this single data point was not undertaken.

Mice treated with etoposide displayed no overt signs of toxicity, even after five weeks of treatment. Contrary to expectations based on previously published work, however, the etoposide dose used did not attenuate tumour growth (Figure 4.2)

A

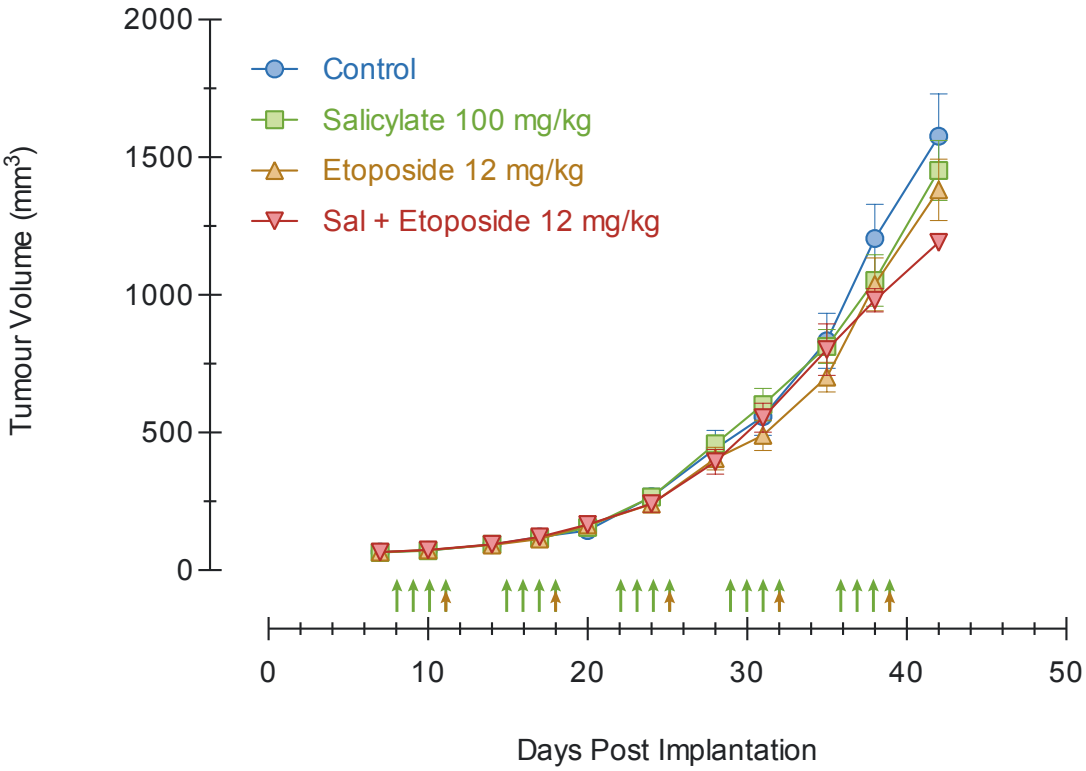
2000
1500
1000
500
0
Tumour Volume (mm3)
Control
Salicylate 100 mg/kg
Etoposide 12 mg/kg
Sal + Etoposide 12 mg/kg
0
10
20
30
40
50
Days Post Implantation

B

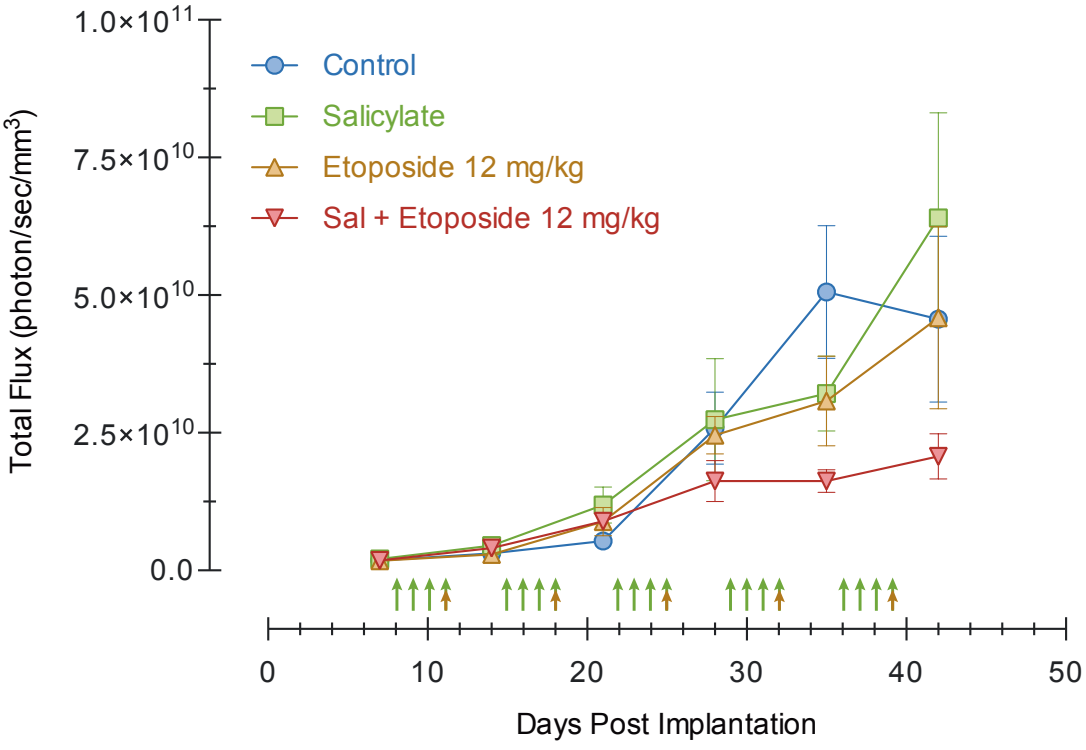
1.0×10^11
7.5×10^10
5.0×10^10
2.5×10^10
0.0
Total Flux (photon/sec/mm3)
Control
Salicylate
Etoposide 12 mg/kg
Sal + Etoposide 12 mg/kg
0
10
20
30
40
50
Days Post Implantation

Figure 4.2 Sub-therapeutic anti-tumour activity in murine xenograft of human breast cancer when treated with 12 mg/kg etoposide. (Experiment 1)

MDA-MB-231-LUC cells were injected into the mammary fat pad of 6 to 7-week-old female SCID C.B-17 mice. Tumour growth was monitored via (A) external caliper measurements (volume = length x width^2/2) and (B) bioluminescence imaging. Treatment began upon tumour establishment (Day 8). Animals were treated IP with control (PBS), salicylate (100 mg/kg), etoposide (12 mg/kg), or salicylate plus etoposide. Vehicle (control) and salicylate (green arrows) were administered on Days 8, 9, 10, and 11, and etoposide (orange arrows) was administered on Day 11. The treatment was repeated weekly for five weeks. Data representing five animals per treatment group from a single experiment are shown. Data were analyzed by multiple unpaired Student's *t*-tests.

(Hainsworth & Greco, 1995). In fact, no difference in tumour growth was observed between any of the treatment groups, regardless of the method used to measure tumour size (bioluminescence or calipers). Bioluminescence data suggest a therapeutic trend, although not statistically significant, in animals co-treated with salicylate and etoposide when compared to all other groups, however this occurred at later stages of tumour growth and likely reflects the increased variability in sample size across groups. By day 42, three (60%) control mice, and two (40%) salicylate-treated mice had been euthanized, compared to only one (20%) etoposide-treated mouse and none of the mice co-treated with etoposide and salicylate. While etoposide alone had no effect on survival outcome, a significant increase in survival was achieved in mice receiving etoposide and salicylate co-treatment ($p < 0.01$) (Figure 4.3). The combined failure to observe either etoposide-induced anti-tumour activity or improved survival over vehicle-treated animals indicated that additional experimentation was required to identify a therapeutic dose at which an anti-tumour effect could be observed, and thus any impact of salicylate on the therapeutic efficacy of etoposide.

In the initial xenograft experiment (Figure 4.2), it was also noted that tumour growth monitored through bioluminescence imaging resulted in substantial apparent variability of tumour size within and between treatment groups. Increased variability of total flux (photons/sec/mm^2) was concurrent with the appearance of central tumour necrosis. The decrease in total flux observed in tumours that are still increasing in physical size is commonly an indication of cell death likely due to either hypoxia or treatment (Lim *et al.*, 2009). As the study progressed, variable degrees of central tumour necrosis were observed in all treatment groups, likely accounting for the inconsistencies

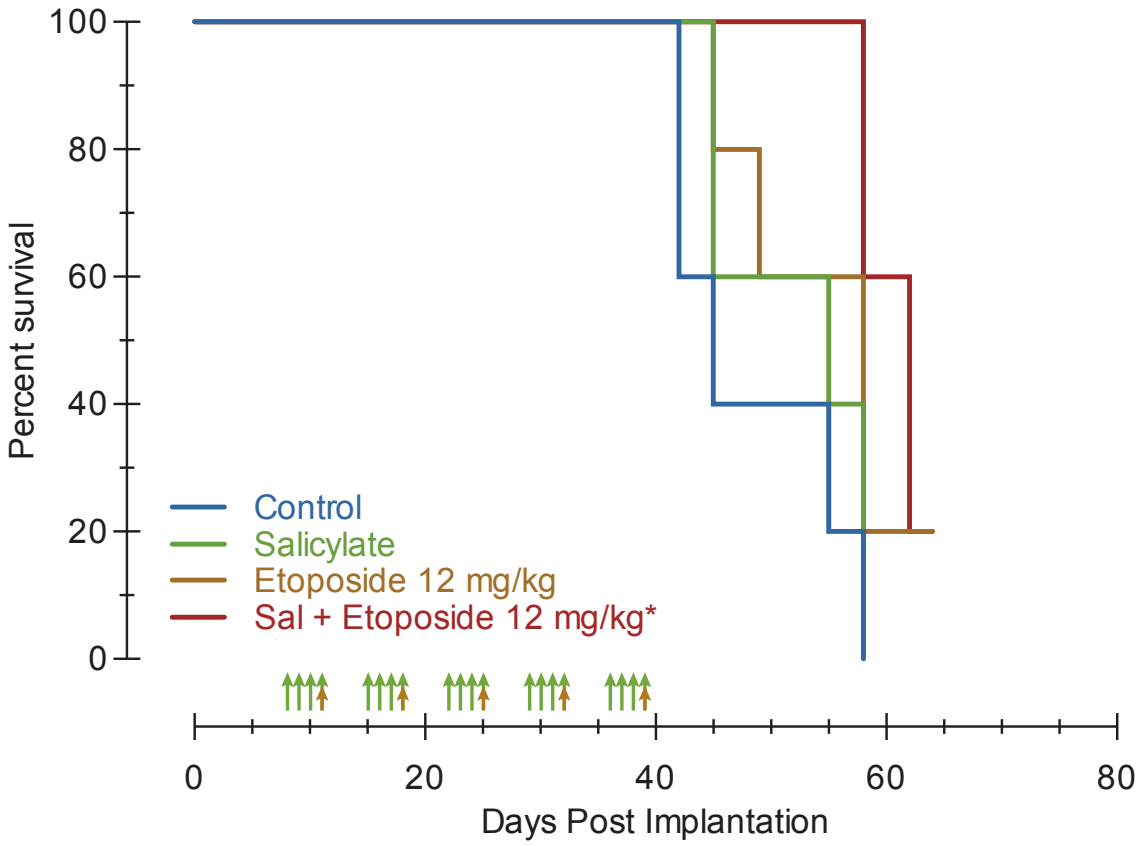
100
80
60
40
20
0
Percent survival
Control
Salicylate
Etoposide 12 mg/kg
Sal + Etoposide 12 mg/kg*
0
20
40
60
80
Days Post Implantation

Figure 4.3 Sub-therapeutic effect on survival rate in murine xenograft of human breast cancer when treated with 12 mg/kg etoposide. (Experiment 1)

MDA-MB-231-LUC cells were injected into the mammary fat pad of 6 to 7-week-old female SCID C.B-17 mice. Treatment began on upon tumour establishment (Day 8). Animals (5 per group) were treated IP with control (PBS), salicylate (100 mg/kg), etoposide (12 mg/kg), or etoposide and salicylate. Vehicle (control) and salicylate (green arrows) were administered on days 8, 9, 10, and 11, and etoposide (orange arrows) was administered on day 11. The treatment was repeated weekly for five weeks. A significant difference in survival was observed in mice receiving salicylate and etoposide, but not etoposide alone, versus control. Kaplan-Meier plot with log-rank (Mantel-Cox) test for curve comparison (* significantly different from control; $p < 0.01$).

observed between the bioluminescence imaging and caliper measurements of tumour growth (Figure 4.2).

In summary, although the dose levels of doxorubicin (8 mg/kg) and etoposide (12 mg/kg) chosen for this study were based on what had been previously reported in the literature, both fell outside of their respective therapeutic windows for SCID C.B.-17 mice bearing MDA-MD-231-LUC tumours (Rezaï *et al.*, 2007; Zhu *et al.*, 2008; Ottewell *et al.*, 2008; Molyneux *et al.*, 2011). Taking into consideration the absence of obvious toxicity, together with the specificity of etoposide for TOP2, and the multiple known mechanisms through which doxorubicin acts, subsequent studies focused on the effect of salicylate co-treatment on the efficacy of etoposide therapy alone.

4.3 Animal study 2 – Salicylate Co-Administration with Etoposide

4.3.1 Experimental Approach

The etoposide treatment regimen used in the preceding animal study (Section 4.2) failed to induce anti-tumour activity. Thus, a therapeutic dose of etoposide needed to be established for SCID C.B-17 mice bearing MDA-MB-231-LUC tumours. The animal study described in this section addressed this issue by focusing on the effect of salicylate co-administration on the efficacy of a range of etoposide doses. MDA-MB-231-LUC cells were injected (4×10^6 cells) into the mammary fat pad of 6 to 7-week-old female SCID C.B-17 mice. Tumour growth was monitored by bioluminescence imaging weekly and external caliper measurements semi-weekly. Palpable tumours were established one week after implantation and mice were then randomly sorted into eight groups, each with

comparable tumour burdens. Group 1 (vehicle control) mice (n = 5) received IP injections of PBS (50 μL) for four consecutive days, repeated weekly. Group 2 (salicylate) mice (n = 5) received IP injections of salicylate (100 mg/kg in 50 μL) for four consecutive days, repeated weekly. Groups 3-5 (12, 18, or 24 mg/kg etoposide, respectively) mice (n = 5) received IP injections of PBS (50 μL) for four consecutive days plus an IP injection of etoposide (12, 18, or 24 mg/kg, respectively in 50 μL PBS) on the fourth day, repeated weekly. Groups 6-8 (salicylate plus etoposide 12, 18, or 24 mg/kg respectively) mice (n = 5) received IP injections of salicylate (100 mg/kg in 50 μL) for four consecutive days plus an IP injection of etoposide (12, 18, or 24 mg/kg respectively in 50 μL PBS) on the fourth day, repeated weekly.

4.3.2 Etoposide Therapeutic Trend Achieved in SCID C.B-17 Mice Bearing MDA-MB-231-LUC Tumours.

Similar to what was reported in section 4.2.2, mice treated with etoposide (12, 18, or 24 mg/kg) demonstrated no overt signs of toxicity. Small to moderate attenuation of tumour growth was observed in mice treated with etoposide alone (Figures 4.4, 4.5, and 4.6). A therapeutic trend was observed across all three etoposide dose regimens; however, statistical significance was not achieved in mice receiving either 18 or 24 mg/kg etoposide, likely due to the considerable variability in tumour size observed within each treatment group. Furthermore, although statistical significance was reached in animals co-treated with salicylate and etoposide at later stages of growth, this was likely due to the increased variability in sample size across groups. No difference in tumour

A

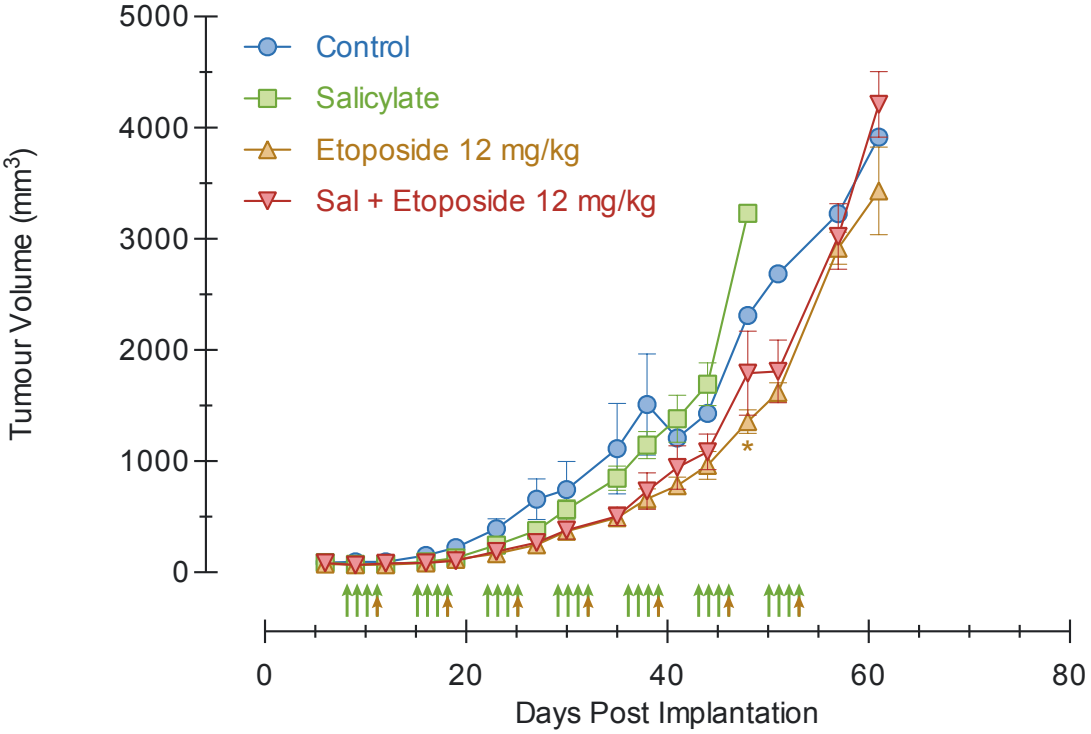
5000
4000
3000
2000
1000
0
Tumour Volume (mm3)
Control
Salicylate
Etoposide 12 mg/kg
Sal + Etoposide 12 mg/kg
*
0
20
40
60
80
Days Post Implantation

B

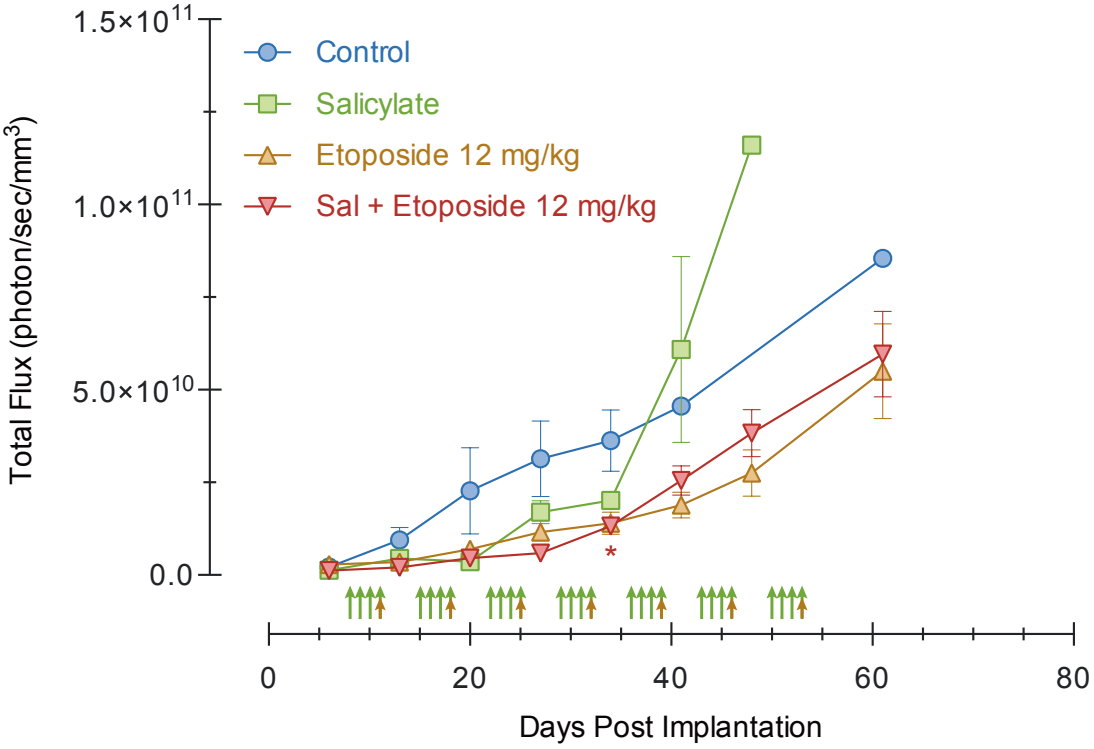
1.5×10^11
1.0×10^11
5.0×10^10
0.0
Total Flux (photon/sec/mm3)
Control
Salicylate
Etoposide 12 mg/kg
Sal + Etoposide 12 mg/kg
*
0
20
40
60
80
Days Post Implantation

Figure 4.4 Etoposide (12 mg/kg) does not induce a significant attenuation of tumour growth in murine xenograft of human breast cancer. (Experiment 2)

Human breast cancer MDA-MB-231 cells expressing luciferase were injected into the mammary fat pad of 6 to 7-week-old female SCID C.B-17 mice. Tumour growth was monitored via (A) external caliper measurements (volume = length x width^2/2) and (B) bioluminescence imaging. Treatment began on upon tumour establishment (Day 8). Animals were treated IP with control (PBS), salicylate (100 mg/kg), etoposide (12 mg/kg), or salicylate and etoposide. Vehicle (control) and salicylate (green arrows) were administered on Days 8, 9, 10, and 11, and etoposide (orange arrows) was administered on Day 11 (treatment schedule was repeated for seven weeks). Etoposide did not significantly attenuate tumour growth irrespective of salicylate co-treatment. Data representing five animals per treatment group from a single experiment are shown. Data were analyzed by multiple unpaired Student's *t*-tests (* significantly different from control; $p < 0.01$).

A

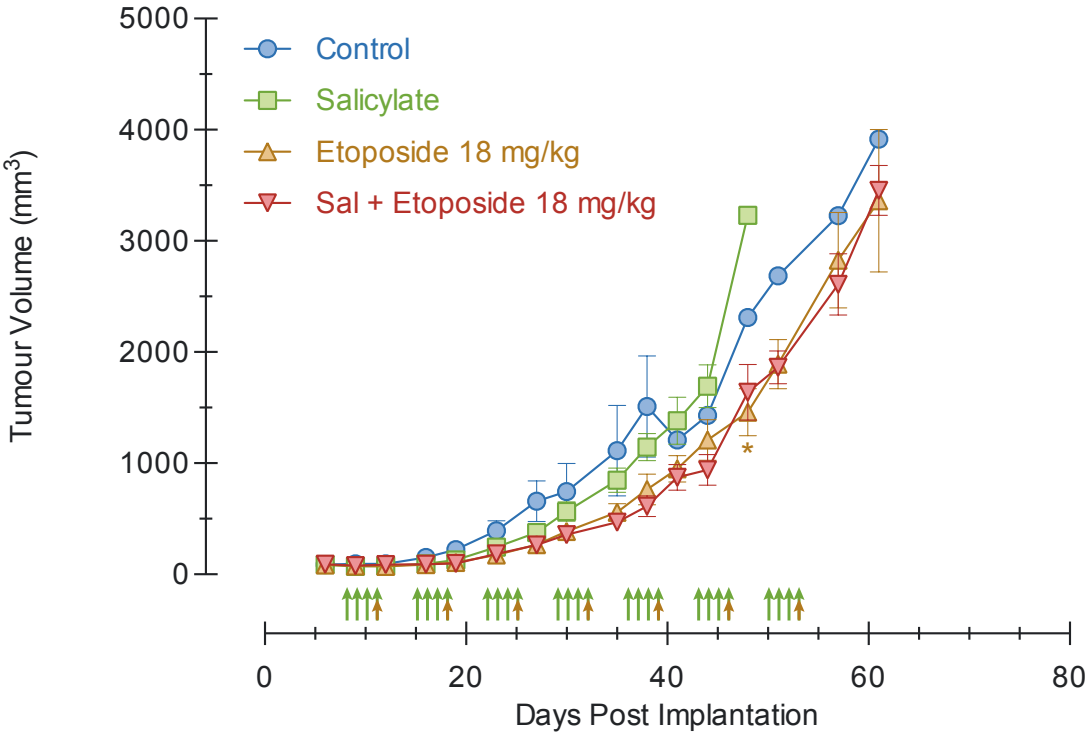
5000
4000
3000
2000
1000
0
Tumour Volume (mm3)
Control
Salicylate
Etoposide 18 mg/kg
Sal + Etoposide 18 mg/kg
*
0
20
40
60
80
Days Post Implantation

B

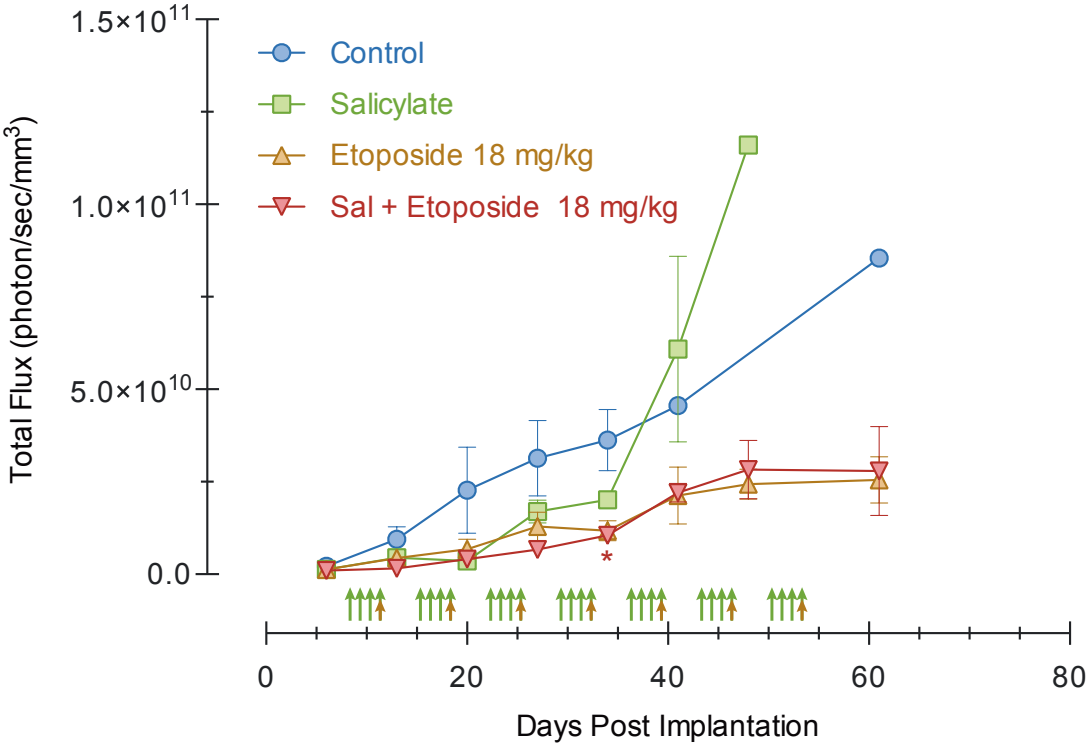
1.5×10^11
1.0×10^11
5.0×10^10
0.0
Total Flux (photon/sec/mm3)
Control
Salicylate
Etoposide 18 mg/kg
Sal + Etoposide 18 mg/kg
*
0
20
40
60
80
Days Post Implantation

Figure 4.5 Etoposide (18 mg/kg) does not induce a significant attenuation of tumour growth in murine xenograft of human breast cancer. (Experiment 2)

Human breast cancer MDA-MB-231 cells expressing luciferase were injected into the mammary fat pad of 6 to 7-week-old female SCID C.B-17 mice. Tumour growth was monitored via (A) external caliper measurements (volume = length x width^2/2) and (B) bioluminescence imaging. Treatment began on upon tumour establishment (Day 8). Animals were treated IP with vehicle control, salicylate (100 mg/kg), etoposide (18 mg/kg), or etoposide and salicylate. Vehicle (control) and salicylate (green arrows) were administered on days 8, 9, 10, and 11, and etoposide (orange arrows) was administered on day 11 (treatment schedule was repeated for seven weeks). Etoposide did not induce significant tumour growth attenuation regardless of salicylate co-treatment. Data representing five animals per treatment group from a single experiment are shown. Data were analyzed by multiple unpaired Student's *t*-tests (* significantly different from vehicle control; $p < 0.01$).

A

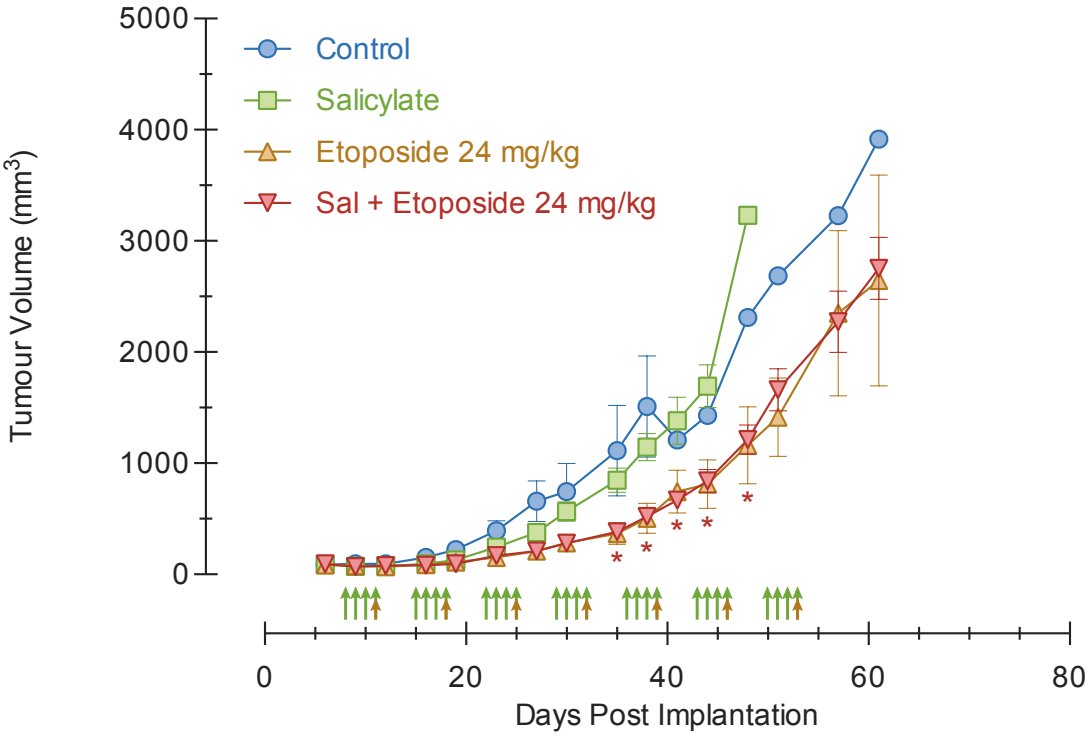
5000
4000
3000
2000
1000
0
Tumour Volume (mm3)
Control
Salicylate
Etoposide 24 mg/kg
Sal + Etoposide 24 mg/kg
*
*
*
*
*
0
20
40
60
80
Days Post Implantation

B

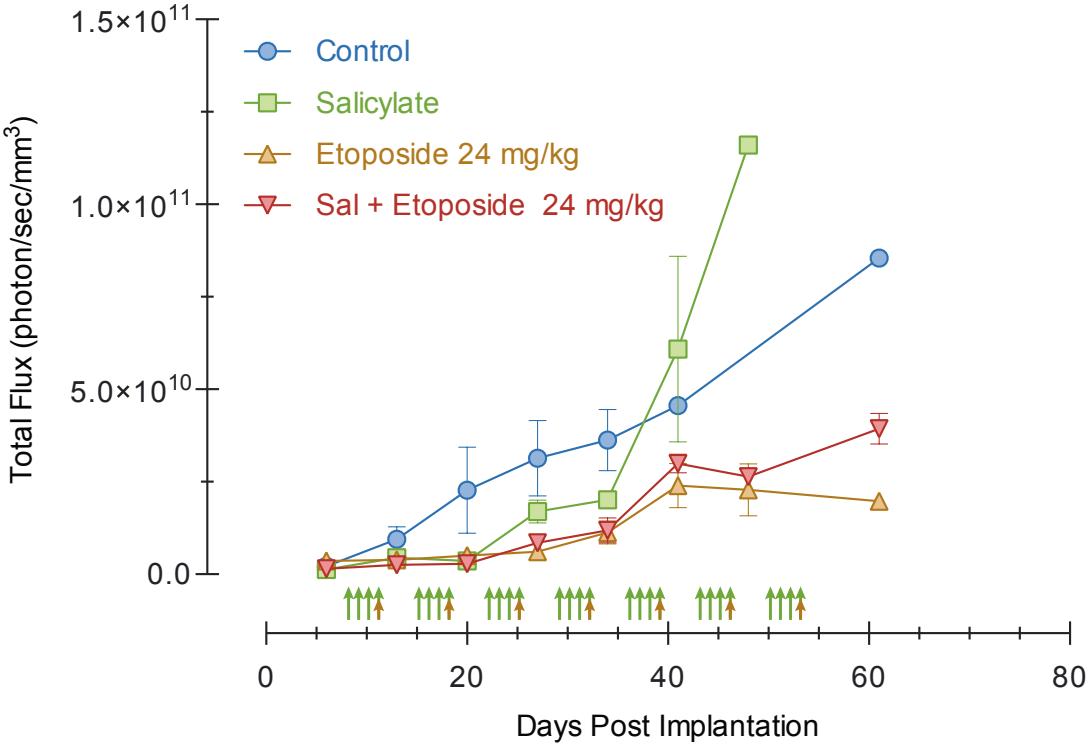
1.5×10^11
1.0×10^11
5.0×10^10
0.0
Total Flux (photon/sec/mm3)
Control
Salicylate
Etoposide 24 mg/kg
Sal + Etoposide 24 mg/kg
0
20
40
60
80
Days Post Implantation

Figure 4.6 Etoposide (24 mg/kg) treatment results in a modest attenuation of tumour growth in murine xenografts of human breast cancer (Experiment 2)

Human breast cancer MDA-MB-231 cells expressing luciferase were injected into the mammary fat pad of 6 to 7-week-old female SCID C.B-17 mice. Tumour growth was monitored via (A) external caliper measurements (volume = length x width^2/2) and (B) bioluminescence imaging. Treatment began on upon tumour establishment (Day 8). Animals were treated IP with control (PBS), salicylate (100 mg/kg), etoposide (24 mg/kg), or etoposide plus salicylate. Vehicle (control) and salicylate (green arrows) were administered on Days 8, 9, 10, and 11, and etoposide (orange arrows) was administered on Day 11. The treatment schedule was repeated for seven weeks. External caliper measurements indicated that etoposide when co-administered with salicylate, but not etoposide alone, significantly attenuated tumour growth. In contrast, a significant difference in tumour growth was not observed in measurements obtained through bioluminescence imaging. Data representing five animals per treatment group from a single experiment are shown. Data were analyzed by multiple unpaired Student's *t*-tests (* significantly different from control; $p < 0.01$)

growth between mice receiving etoposide alone and those receiving salicylate co-treatment was observed.

There was substantial variation in tumour size within each treatment group, documented by both tumour volume and total measured bioluminescence. Similar to what was reported in the section 4.2.2, total flux of bioluminescent imaging-derived tumour signals was inconsistent with tumour size measured by external calipers. Similarly, varying degrees of central tumour necrosis were observed in all treatment groups, with ulceration increasing in size as the study progressed.

Evidence of a therapeutic trend was also provided by the improved survival observed in mice treated with either 18 or 24 mg/kg, but not 12 mg/kg, etoposide ($p < 0.01$) (Figures 4.7, 4.8, and 4.9). Similarly, mice receiving salicylate and etoposide (12, 18, or 24 mg/kg) co-treatment exhibited a better survival outcome when compared to control mice ($p < 0.01$). However, no significant difference in survival outcome was observed in mice receiving salicylate and etoposide co-treatment when compared to mice receiving etoposide treatment alone.

In summary, a moderate etoposide-induced therapeutic trend was achieved; however, the high degree of within-group variation in etoposide efficacy persisted. Given that the intention of this study was to measure the effect of salicylate co-treatment on the therapeutic efficacy of etoposide, a sufficient therapeutic baseline was not yet deemed to have been established. Similar to what was reported in section 4.2.2, bioluminescence imaging appeared to be considerably less consistent than external calipers for monitoring tumour growth. This can most likely be attributed to bioluminescent signal interference due to the prevalence of central tumour necrosis across treatment groups. Nevertheless,

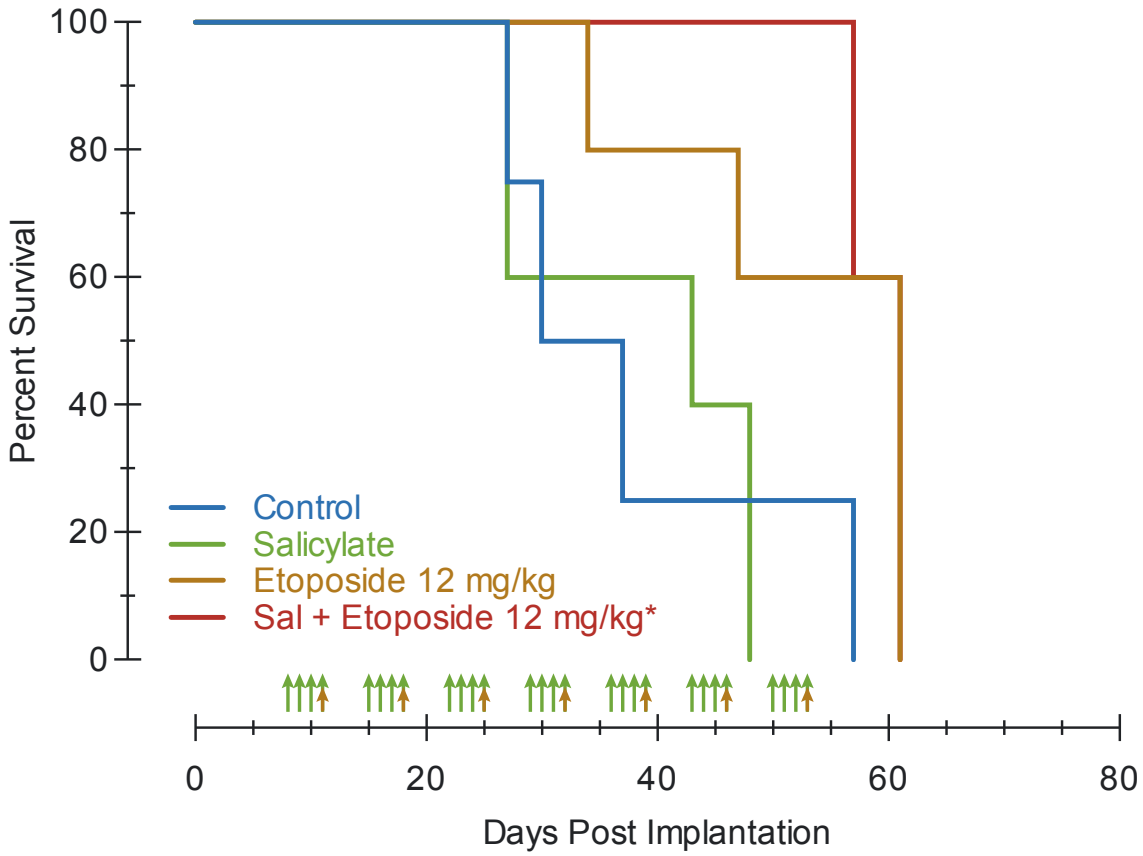
100
80
60
40
20
0
Percent Survival
Control
Salicylate
Etoposide 12 mg/kg
Sal + Etoposide 12 mg/kg*
0
20
40
60
80
Days Post Implantation

Figure 4.7 Etoposide (12 mg/kg) treatment co-administered with salicylate increases survival rate in a murine xenograft model of human breast cancer. (Experiment 2)

Human breast cancer MDA-MB-231 cells expressing luciferase were injected into the mammary fat pad of 6 to 7-week-old female SCID C.B-17 mice. Treatment began on upon tumour establishment (Day 8). Animals were treated IP with control (PBS), salicylate (100 mg/kg), etoposide (12 mg/kg), or etoposide plus salicylate. Control and salicylate (green arrows) were administered on Days 8, 9, 10, and 11, and etoposide (orange arrows) was administered on Day 11 (treatment schedule was repeated for seven weeks). A significant difference in survival was observed in mice receiving etoposide and salicylate, but not etoposide alone, versus mice receiving vehicle control, or salicylate alone. Kaplan-Meier plot with log-rank (Mantel-Cox) test for curve comparison (*significantly different from control; $p < 0.01$).

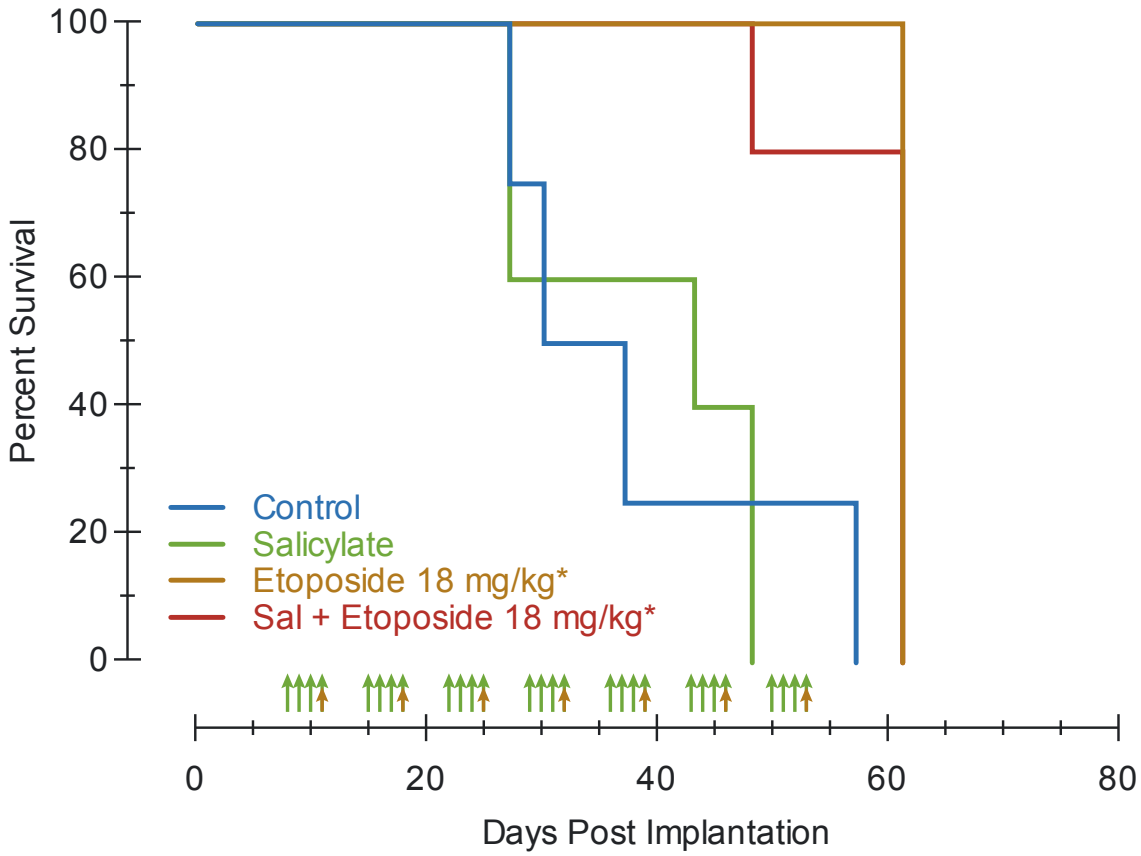
100
80
60
40
20
0
Percent Survival
Control
Salicylate
Etoposide 18 mg/kg*
Sal + Etoposide 18 mg/kg*
0
20
40
60
80
Days Post Implantation

Figure 4.8 Etoposide (18 mg/kg) alone or co-administered with salicylate increases survival in a murine xenograft model of human breast cancer. (Experiment 2)

Human breast cancer MDA-MB-231 cells expressing luciferase were injected into the mammary fat pad of 6 to 7-week-old female SCID C.B-17 mice. Treatment began on upon tumour establishment (Day 8). Animals were treated IP. with control (PBS), salicylate (100 mg/kg), etoposide (18 mg/kg), or etoposide plus salicylate. Control and salicylate (green arrows) were administered on Days 8, 9, 10, and 11, and etoposide (orange arrows) was administered on Day 11 (treatment schedule was repeated for seven weeks). A significant difference in survival outcome was observed in mice receiving etoposide, regardless of salicylate co-administration, versus mice receiving vehicle control, or salicylate alone. Kaplan-Meier plot with log-rank (Mantel-Cox) test for curve comparison (*significantly different from control; $p < 0.01$).

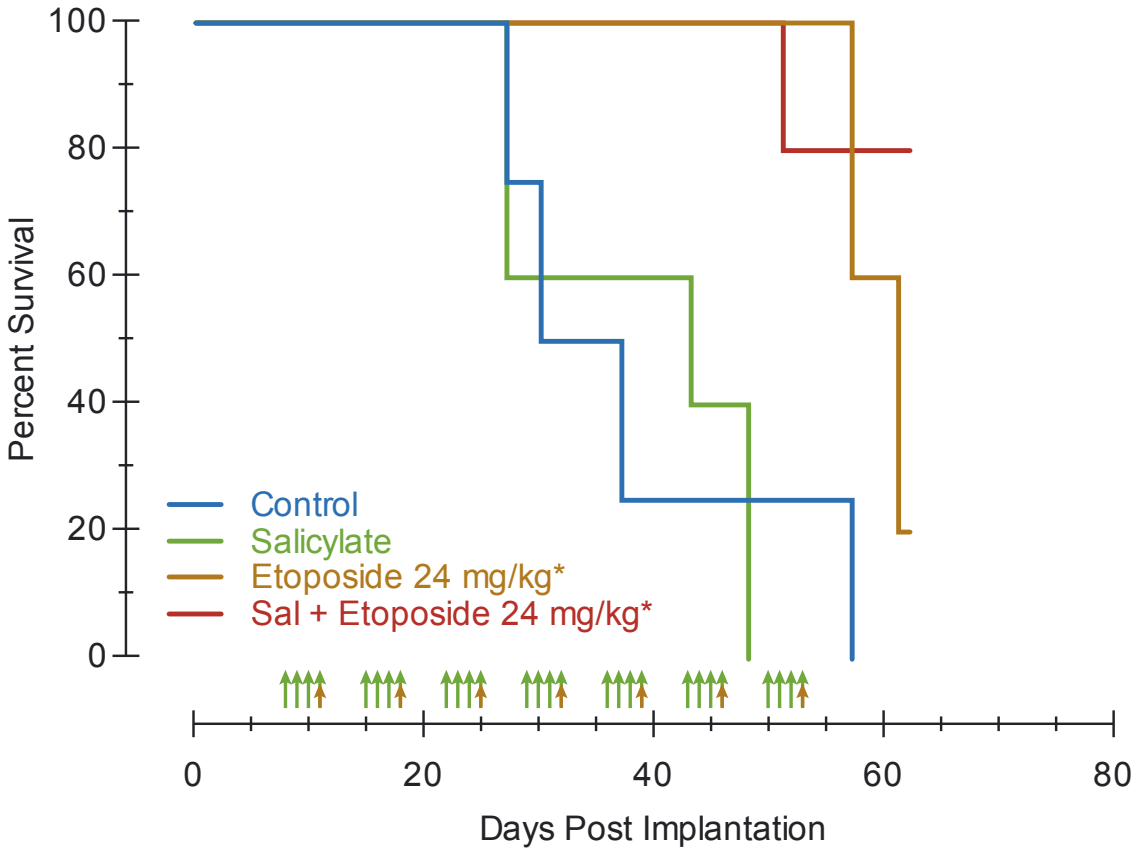
100
80
60
40
20
0
Percent Survival
Control
Salicylate
Etoposide 24 mg/kg*
Sal + Etoposide 24 mg/kg*
0
20
40
60
80
Days Post Implantation

Figure 4.9 Etoposide (24 mg/kg) alone or co-administered with salicylate increases survival in a murine xenograft model of human breast cancer. (Experiment 2)

Human breast cancer MDA-MB-231 cells expressing luciferase were injected into the mammary fat pad of 6 to 7-week-old female SCID C.B-17 mice. Treatment began on upon tumour establishment (Day 8). Animals were treated IP. with control (PBS), salicylate (100 mg/kg), etoposide (24 mg/kg), or etoposide plus salicylate. Control and salicylate (green arrows) were administered on Days 8, 9, 10, and 11, and etoposide (orange arrows) was administered on Day 11 (treatment schedule was repeated for seven weeks). A significant difference in survival outcome was observed in mice receiving etoposide, regardless of salicylate co-administration, versus mice receiving vehicle control, or salicylate alone. Kaplan-Meier plot with log-rank (Mantel-Cox) test for curve comparison (*significantly different from control; $p < 0.01$).

bioluminescence imaging proved to be a valuable tool for confirming the xenotransplantation site and monitoring the internal spread of tumour tissue.

4.4 Animal study 3 – Salicylate Co-Administration with Etoposide (Dose Escalation)

4.4.1 Experimental Approach

While the earlier study identified an etoposide regimen resulting in a moderate therapeutic trend, measurable both by tumour growth and survival outcome, it was not sufficiently robust to effectively test the consequence of salicylate co-treatment. To address this issue in the follow-up study, the etoposide dose range was escalated to induce a more significant etoposide-mediated anticancer outcome. Furthermore, it was determined that the investigation should proceed as an *in vivo* proof of principle study. Consequently, the salicylate regimen was altered by increasing the dose to 200 mg/kg while maintaining the same treatment schedule used in the previous study.

Here, MDA-MB-231-LUC cells were injected (4×10^6 cells) into the mammary fat pad of 6 to 7-week-old female SCID C.B-17 mice. Tumour growth was monitored by bioluminescence imaging and external caliper measurements. After one week, palpable tumours were established and mice were randomly sorted into eight groups each with comparable tumour burdens. Group 1 (vehicle control) mice (n = 5) received IP injections of PBS (50 μL) for four consecutive days, repeated weekly. Group 2 (salicylate) mice (n = 5) received IP injections of salicylate (200 mg/kg in 50 μL) for four consecutive days, repeated weekly. Groups 3-5 (etoposide 24, 36, or 48 mg/kg in PBS, respectively) mice (n = 5) received IP injections of PBS (50 μL) for four consecutive days plus an IP

injection of etoposide (24, 36, or 48 mg/kg in 50 μL PBS, respectively) on the fourth day, repeated weekly. Groups 6-8 (salicylate plus etoposide 24, 36, or 48 mg/kg in PBS, respectively) mice (n = 5) received IP injections of salicylate (200 mg/kg in 50 μL PBS) for four consecutive days plus an IP injection of etoposide (24, 36, or 48 mg/kg in 50 μL PBS, respectively) on the fourth day, repeated weekly.

4.4.2 Dose Modification Due to Issues with Etoposide Solubility

After two rounds of treatment, it came to light that etoposide was precipitating out of solution when PBS was used as the solvent. Additional dilution in PBS was not possible given that 10 μL/g is the maximum recommended volume for IP administration in mice (Morton *et al.*, 2001). Based on a comprehensive literature review, corn oil was identified as a suitable solvent for IP administration of etoposide (Joel *et al.*, 1995; Lee *et al.*, 1995; Spronck & Kirkland, 2002; Jiang & Kang, 2004). Anticipating that the actual (soluble) dose of etoposide received by mice when using PBS was lower than that intended, and due to concern for subsequent toxicity, dose levels were modified for etoposide dissolved in corn oil. Hence, the doses for groups 3-8, receiving 24, 36, and 48 mg/kg etoposide at the start of the experiment, were decreased to 18, 24, and 36 mg/kg etoposide, respectively, administered in 150 μL of corn oil. In addition, treatment groups receiving vehicle control, or salicylate alone also received 150 μL of corn oil to account for any effects of the vehicle on tumour growth or animal well-being. The modified regimens commenced on day 23 post-implantation.

4.4.3 Salicylate Co-Administration Significantly Reduces Both Etoposide-Induced Attenuation of Tumour Growth, and Etoposide-Mediated Survival

As expected, tumours in mice treated with salicylate alone showed no significant change in tumour growth from that observed in mice receiving vehicle control alone (Figure 4.10). However, by day 54, the tumours of mice receiving 18, 24, or 36 mg/kg etoposide showed significant attenuation of growth (Figures 4.10, 4.11 and 4.12). More importantly, co-administration of salicylate significantly reduced etoposide-induced attenuation of tumour growth in mice co-treated with 36 mg/kg etoposide (Figure 4.12), but not in those co-treated with etoposide at 18 or 24 mg/kg (Figures 4.10 and 4.11). Within-group variance of tumour growth was notably lower than that observed in the preceding two studies in which etoposide was administered in PBS. The escalated etoposide regimen did not result in toxicity even at the highest dose administered. Improved and consistent therapeutic effect of etoposide can almost certainly be attributed to its higher solubility in corn oil (Slevin, 1991). Furthermore, the onset of central tumour necrosis was delayed in mice treated with 24 or 36 mg/kg etoposide but not in matching groups co-treated with salicylate.

Changes in tumour growth, as indicated by caliper measurements, were accompanied by a corresponding significant difference in survival outcome (Figures 4.13, 4.14 and 4.15). Mice treated with 18, 24, or 36 mg/kg etoposide alone had significantly better survival outcomes when compared to either vehicle or salicylate only controls ($p < 0.01$). More importantly, when salicylate was co-administered in mice receiving 36 mg/kg etoposide, there was as significant attenuation in etoposide-induced survival ($p <$

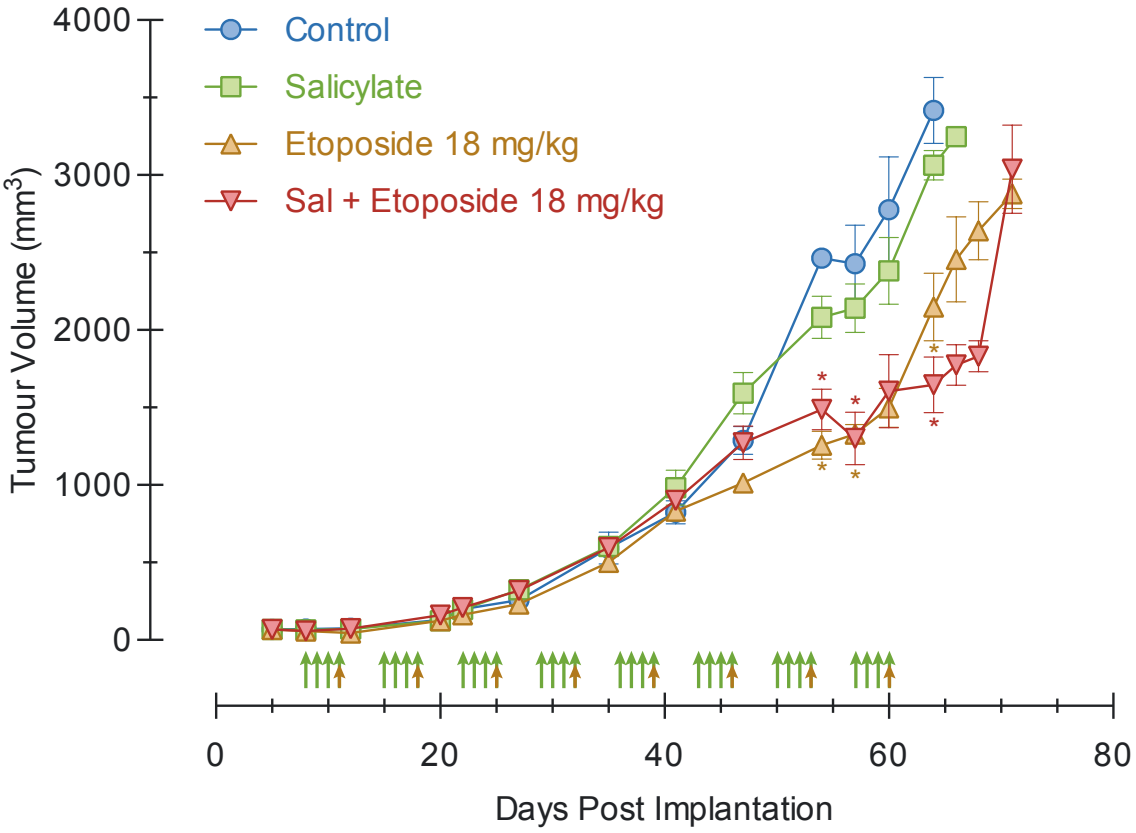
Control
Salicylate
Etoposide 18 mg/kg
Sal + Etoposide 18 mg/kg
Tumour Volume (mm3)
4000
3000
2000
1000
0
0
20
40
60
80
Days Post Implantation

Figure 4.10 Salicylate co-administration does not affect the therapeutic efficacy of etoposide (18 mg/kg) in a xenograft model of human breast cancer. (Experiment 3)

Human breast cancer MDA-MB-231 cells expressing luciferase were injected into the mammary fat pad of 6 to 7-week-old female SCID C.B-17 mice. Tumour growth was monitored via external caliper measurements (volume = length x width^2/2). Treatment began on upon tumour establishment (Day 8). Animals were treated IP with control (PBS and corn oil), salicylate, etoposide (18 mg/kg), or salicylate plus etoposide. Control and salicylate were administered on Days 8, 9, 10, and 11, and etoposide was administered on Day 11 (repeated weekly for eight weeks). Data representing five animals per treatment group from a single experiment are shown. Data were analyzed by multiple unpaired Student's t-tests (*significantly different from control; $p < 0.01$).

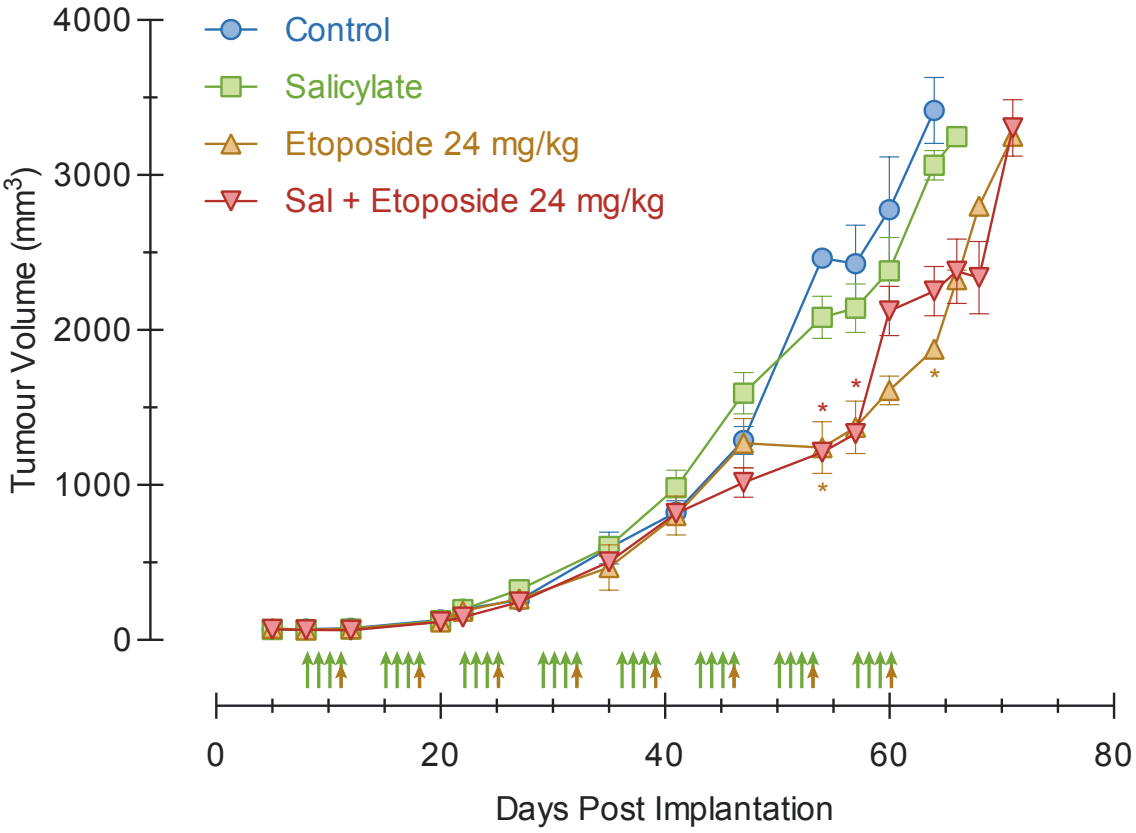
Control
Salicylate
Etoposide 24 mg/kg
Sal + Etoposide 24 mg/kg
Tumour Volume (mm3)
4000
3000
2000
1000
0
0
20
40
60
80
Days Post Implantation
*
*
*
*

Figure 4.11 Salicylate co-administration does not impact the therapeutic efficacy of etoposide (24 mg/kg) in a xenograft model of human breast cancer. (Experiment 3)

Human breast cancer MDA-MB-231 cells expressing luciferase were injected into the mammary fat pad of 6 to 7-week-old female SCID C.B-17 mice. Tumour growth was monitored via external caliper measurements (volume = length x $width^2/2$). Treatment began on upon tumour establishment (Day 8). Animals were treated IP with control (PBS and corn oil), salicylate, etoposide (24 mg/kg), or salicylate plus etoposide. Control and salicylate were administered on Days 8, 9, 10, and 11, and etoposide was administered on Day 11 (repeated weekly for eight weeks). Data representing five animals per treatment group from a single experiment are shown. Data were analyzed by multiple unpaired Student's t-tests (*significantly different from control; $p < 0.01$).

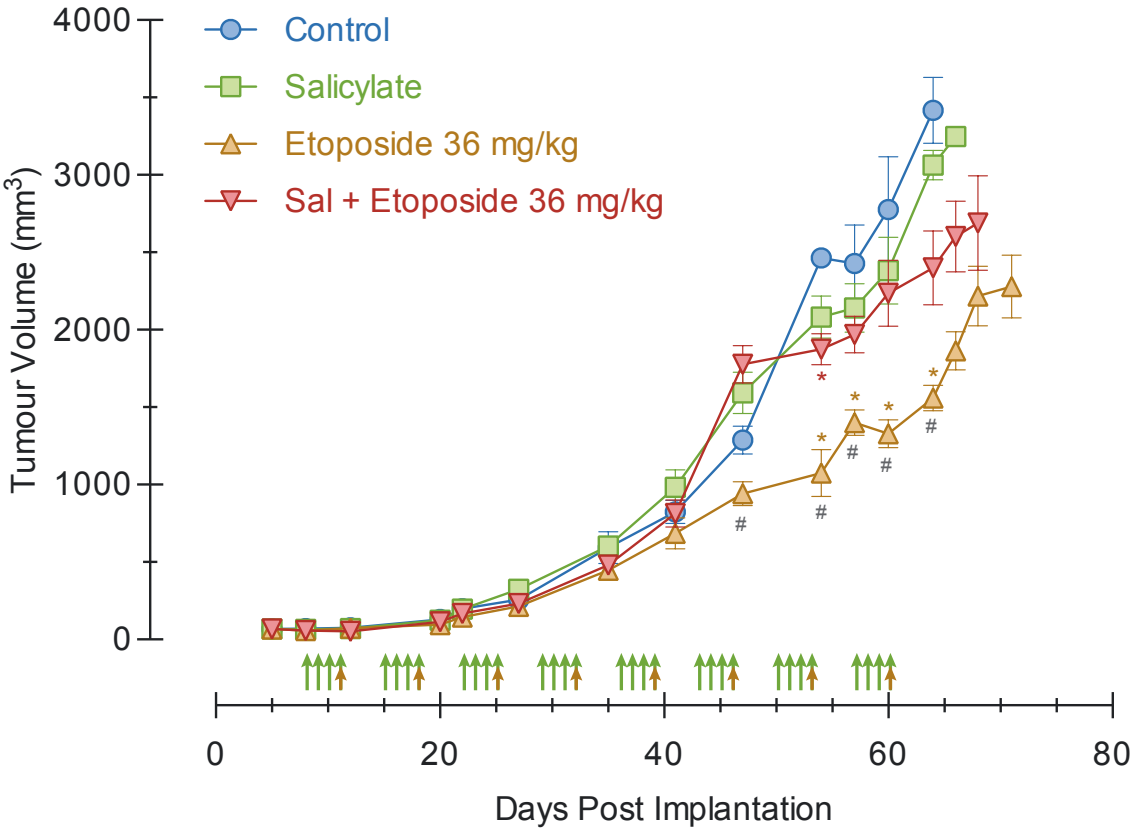
Control
Salicylate
Etoposide 36 mg/kg
Sal + Etoposide 36 mg/kg
Tumour Volume (mm3)
4000
3000
2000
1000
0
0
20
40
60
80
Days Post Implantation

Figure 4.12 Salicylate co-administration reduces the efficacy of etoposide-induced attenuation of tumour growth in a xenograft model of human breast cancer. (Experiment 3)

Human breast cancer MDA-MB-231 cells expressing luciferase were injected into the mammary fat pad of 6 to 7-week-old female SCID C.B-17 mice. Tumour growth was monitored via external caliper measurements (volume = length x width^2/2). Treatment began on upon tumour establishment (Day 8). Animals were treated IP with control (PBS and corn oil), salicylate, etoposide (36 mg/kg), or salicylate plus etoposide. Control and salicylate were administered on Days 8, 9, 10, and 11, and etoposide was administered on Day 11 (repeated weekly for eight weeks). Data representing five animals per treatment group from a single experiment are shown. Data were analyzed by multiple unpaired Student's t-tests (* significantly different from control; # etoposide vs. salicylate plus etoposide; $p < 0.01$).

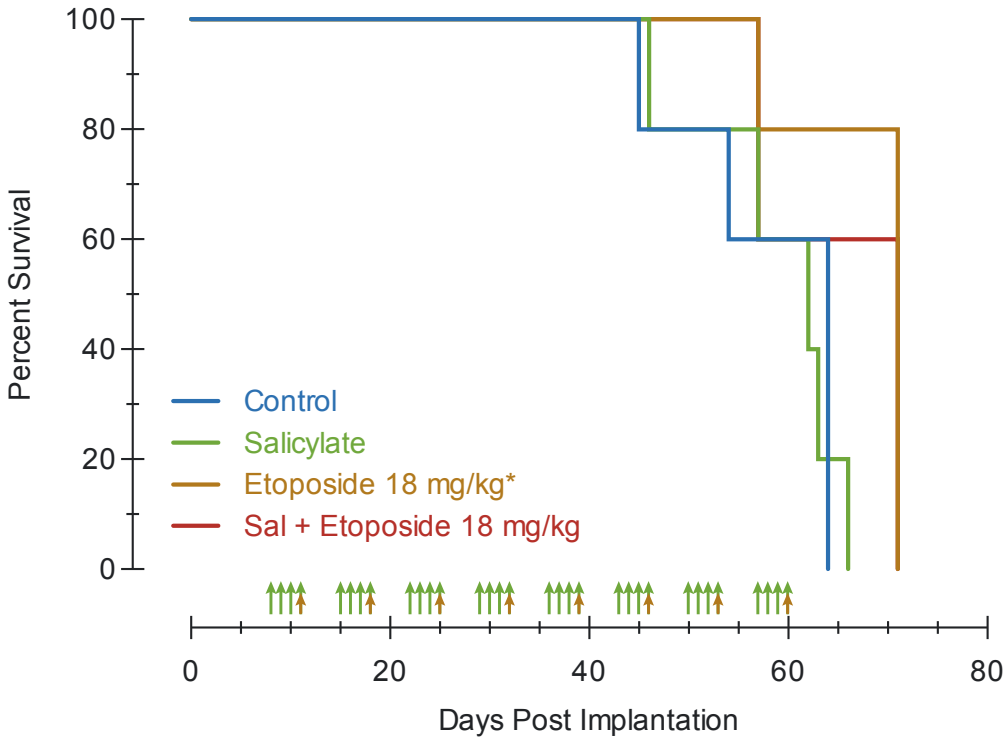
100
80
60
40
20
0
Percent Survival
Control
Salicylate
Etoposide 18 mg/kg*
Sal + Etoposide 18 mg/kg
0
20
40
60
80
Days Post Implantation

Figure 4.13 Etoposide (18 mg/kg) alone, but not in combination with salicylate, moderately increased survival in a murine xenograft model of human breast cancer. (Experiment 3)

Human breast cancer MDA-MB-231 cells expressing luciferase were injected into the mammary fat pad of 6 to 7-week-old female SCID C.B-17 mice. Treatment began on upon tumour establishment (Day 8). Animals were treated IP with control (PBS and corn oil), salicylate, etoposide (18 mg/kg), or salicylate and etoposide. Control and salicylate were administered on Days 8, 9, 10, and 11, and etoposide was administered on Day 11 (repeated weekly for eight weeks). Data representing five animals per treatment group from a single experiment are shown. Kaplan-Meier plot with log-rank (Mantel-Cox) test for curve comparison (*significantly different from control; $p < 0.01$).

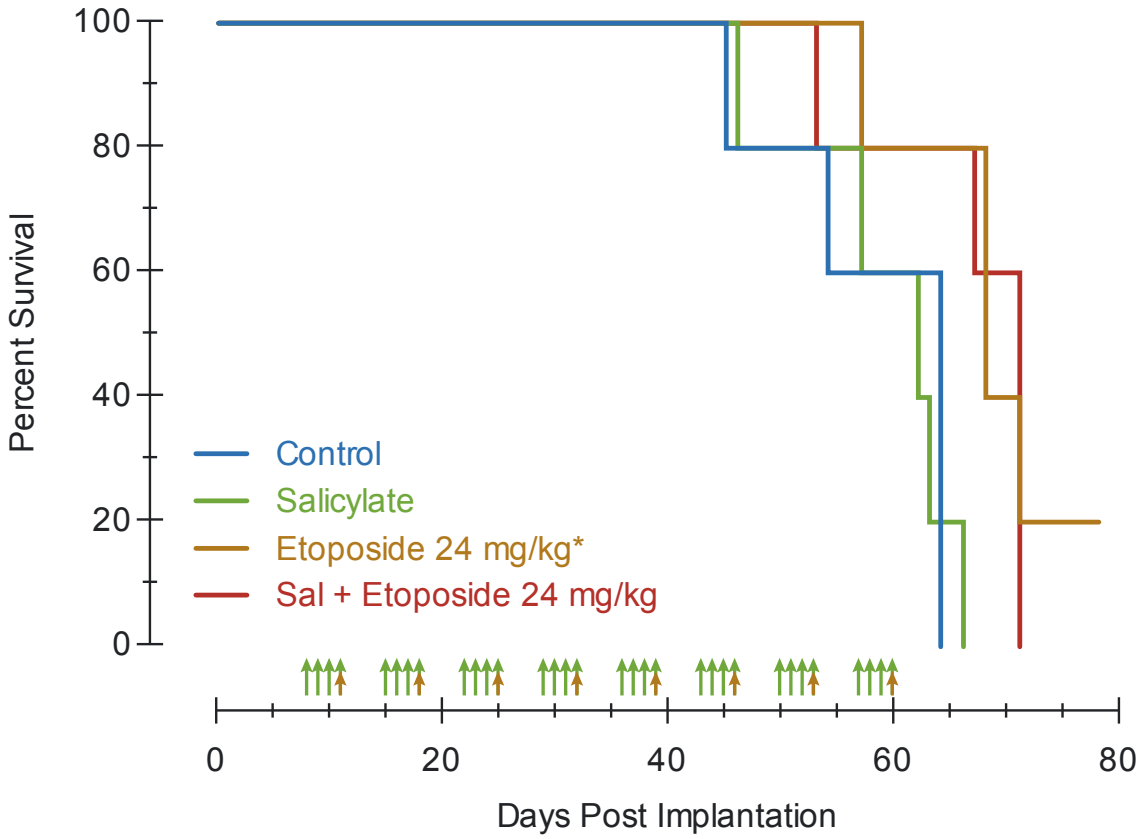
100
80
60
40
20
0
Percent Survival
Control
Salicylate
Etoposide 24 mg/kg*
Sal + Etoposide 24 mg/kg
0
20
40
60
80
Days Post Implantation

Figure 4.14 Etoposide (24 mg/kg) alone, but not in combination with salicylate, moderately increases survival in a murine xenograft model of human breast cancer. (Experiment 3)

Human breast cancer MDA-MB-231 cells expressing luciferase were injected into the mammary fat pad of 6 to 7-week-old female SCID C.B-17 mice. Treatment began on upon tumour establishment (Day 8). Animals were treated IP with control (PBS and corn oil), salicylate, etoposide (24 mg/kg), or salicylate plus etoposide. Control and salicylate were administered on Days 8, 9, 10, and 11, and etoposide was administered on Day 11 (repeated weekly for eight weeks). Data representing five animals per treatment group from a single experiment are shown. Kaplan-Meier plot with log-rank (Mantel-Cox) test for curve comparison (*significantly different from control; $p < 0.01$).

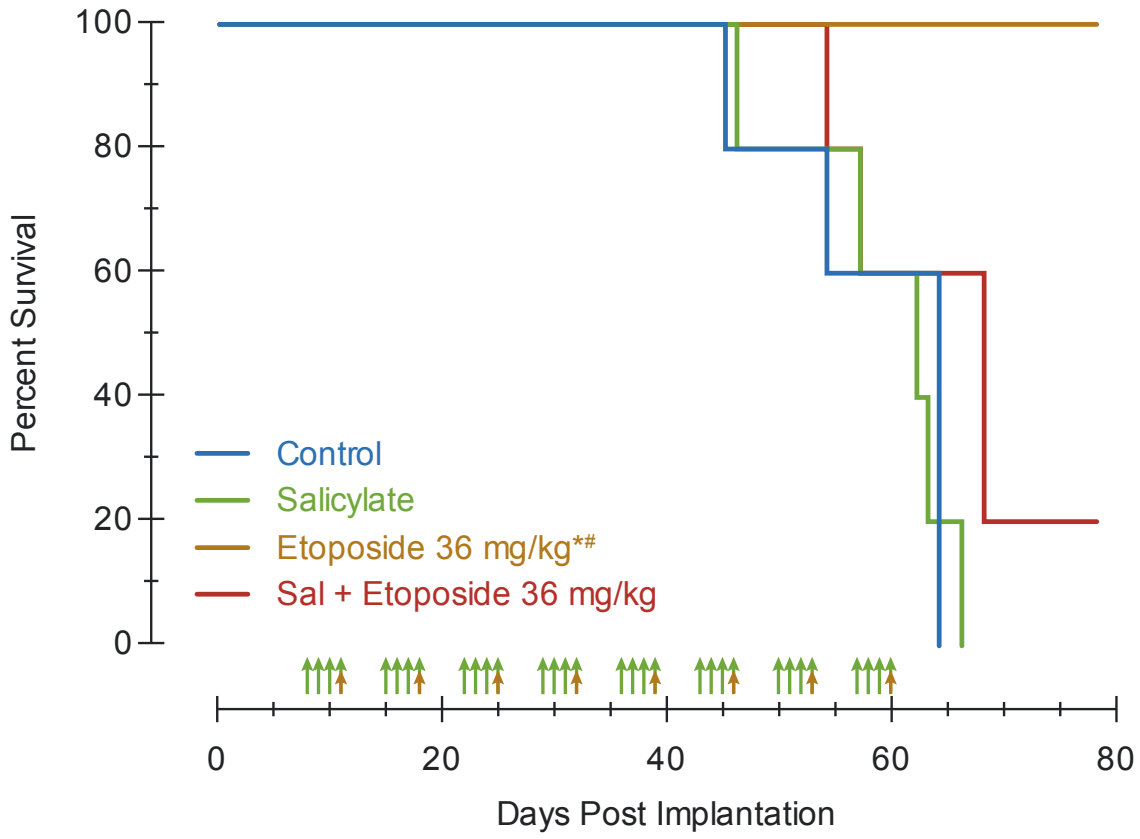
100
80
60
40
20
0
Percent Survival
Control
Salicylate
Etoposide 36 mg/kg*#
Sal + Etoposide 36 mg/kg
0
20
40
60
80
Days Post Implantation

Figure 4.15 Salicylate co-administration significantly attenuates etoposide-induced survival in a murine xenograft model of human breast cancer. (Experiment 3)

Human breast cancer MDA-MB-231 cells expressing luciferase were injected into the mammary fat pad of 6 to 7-week-old female SCID C.B-17 mice. Treatment began on upon tumour establishment (Day 8). Animals were treated IP with control (PBS and corn oil), salicylate, etoposide (36 mg/kg), or salicylate plus etoposide. Control and salicylate were administered on Days 8, 9, 10, and 11, and etoposide was administered on Day 11 (repeated weekly for eight weeks). Data representing five animals per treatment group from a single experiment are shown. Kaplan-Meier plot with log-rank (Mantel-Cox) test for curve comparison (*significantly different from control; # etoposide vs. salicylate plus etoposide alone; $p < 0.01$).

0.01) (Figure 4.15). Despite this, salicylate co-administration had no significant effect on etoposide-induced survival in mice receiving either 18 or 24 mg/kg etoposide (Figures 4.13 and 4.14).

In summary, co-administration of 200 mg/kg salicylate reduced both etoposide-induced attenuation of tumour growth and etoposide-induced survival in mice treated with 36 mg/kg etoposide. However, given the modification of etoposide vehicle and the corresponding dose revisions, a replicate study was needed to validate these findings.

4.5 Animal study 4 – Salicylate Co-Administration with Etoposide (Dose Modification)

4.5.1 Experimental Approach

Because of the mid-experiment treatment modification described in section 4.4.2, a second xenograft study was carried out to examine the effect of salicylate co-administration on a single dose regimen of etoposide (36 mg/kg). MDA-MB-231-LUC cells were injected (4×10^6 cells) into the mammary fat pad of 6 to 7-week-old female SCID C.B-17 mice. Tumour growth was monitored by bioluminescence imaging and external caliper measurements. After one week, palpable tumours were established and mice were randomly sorted into four groups, each with comparable tumour burdens. Group 1 (vehicle control) mice (n = 5) received IP injections of PBS (50 µL) for four consecutive days plus an IP injection of corn oil (150 µL) on the fourth day, repeated weekly. Group 2 (salicylate) mice (n = 5) received IP injections of salicylate (200 mg/kg in 50 µL PBS) for four consecutive days plus an IP injection of corn oil (150 µL) on the

fourth day, repeated weekly. Groups 3 (etoposide) mice (n = 5) received IP injections of PBS (50 µL) for four consecutive days plus an IP injection of etoposide (36 mg/kg in 150 µL corn oil) on the fourth day, repeated weekly. Group 4 (salicylate plus etoposide) mice (n = 5) received IP injections of salicylate (200 mg/kg in 50 µL PBS) for four consecutive days plus an IP injection of etoposide (36 mg/kg in 150 µL corn oil) on the fourth day, repeated weekly.

4.5.2 Co-Administration of Salicylate Significantly Reduces Both Etoposide-Induced Attenuation of Tumour Growth, and Etoposide-Induced Survival.

Etoposide anti-tumour activity was observed as early as Day 30 post implantation, noticeably earlier than what was reported in section 4.4, in mice receiving 36 mg/kg etoposide alone (Figure 4.16). Nevertheless, mice receiving etoposide alone presented no overt signs of toxicity. Similarly, there was no significant loss in body weight in any of the mice. MDA-MB-231-LUC xenograft tumours were significantly smaller in mice receiving etoposide alone versus either vehicle or salicylate control ($p < 0.01$) (Figure 4.16). Co-treatment with salicylate, however, significantly diminished etoposide-induced attenuation of tumour growth ($p < 0.01$). Etoposide alone effectively supressed tumour growth by 72.9% (Day 53), whereas when salicylate was co-administered only 43.8% growth inhibition was achieved (Day 53). Central tumour necrosis was observed in all mice regardless of treatment; however, onset was delayed in mice receiving etoposide alone and in combination with salicylate (Figure 4.17).

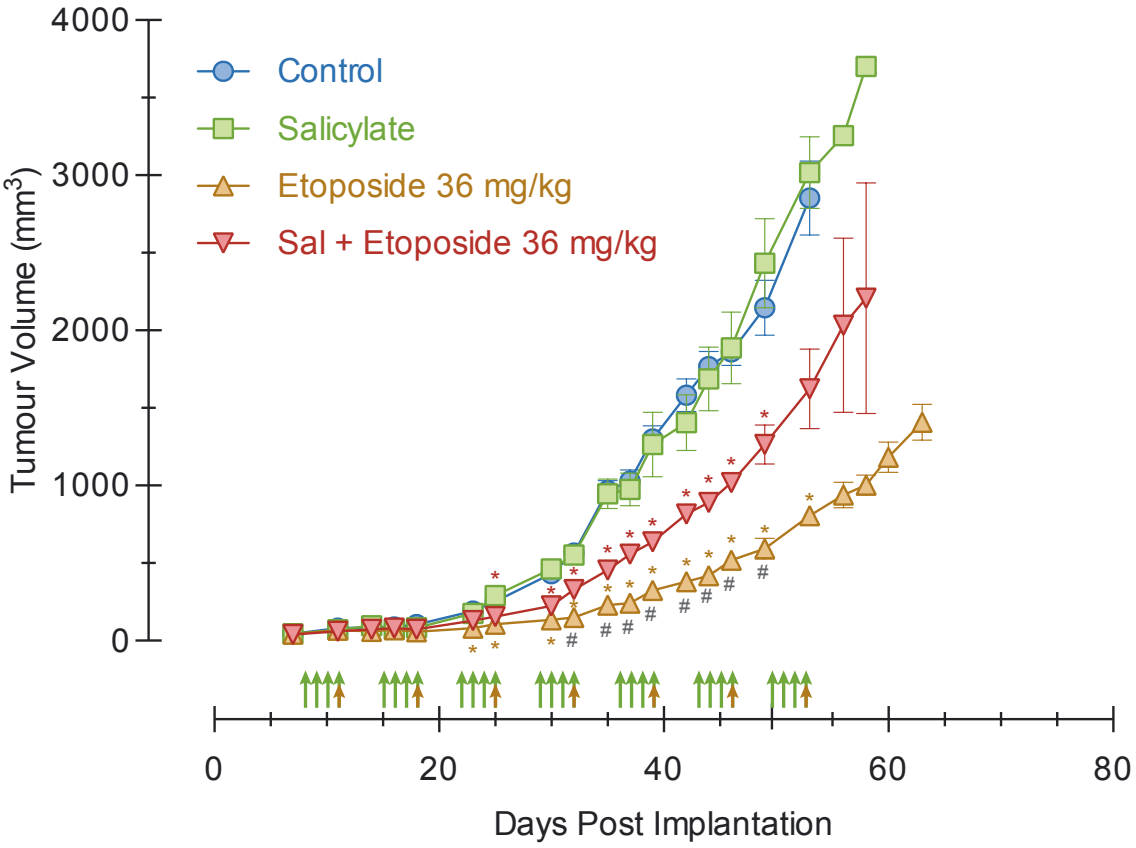
Control
Salicylate
Etoposide 36 mg/kg
Sal + Etoposide 36 mg/kg
Tumour Volume (mm3)
4000
3000
2000
1000
0
0
20
40
60
80
Days Post Implantation

Figure 4.16 Salicylate co-administration reduces the efficacy of etoposide anti-tumour activity in murine xenograft model of human breast cancer. (Experiment 4)

Human breast cancer MDA-MB-231 cells expressing luciferase were injected into the mammary fat pad of 6 to 7-week-old female SCID C.B-17 mice. Treatment began upon tumour establishment (Day 8). Animals were treated IP with control (PBS and corn oil), salicylate, etoposide (36 mg/kg in corn oil), or salicylate plus etoposide. Control and salicylate were administered on Days 8, 9, 10, and 11, and etoposide was administered on Day 11 (repeated weekly for seven weeks). Treatments were repeated on a weekly basis for eight consecutive weeks. Data representing five animals per treatment group from a single experiment are shown. Data were analyzed by multiple unpaired Student's t-tests (*significantly different from control; # etoposide vs. salicylate plus etoposide; $p < 0.01$).

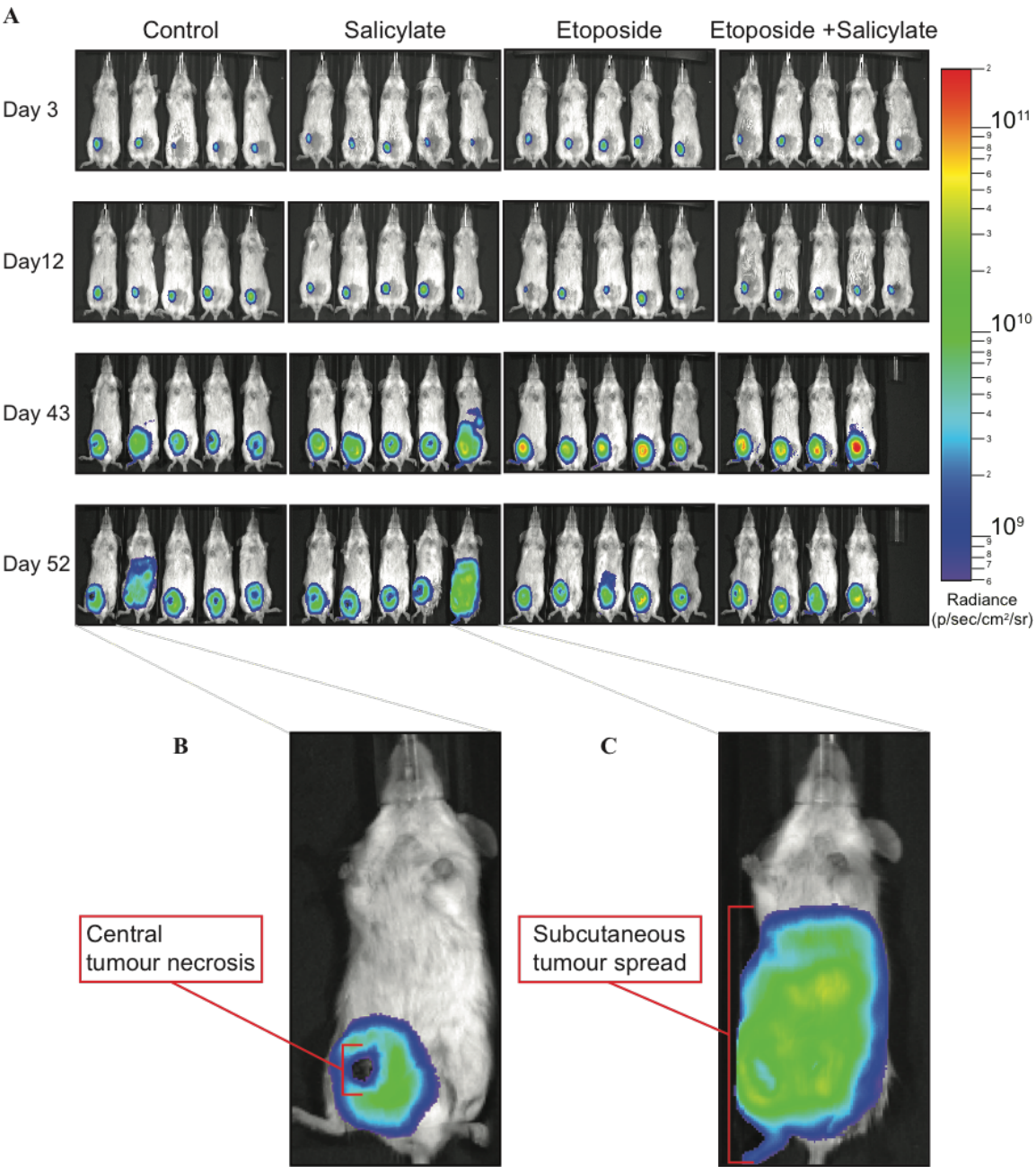
A
Control
Salicylate
Etoposide
Etoposide +Salicylate
Day 3
Day12
Day 43
Day 52
10^{11}
10^{10}
10^{9}
Radiance
(p/sec/cm²/sr)
B
C
Central
tumour necrosis
Subcutaneous
tumour spread

Figure 4.17 *In vivo* bioluminescence imaging of orthotopic MDA-MB-231 tumours shows central tumour necrosis and subcutaneous spread in SCID mice.

A) To monitor tumour progression and metastatic dissemination, animals were imaged immediately before, and 1, 6, and 8 weeks after the commencement of treatment. Selected ventral view of representative mice demonstrating B) central tumour necrosis, and corresponding bioluminescence signal disruption and C) subcutaneous tumour spread and more distant metastases. Images were set to the same pseudocolour scale to demonstrate relative bioluminescent signals.

Anti-tumour activity of etoposide therapy, as indicated by caliper measurements of tumour size, was accompanied by a corresponding significant difference in survival outcome ($p < 0.01$) (Figure 4.18). As hypothesized, when salicylate was co-administered, etoposide-induced survival was significantly reduced ($p < 0.01$). All mice treated with etoposide alone survived until the end of the experiment (Day 63). In contrast, by Day 54 100% (5/5) of vehicle treated mice, 80% (4/5) of salicylate-treated mice, and 60% (3/5) of mice co-treated with salicylate and etoposide had been euthanized due to the size of their tumours.

In summary, a regimen of 200 mg/kg salicylate significantly diminished etoposide-induced attenuation of tumour growth and etoposide-induced survival in mice co-treated with 36 mg/kg etoposide, thus replicating the findings reported in section 4.4.

4.6 Summary and Significance

As mentioned previously, translational research tests hypotheses, based on *in vitro* and/or *in cyto* observations, in models that better represent the complexity of a whole organism and what may be observed in a clinical environment. Living systems are complex; consequently, the therapeutic window of a drug reported in one *in vivo* cancer model may shift significantly depending on variables including the genetic background of the host and the susceptibility of the cancer to treatment. The hyper-toxicity of doxorubicin and the prolonged process of identifying a therapeutic etoposide regimen reported in this chapter exemplify the challenges of using *in vivo* models.

Following optimization, 36 mg/kg etoposide was identified as a therapeutic treatment regimen that induced significant anti-tumour activity in SCID C.B-17 mice

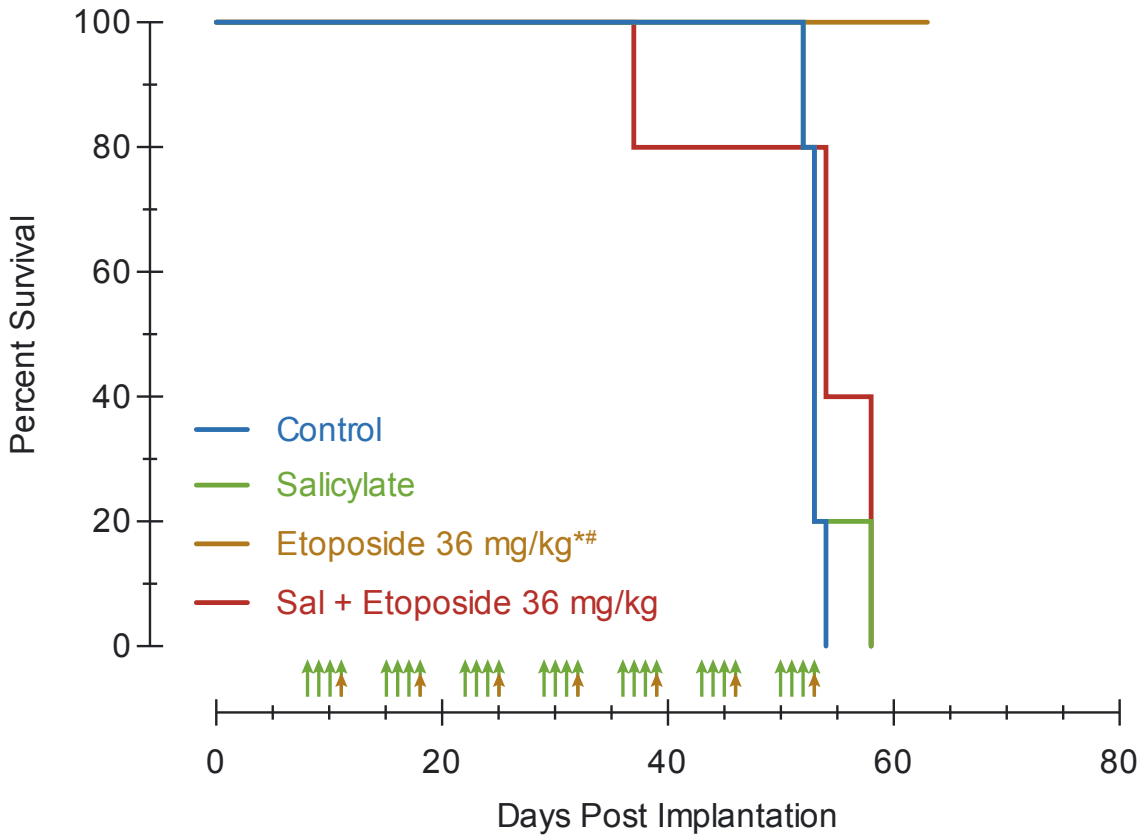
100
80
60
40
20
0
Percent Survival
Control
Salicylate
Etoposide 36 mg/kg*#
Sal + Etoposide 36 mg/kg
0
20
40
60
80
Days Post Implantation

Figure 4.18 Salicylate co-administration significantly reduces etoposide-induced survival in murine xenograft model of human breast cancer. (Experiment 4)

Human breast cancer MDA-MB-231 cells expressing luciferase were injected into the mammary fat pad of 6 to 7-week-old female SCID C.B-17 mice. Treatment began on upon tumour establishment (Day 8). Animals were treated IP with control (PBS and corn oil), salicylate, etoposide (36 mg/kg), or salicylate plus etoposide. Control and salicylate were administered on Days 8, 9, 10, and 11, and etoposide was administered on Day 11 (repeated weekly for seven weeks). Data representing five animals per treatment group from a single experiment are shown. Kaplan-Meier plot with log-rank (Mantel-Cox) test for curve comparison (*significantly different from control; # etoposide vs. salicylate plus etoposide; $p < 0.01$).

bearing MDA-MB-231-LUC human breast cancer tumours. However, etoposide-induced anti-tumour activity and etoposide-induced survival were significantly diminished in mice co-treated with 200 mg/kg salicylate. This finding supports the hypothesis that the co-administration of the salicylate, the primary metabolite of ASA, significantly reduces the anticancer efficacy of etoposide *in vivo*.

Chapter Five: Discussion

5.1 Summary

The advent of ASA in the late 19th century, and its subsequent commercial marketing under the trade name Aspirin by Bayer Pharmaceuticals in 1899, spurred the globally pervasive use observed today. The primary metabolite of ASA is salicylate, a compound that has been used in the form of plant extracts for millennia to treat various medical ailments. Albeit a highly effective anti-inflammatory, anti-platelet, and anti-pyretic drug, today ASA is most commonly used daily in low-dose for the prevention of secondary occlusive vascular events (*i.e.* heart attack or stroke) (Antithrombotic Trialists' Collaboration, 2002). Accumulating evidence suggests that the broad pharmacologic effects of ASA are not dependent on COX inhibition (Kopp & Ghosh, 1994; Bozza *et al.*, 1996; Takahashi *et al.*, 2008; Gurpinar *et al.*, 2013). Salicylate and ASA have multiple cellular targets, such as AMPK, AKT, ERK, NFκB, and p38 MAPK (Figure 1.5); however, the full mechanistic network by which ASA and salicylate act is still unknown (Kopp & Ghosh, 1994; Schwenger *et al.*, 1998; Ricchi *et al.*, 2003; Chae *et al.*, 2004; Stark *et al.*, 2007; Serizawa *et al.*, 2014).

Recently, salicylate was identified as a catalytic inhibitor of the essential nuclear enzyme TOP2A (Bau & Kurz, 2011; Bau *et al.*, 2014). TOP2A resolves constraints in DNA topology that interfere with critical cellular processes. The enzyme acts by inducing transient DNA DSBs to aid in the management of DNA supercoiling and catenanes. TOP2 inhibition can be achieved through either poisoning, where the TOP2-DNAcc is covalently stabilized leading to the accumulation of lethal DNA DSBs, or through

catalytic inhibition, where essential TOP2 activity is compromised without the covalent stabilization of the TOP2-DNAcc. Several long-standing chemotherapeutic agents are TOP2 poisons. The anti-tumour activity of drugs like doxorubicin, the gold-standard treatment for breast cancer, and etoposide are reliant on the induction of these cytotoxic TOP2-mediated DNA DSBs. Salicylate, in contrast, catalytically inhibits TOP2A by inhibiting DNA cleavage and, to a lesser degree, by non-competitively inhibiting ATPase activity (Bau *et al.*, 2014). Through these actions, salicylate prevents the formation of the TOP2-DNAcc that TOP2 poisons stabilize. Salicylate pretreatment attenuates not only the formation of TOP2 poison-mediated DSBs, but also TOP2 poison-induced cytotoxicity in MCF-7 cells (Bau & Kurz, 2011).

In this thesis, the effect of salicylate on the cellular response to the TOP2 poisons doxorubicin and etoposide was further characterised in a panel of human and murine breast cancer cell lines. The cell lines were chosen to reflect the molecular heterogeneity observed in populations of breast cancer patients. At concentrations similar to those reported in the plasma of patients taking anti-inflammatory doses of ASA, salicylate co-treatment significantly attenuated TOP2 poison-mediated cytotoxicity in luminal A, basal, claudin-low, and, to a lesser degree, HER2-overexpressing subtypes of human breast cancer. Furthermore, the cytoprotective effect of salicylate against TOP2 poisons was conserved in murine breast cancer cells. TOP2A expression directly correlates with TOP2 poison sensitivity (Burgess *et al.*, 2008). However, relative TOP2A expression was similar across molecular subtypes, and thus could not account for the variation observed across the cell lines.

Salicylate-mediated attenuation of TOP2 poison cytotoxicity in HER2+ SK-BR-3 cells was the least pronounced of the cell lines analyzed. HER2 is a receptor tyrosine kinase located upstream of several signal transduction pathways that regulate cellular processes associated with proliferation, migration, survival, and cell growth. Some of the affected pathways include RAS-MAPK (mitogen-activated protein kinase), PI3K (phosphatidylinositol 3-kinase)-AKT, SRC tyrosine kinase, and STAT (signal transducer and activator of transcription) (Hynes & Lane, 2005; Carpenter & Lo, 2013). HER2 overexpression promotes PI3K-AKT signalling and subsequent activation of NFκB signaling pathways is known to inhibit apoptosis, stimulate cell proliferation, and promote cancer cell migration and invasion (Beg & Baltimore, 1996; Liu *et al.*, 1996; Van Antwerp *et al.*, 1996; Wang *et al.*, 1996; Joyce *et al.*, 2001; Huang *et al.*, 2001). Given the complexity of HER2 overexpression on cancer-related pathways, the cellular promiscuity of salicylate, and the prominent nodes of signalling crosstalk shared by the two systems (*e.g.* PI3K, AKT, STAT, NFκB, and MAPK), further research is required to explain the diminished cytoprotective effect of salicylate on TOP2 poison-induced cytotoxicity in HER2+ cells (Kopp & Ghosh, 1994; Schwenger *et al.*, 1998; Ricchi *et al.*, 2003; Chae *et al.*, 2004; Hynes & Lane, 2005; Stark *et al.*, 2007; Carpenter & Lo, 2013; Serizawa *et al.*, 2014).

A murine xenograft model of human breast cancer was used to establish the effect of salicylate co-administration on TOP2 poison based chemotherapy *in vivo*. The effect was first monitored in SCID C.B.-17 mice bearing MDA-MB-231 tumours and receiving either doxorubicin or etoposide treatment. Although the dose levels and schedule were based on those reported in the literature, the chosen dose of doxorubicin proved toxic and

etoposide produced no observable therapeutic effect independent of salicylate co-administration. The observed intolerance to doxorubicin treatment, and because doxorubicin acts through TOP2-independent mechanisms, it was decided that doxorubicin would not be used for subsequent *in vivo* experiments in this study. Instead, the remaining *in vivo* experiments were carried out using the uniquely TOP2-specific drug etoposide. Appropriate adjustments were made to etoposide treatment regimens until a therapeutic window was achieved and drug solubility had been optimized.

Once a therapeutic etoposide regimen was identified, the effect of salicylate co-administration was observable in tumour-bearing mice. As predicted, the co-administration of salicylate significantly reduced etoposide-mediated anti-tumour activity. Furthermore, etoposide-mediated survival was significantly attenuated by salicylate co-administration. This adds further support to the hypothesis that salicylate co-administration would be detrimental to the treatment outcome of women receiving TOP2 poison-based chemotherapy for the treatment of breast cancer.

5.2 Translational Implications of Salicylate-Induced Attenuation of Etoposide Therapeutic Efficacy in Breast Cancer.

Given the widespread use of ASA, the observations presented in this thesis could have significant clinical implications for women taking salicylates and undergoing TOP2 poison-based chemotherapy for the treatment of breast cancer. Salicylates, when administered at therapeutic doses, can reach high micromolar/low millimolar concentrations in patient plasma (Grosser *et al.*, 2011). Although a major source of salicylates, exposure to salicylates is not limited to the consumption of salicylate-based

pharmaceuticals (*i.e.* ASA, sulfasalazine, and diflunisal). The ingestion of plant-based foods containing high levels of salicylic acid, a ubiquitous plant hormone, is another common source of salicylates (Swain *et al.*, 1985; Wood *et al.*, 2011). Estimates of the dietary intake of salicylate range from less than 5 mg/day up to 200 mg/day (Swain *et al.*, 1985; Wood *et al.*, 2011). Like other phytochemicals, factors such as plant varieties, growing conditions, processing, storage and preparation may influence the salicylate content of food (Cermak *et al.*, 2009). Major dietary sources of salicylates include alcoholic beverages (22% of total salicylate intake), herbs and spices (17%), fruit (16%), non-alcoholic beverages (13%), tomato-based sauces (12%), and vegetables (9%) (Wood *et al.*, 2011). Although there are no data on the effect of a specifically salicylate-rich diet on salicylate plasma, one study did, however, look at the serum levels of salicylic acid in vegetarians, non-vegetarians, and non-vegetarians taking daily low-dose ASA (75 mg/day). Serum levels of salicylic acid were significantly higher in vegetarians (0.04–2.47 μM) than non-vegetarians (0.02-0.20 μM), but only a fraction of what was measured in those taking low-dose ASA (0.23–25.40 μM) (Blacklock *et al.*, 2001). Given that salicylate concentrations as low as 0.1 μM can inhibit COX-2 transcription, a salicylate-rich diet could have clinically relevant implications.

The work presented in this thesis demonstrates that salicylate attenuation of TOP2 poison activity in cultured human breast cancer cells is conserved in murine breast cancer cells and across cells representing human breast cancer subtypes. Furthermore, *in vivo* work presented herein demonstrates that salicylate attenuates the efficacy of etoposide and negatively impacts survival in a xenograft model of human breast cancer. These

observations add further evidence that salicylate exposure may pose a significant risk for women receiving TOP2 poison-based chemotherapy for the treatment of breast cancer.

5.3 Challenges of Animal Models

The use of preclinical animal models is an essential step for the translation of research findings from bench to bedside. A preclinical model, by definition, approximates a clinical condition. To maintain translatable clinical value, several factors must be considered in the experimental design. First, the dose, route of administration, and treatment schedule should reflect the drug concentrations and dosing regimens used in patients. Inappropriate dose translation can often explain drug ineffectiveness between species (Reagan-Shaw *et al.*, 2008; Blanchard & Smoliga, 2015). Second, choosing endpoints that are clinically relevant to patient outcome enhances translational value. For example, tumour size is often used as the primary endpoint in animal models of cancer, while overall or progression-free survival is a more common endpoint in cancer clinical trials. Third, in model systems, treatment is often initiated before or just after disease initiation, whereas in the clinic, treatment initiation occurs after the onset of symptoms and a clear diagnosis. This inconsistency can lead to an overestimation of the pharmacological effect due to therapeutic intervention earlier in the disease process. Lastly, special conditions of the pathophysiology and target of interest must be considered. Even the best-suited animal model will not yield conclusive results if any one of these factors is overlooked in the experimental design process.

The *in vivo* study presented here is a prime example of the challenges faced in translational research. The doses and treatment schedule of doxorubicin and etoposide

administered in the first *in vivo* experiment were selected based on respective therapeutic windows reported in similar models (Wheeler *et al.*, 1982; Reichman *et al.*, 1989; Bellamy *et al.*, 1993; Remichkova *et al.*, 2008). However, the selected treatment regimens did not perform as predicted. In MDA-MB-231 tumour-bearing SCID mice, a single administration of 8 mg/kg doxorubicin was unexpectedly toxic. Conversely, weekly administration of 12 mg/kg etoposide was not toxic, and had no measurable therapeutic effect. Further *in vivo* work with doxorubicin was abandoned due to its toxicity in this model system. The SCID phenotype is the result of a spontaneous mutation in the $Prkdc^{scid}$ gene, which encodes the DNA-dependent protein kinase catalytic subunit (DNA-PKcs) (Jhappan *et al.*, 1997). DNA-PKcs is the catalytic subunit of DNA-dependent protein kinase (DNA-PK), a nuclear protein required for DNA damage repair through non-homologous end joining, a DNA repair pathway that rejoins DNA DSBs and is essential for the V(D)J recombination required for T and B cell maturation (Hendrickson *et al.*, 1991; Blunt *et al.*, 1995). In SCID mice, a nonsense mutation located in the sequence encoding the C-terminal region of DNA-PKcs results in a truncated DNA-PKcs missing the last 83 amino acids of the kinase domain (Blunt *et al.*, 1996; Danska *et al.*, 1996; Araki *et al.*, 1997). Although the motifs required for kinase activity are preserved, the truncated protein is highly unstable, resulting in low levels of DNA-PKcs protein, ultimately leading to profound attenuation of DNA DSB repair (Danska *et al.*, 1996; Kurimasa *et al.*, 1999). Doxorubicin and etoposide induce DNA DSBs through stabilization of the TOP2-DNAcc. However, a significant portion of etoposide-mediated DNA damage is the consequence of DNA SSBs (Bromberg *et al.*, 2003). The majority of doxorubicin-mediated DNA damage results in DNA DSBs,

supplemented by DNA intercalation and oxidative damage (Goodman & Hochstein, 1977; Thorn *et al.*, 2011). These discrepancies between the mechanisms of the doxorubicin and etoposide could explain why doxorubicin, and not etoposide, was lethal in SCID C.B.-17 mice.

Subsequent *in vivo* experiments focused on the optimization of the etoposide dose; however, further issues arose. The large volume of aqueous solvent required to prevent etoposide precipitation far exceeded the maximum drug administration volume recommended for this model system. To resolve this, a hydrophobic solvent (*i.e.* corn oil) was used. Modifying the etoposide solvent reduced previous variation observed in both etoposide-mediated anti-tumour activity and survival. High intra- and inter-group variation in groups receiving aqueous etoposide suspension was likely due to drug precipitation post-administration. The bioavailability of a drug decreases significantly if it precipitates out of solution; etoposide, in particular, becomes significantly less stable as a precipitate (Joel *et al.*, 1995).

5.4 Future Directions

The findings presented in this thesis form a solid foundation for further research that could significantly improve our understanding of the relationship between salicylates and TOP2 poisons *in vivo*. Admittedly, these observations were made in immunocompromised mice bearing tumours initiated from a single human breast cancer cell line. Because of the complexity and heterogeneity of breast cancer, this one model alone cannot be expected to recapitulate all facets of this disease. The predictive nature of xenografts has been shown to improve when preclinical outcomes are observed in more

than a single model system (Gould *et al.*, 2015). Thus, to establish conclusive clinically relevance, further preclinical studies using a variety of models should be conducted to avoid a preclinical-clinical disconnect.

5.4.1 Determining if the Salicylate-Induced Attenuation of Anti-Cancer Therapy Observed In Vivo is TOP2-Dependent

Here, salicylate co-treatment negatively influenced the chemotherapeutic efficacy of the TOP2 poison etoposide in a xenograft model of human breast cancer. *In vivo* models are complex, and isolating cause and effect can be challenging given the interconnectedness of cellular processes and signalling pathways. Salicylate is a highly promiscuous compound affecting numerous cellular processes including cell cycle progression, proliferation, inflammation and apoptosis through its many targets. Although the results presented here highlight that salicylate attenuates the efficacy of etoposide, further inquiry is needed to establish whether this effect is due to the catalytic inhibition of TOP2A by salicylate. One way to provide more evidence that this effect is TOP2A-dependent would be to replicate the final *in vivo* experiment presented in this thesis with a non-TOP2 targeting chemotherapeutic such as cisplatin. Female SCID mice bearing MDA-MB-231 tumours would be split into four treatment groups: (1) vehicle control, (2) 200 mg/kg salicylate alone, (3) 20 mg/kg cisplatin alone, or (4) salicylate and cisplatin (Wang *et al.*, 2012). A weekly treatment schedule of salicylate administration on days 1, 2, 3, and 4, and cisplatin administration on day 4 would be repeated for eight cycles. If salicylate co-administration were to elicit a decrease in the efficacy of non-TOP2 targeting drugs, then it could be concluded that the observed effects of salicylate are

TOP2A-independent. Follow-up studies could investigate the effect in a xenograft model of a different breast cancer subtype. Furthermore, the *in vivo* effect of salicylate co-administration on the efficacy of doxorubicin could also be revisited in a less sensitive xenograft model.

5.4.2 Validating the In Vivo Effect of Salicylate Co-Administration on the Therapeutic Efficacy of Etoposide in an Immunocompetent Model of Breast Cancer

The *in vivo* results presented here were obtained from SCID C.B.17 mice bearing human breast cancer tumours. As previously stated, the SCID phenotype is the result of a mutation in the gene encoding DNA-PKcs, a protein required for V(D)J recombination and immune system maturation. Without DNA-PKcs activity, T- and B-lymphocytes, involved in cell-mediated and antibody-mediated immunity, respectively, cannot mature. Thus, the SCID mutation results in a lack of functional lymphocytes, rendering affected mice severely immunocompromised. In preclinical research, immunodeficient hosts are beneficial because human tumour cells can be implanted without fear of immune-mediated host-versus-graft rejection. However, using an immunocompromised model for cancer research also has its drawbacks.

There is considerable evidence that supports an important functional role for immune cells in the tumour microenvironment (Grivennikov *et al.*, 2010; DiDonato *et al.*, 2012; Nakanishi & Rosenberg, 2013). Lymphocytes affect cancer cells through production of chemokines, cytokines, growth factors, prostaglandins, and reactive oxygen and nitrogen species. Inflammation affects every stage of tumorigenesis, from initiation and tumour growth, to tumour metastasis (Grivennikov *et al.*, 2010). Without a functional

immune system, the complex balance of interactions between anti-cancer therapies and immunoresponsive cell types cannot be fully appreciated.

Tumour-promoting inflammation can contribute to malignant disease through supplying the tumour microenvironment with bioactive molecules that sustain proliferative signaling, limit cell death, promote angiogenesis, invasion and metastasis, and activate epithelial-to-mesenchymal transition (Sparmann & Bar-Sagi, 2004; Condeelis & Pollard, 2006; Yu *et al.*, 2007; Bollrath *et al.*, 2009). Inflammatory signalling pathways often operate under positive feed-forward loops. An example of this can be found in tumour-infiltrating immune cells, where activation of NFκB promotes the production of cytokines that, in turn, signal adjacent tumour cells to activate NFκB, producing chemokines that attract more infiltrating immune cells (DiDonato *et al.*, 2012). This is especially relevant given the anti-inflammatory action salicylate elicits through modulating the NFκB signalling pathway (Kopp & Ghosh, 1994).

Combined, these observations suggest the introduction of immunocompetency has the potential to alter the effect of salicylate on etoposide efficacy observed in the current xenograft model. Thus, further research using a syngeneic model is warranted. The cytotoxicity assays using the murine breast cancer cell line EMT-6 reported here were conducted with future syngeneic experiments in mind. To determine the effects of immunocompetence, a syngeneic model of murine breast cancer, where EMT-6 cells are transplanted into female Balb/c mice, could be used. Once tumours were established, mice would be sorted randomly into one of four treatment groups, each carrying equal average tumour burdens: (1) vehicle control, (2) 200 mg/kg salicylate alone, (3) etoposide alone (dose to be determined through preliminary work), or (4) salicylate and etoposide.

A weekly treatment schedule of salicylate administration on days 1, 2, 3, and 4, and etoposide administration on day 4 would be repeated for eight cycles. If the results reflect those observed in the xenograft model, then it could be concluded that effect of salicylate is present in animals with functioning immune systems, adding further support to the clinical relevance of this model.

5.4.3 Exploring the Effect of ASA Co-Administration on Doxorubicin-Induced Cardiomyopathy In Vivo

Doxorubicin, although one of the most effective chemotherapeutics in use today, is cytotoxic. Some side effects of its use include alopecia, extravasation, hematopoietic suppression, nausea, and vomiting; however, the greatest concern is cardiotoxicity and the resulting development of heart failure. The single greatest risk factor for the development of doxorubicin-induced heart failure is the cumulative lifetime dose of doxorubicin a patient receives. The risk significantly increases after the cumulative dose of 400 mg/m^2 at 5% prevalence of heart failure, to 26% and 48% at cumulative doses of 500 mg/m^2 and 700 mg/m^2, respectively (Gianni *et al.*, 2007; Octavia *et al.*, 2012).

Multiple molecular mechanisms are involved in doxorubicin cardiotoxicity. These mechanisms include oxidative stress, apoptotic signalling, intracellular Ca^{2+} dysregulation, and novel cytotoxic mechanisms including COX-2 inhibition and TOP2B poisoning. ASA acts as both a potent antioxidant and a COX-2 inhibitor. Thus, the effect of ASA co-administration on doxorubicin-induced cardiomyopathy, whether cytoprotective (through its antioxidant activity) or synergistically toxic (through COX-2 inhibition), has potential clinical importance. This knowledge could provide further

insight in to determining if the use of ASA-containing pharmaceuticals should be discouraged in patients receiving doxorubicin anticancer therapy.

Although the animal model used in the work presented in this thesis did not tolerate doxorubicin treatment, studies investigating doxorubicin-induced cardiotoxicity *in vivo* have developed models that are more tolerant of the drug (Nagendran *et al.*, 2013; Milano *et al.*, 2014). One such model induces cardiomyopathy in CB57BL/6J mice by a single IP injection of 15 mg/kg doxorubicin. Significant functional deterioration of cardiac tissue was reported two weeks after disease induction. To establish the effect co-administration of ASA may have on doxorubicin-induced cardiomyopathy, a similar model could be employed with mice receiving one of four treatments: (1) vehicle control, (2) 200 mg/kg ASA alone, (3) 15 mg/kg doxorubicin alone, or (4) ASA and doxorubicin, with salicylate administered as a daily dose starting one week prior to doxorubicin exposure. Two weeks after doxorubicin treatment, the effect of salicylate co-administration could be characterized using echocardiography, cardiac catheterization, and pathological assays to compare the degree of functional and pathological cardiac deterioration between treatment groups. If ASA co-treatment resulted in a cytoprotective effect (*i.e*. doxorubicin-induced cardiotoxicity were significantly decreased), then ASA could potentially be used as a prophylactic therapy for the prevention of doxorubicin-induced cardiotoxicity, provided it does not compromise chemotherapeutic efficacy. However, if ASA co-treatment elicited a synergistically cardiotoxic effect (*i.e*. doxorubicin-induced cardiotoxicity was significantly increased), it would provide further evidence that ASA use by patients receiving doxorubicin therapy should be discouraged.

5.5 Final Remarks and Conclusion

The work presented in this thesis has significantly enhanced the understanding of the effects of salicylate on the efficacy of TOP2 poisons. Through this work, I have demonstrated that salicylate attenuates TOP2 poison-mediated cytotoxicity in an array of breast cancer cell lines. Moreover, I have demonstrated that the addition of daily salicylate treatment significantly reduces the efficacy of etoposide anti-tumour therapy in orthotopic murine xenografts of human breast cancer. Given the prominence of TOP2 poison-based chemotherapy, the widespread use of ASA, and the prevalence of other salicylates, this work provides a substantial foundation for further investigation to establish if salicylate use should be discouraged in women receiving TOP2 poison-based for the treatment of breast cancer.

References

Ajani UA, Ford ES, Greenland KJ, Giles WH & Mokdad AH (2006). Aspirin Use among U.S. Adults: Behavioral Risk Factor Surveillance System. *Am J Prev Med* **30,** 74–77.

Akimitsu N, Adachi N, Hirai H, Hossain MS, Hamamoto H, Kobayashi M, Aratani Y, Koyama H & Sekimizu K (2003). Enforced Cytokinesis Without Complete Nuclear Division in Embryonic Cells Depleting the Activity of DNA Topoisomerase IIα. *Genes to Cells* **8,** 393–402.

Algra AM & Rothwell PM (2012). Effects of Regular Aspirin on Long-Term Cancer Incidence and Metastasis: A Systematic Comparison of Evidence from Observational Studies versus Randomised Trials. *Lancet Oncol* **13,** 518–527.

Antithrombotic Trialists' Collaboration (2002). Collaborative Meta-Analysis of Randomised Trials of Antiplatelet Therapy for Prevention of Death, Myocardial Infarction, and Stroke in High Risk Patients. *BMJ* **324,** 71–86.

Araki R, Fujimori A, Hamatani K, Mita K, Saito T, Mori M, Fukumura R, Morimyo M, Muto M, Itoh M, Tatsumi K & Abe M (1997). Nonsense Mutation at Tyr-4046 in the DNA-Dependent Protein Kinase Catalytic Subunit of Severe Combined Immune Deficiency Mice. *Proc Natl Acad Sci U S A* **94,** 2438–2443.

Arcamone F, Cassinelli G, Fantini G, Grein A, Orezzi P, Pol C & Spalla C (1969). Adriamycin, 14-Hydroxydaunomycin, a New Antitumor Antibiotic from S. Peucetius Var. Caesius. *Biotechnol Bioeng* **11,** 1101–1110.

Ashour ME, Atteya R & El-Khamisy SF (2015). Topoisomerase-Mediated Chromosomal Break Repair: An Emerging Player in Many Games. *Nat Rev Cancer* **15,** 137–151.

Austin CA, Sng JH, Patel S & Fisher LM (1993). Novel HeLa Topoisomerase II Is the II Beta Isoform: Complete Coding Sequence and Homology with Other Type II Topoisomerases. *Biochim Biophys Acta* **1172,** 283–291.

Baigent C, Collins R, Appleby P, Parish S, Sleight P & Peto R (1998). ISIS-2: 10 Year Survival among Patients with Suspected Acute Myocardial Infarction in Randomised Comparison of Intravenous Streptokinase, Oral Aspirin, Both, or Neither. The ISIS-2 (Second International Study of Infarct Survival) Collaborative Group. *BMJ* **316,** 1337–1343.

Barnes PJ & Karin M (1997). Nuclear Factor-κB — A Pivotal Transcription Factor in Chronic Inflammatory Diseases. *N Engl J Med* **336,** 1066–1071.

Barpe DR, Rosa DD & Froehlich PE (2010). Pharmacokinetic Evaluation of Doxorubicin Plasma Levels in Normal and Overweight Patients with Breast Cancer and Simulation of Dose Adjustment by Different Indexes of Body Mass. *Eur J Pharm Sc* **41,** 458–463.

Bau JT, Kang Z, Austin CA & Kurz EU (2014). Salicylate, a Catalytic Inhibitor of Topoisomerase II, Inhibits DNA Cleavage and Is Selective for the α Isoform. *Mol Pharmacol* **85,** 198–207.

Bau JT & Kurz EU (2011). Sodium Salicylate Is a Novel Catalytic Inhibitor of Human DNA Topoisomerase II Alpha. *Biochem Pharmacol* **81,** 345–354.

Bau JT & Kurz EU (2014). Structural Determinants of the Catalytic Inhibition of Human Topoisomerase IIα by Salicylate Analogs and Salicylate-Based Drugs. *Biochem Pharmacol* **89,** 464–476.

Baxter J & Diffley JFX (2008). Topoisomerase II Inactivation Prevents the Completion of DNA Replication in Budding Yeast. *Mol Cell* **30,** 790–802.

Beg AA & Baltimore D (1996). An Essential Role for NF-kB in Preventing TNF-α - Induced Cell Death. *Science* **274,** 782–784.

Bellamy WT, Odeleye A, Finley P, Huizenga B, Dalton WS, Weinstein RS, Hersh EM & Grogan TM (1993). An In Vivo Model of Human Multidrug-Resistant Multiple Myeloma in SCID Mice. *Am J Pathol* **142,** 691–697.

Bennett A & Del Tacca M (1975). Proceedings: Prostaglandins in Human Colonic Carcinoma. *Gut* **16,** 409.

Berger JM, Gamblin SJ, Harrison SC & Wang JC (1996). Structure and Mechanism of DNA Topoisomerase II. *Nature* **379,** 225–232.

Bergh J, Norberg T, Sjögren S, Lindgren A & Holmberg L (1995). Complete Sequencing of the p53 Gene Provides Prognostic Information in Breast Cancer Patients, Particularly in Relation to Adjuvant Systemic Therapy and Radiotherapy. *Nat Med* **1,** 1029–1034.

Blacklock CJ, Lawrence JR, Wiles D, Malcolm EA, Gibson IH, Kelly CJ & Paterson JR (2001). Salicylic Acid in the Serum of Subjects Not Taking Aspirin. Comparison of Salicylic Acid Concentrations in the Serum of Vegetarians, Non-Vegetarians, and Patients Taking Low Dose Aspirin. *J Clin Pathol* **54,** 553–555.

Blanchard OL & Smoliga JM (2015). Translating Dosages from Animal Models to Human Clinical Trials—Revisiting Body Surface Area Scaling. *FASEB J* **29,** 1629–1634.

Blunt T, Finnie NJ, Taccioli GE, Smith GCM, Demengeot J, Gottlieb TM, Mizuta R, Varghese AJ, Alt FW, Jeggo PA & Jackson SP (1995). Defective DNA-Dependent Protein Kinase Activity is Linked to V(D)J Recombination and DNA Repair Defects Associated with whe Murine SCID Mutation. *Cell* **80,** 813–823.

Blunt T, Gell D, Fox M, Taccioli GE, Lehmann AR, Jackson SP & Jeggo PA (1996). Identification of a Nonsense Mutation in the Carboxyl-Terminal Region of DNA-Dependent Protein Kinase Catalytic Subunit in the Scid Mouse. *Proc Natl Acad Sci USA* **93,** 10285–10290.

Bollrath J, Phesse TJ, von Burstin VA, Putoczki T, Bennecke M, Bateman T, Nebelsiek T, Lundgren-May T, Canli Ö, Schwitalla S, Matthews V, Schmid RM, Kirchner T, Arkan MC, Ernst M & Greten FR (2009). gp130-Mediated Stat3 Activation in Enterocytes Regulates Cell Survival and Cell-Cycle Progression during Colitis-Associated Tumorigenesis. *Cancer Cell* **15,** 91–102.

Børresen AL, Andersen TI, Eyfjörd JE, Cornelis RS, Thorlacius S, Borg A, Johansson U, Theillet C, Scherneck S & Hartman S (1995). TP53 Mutations and Breast Cancer Prognosis: Particularly Poor Survival Rates for Cases with Mutations in the Zinc-Binding Domains. *Genes Chromosomes Cancer* **14,** 71–75.

Box VGS (2007). The Intercalation of DNA Double Helices with Doxorubicin and Nogalamycin. *J Mol Graph Model* **26,** 14–19.

Bozza PT, Payne JL, Morham SG, Langenbach R, Smithies O & Weller PF (1996). Leukocyte Lipid Body Formation and Eicosanoid Generation: Cyclooxygenase-Independent Inhibition by Aspirin. *Proc Natl Acad Sci USA* **93,** 11091–11096.

Brase JC, Schmidt M, Fischbach T, Sültmann H, Bojar H, Koelbl H, Hellwig B, Rahnenführer J, Hengstler JG & Gehrmann MC (2010). ERBB2 and TOP2A in Breast Cancer: A Comprehensive Analysis of Gene Amplification, RNA Levels, and Protein Expression and Their Influence on Prognosis and Prediction. *Clin Cancer Res* **16,** 2391–2401.

Bromberg KD, Burgin AB & Osheroff N (2003). A Two-Drug Model for Etoposide Action Against Human Topoisomerase II Alpha. *J Biol Chem* **278,** 7406–7412.

Brown P, Peebles C & Cozzarelli N (1979). Topoisomerase from Escherichia Coli Related to DNA Gyrase. *Proc Natl Acad Sci U S A* **76,** 6110–6114.

Burgess DJ, Doles J, Zender L, Xue W, Ma B, McCombie WR, Hannon GJ, Lowe SW & Hemann MT (2008). Topoisomerase Levels Determine Chemotherapy Response In Vitro and In Vivo. *Proc Natl Acad Sci U S A* **105,** 9053–9058.

Canadian Cancer Society's Advisory Committee on Cancer Statistics (2015). *Canadian Cancer Statistics 2015*. Canadian Cancer Society, Toronto, ON.

Capranico G, Tinelli S, Austin CA, Fisher ML & Zunino F (1992). Different Patterns of Gene Expression of Topoisomerase II Isoforms in Differentiated Tissues during Murine Development. *Biochim Biophys Acta* **1132,** 43–48.

Carpenter RL & Lo H-W (2013). Regulation of Apoptosis by HER2 in Breast Cancer. *J Carcinog Mutagen* **2013,** 1–13.

Carvalho C, Santos RX, Cardoso S, Correia S, Oliveira PJ, Santos MS & Moreira PI (2009). Doxorubicin: The Good, the Bad and the Ugly Effect. *Curr Med Chem* **16,** 3267–3285.

Cermak R, Durazzo A, Maiani G, Boehm V, Kammerer DR, Carle R, Wiczkowski W, Piskula MK & Galensa R (2009). The Influence of Postharvest Processing and Storage of Foodstuffs on the Bioavailability of Flavonoids and Phenolic Acids. *Mol Nutr Food Res* **53,** S184–S193.

Chae H-J, Chae S-W, Reed JC & Kim H-R (2004). Salicylate Regulates COX-2 Expression through ERK and Subsequent NF-KappaB Activation in Osteoblasts. *Immunopharmacol Immunotoxicol* **26,** 75–91.

Champoux JJ (1981). DNA is Linked to the Rat-Liver DNA Nicking-Closing Enzyme by a Phosphodiester Bond to Tyrosine. *J Biol Chem* **256,** 4805–4809.

Champoux JJ (2001). DNA Topoisomerases: Structure, Function, and Mechanism. *Annu Rev Biochem* **70,** 369–413.

Chan AT, Arber N, Burn J, Chia WK, Elwood P, Hull MA, Logan RF, Rothwell PM, Schrör K & Baron JA (2012). Aspirin in the Chemoprevention of Colorectal Neoplasia: An Overview. *Cancer Prev Res* **5,** 164–178.

Chan AT, Ogino S & Fuchs CS (2007). Aspirin and the Risk of Colorectal Cancer in Relation to the Expression of COX-2. *N Engl J Med* **356,** 2131–2142.

Chariot A (2009). The NF-KappaB-Independent Functions of IKK Subunits in Immunity and Cancer. *Trends Cell Biol* **19,** 404–413.

Cheang MCU, Chia SK, Voduc D, Gao D, Leung S, Snider J, Watson M, Davies S, Bernard PS, Parker JS, Perou CM, Ellis MJ & Nielsen TO (2009). Ki67 Index, HER2 Status, and Prognosis of Patients with Luminal B Breast Cancer. *J Natl Cancer Inst* **101,** 736–750.

Cheang MCU, Voduc KD, Tu D, Jiang S, Leung S, Chia SK, Shepherd LE, Levine MN, Pritchard KI, Davies S, Stijleman IJ, Davis C, Ebbert MTW, Parker JS, Ellis MJ, Bernard PS, Perou CM & Nielsen TO (2012). Responsiveness of Intrinsic Subtypes to Adjuvant Anthracycline Substitution in the NCIC.CTG MA.5 Randomized Trial. *Clin Cancer Res* **18,** 2402–2412.

Classen S, Olland S & Berger JM (2003). Structure of the Topoisomerase II ATPase Region and Its Mechanism of Inhibition by the Chemotherapeutic Agent ICRF-187. *Proc Natl Acad Sci USA* **100,** 10629–10634.

Coates AS, Winer EP, Goldhirsch A, Gelber RD, Gnant M, Piccart-Gebhart M, Thürlimann B, Senn H-J & Panel Members (2015). Tailoring Therapies--Improving the Management of Early Breast Cancer: St Gallen International Expert Consensus on the Primary Therapy of Early Breast Cancer 2015. *Ann Oncol* **26,** 1533–1546.

Collaboration AT (1994). Collaborative Overview of Randomised Trials of Antiplatelet Therapy Prevention of Death, Myocardial Infarction, and Stroke by Prolonged Antiplatelet Therapy in Various Categories of Patients. *BMJ* **308,** 81–106.

Condeelis J & Pollard JW (2006). Macrophages: Obligate Partners for Tumor Cell Migration, Invasion, and Metastasis. *Cell* **124,** 263–266.

Cutts SM, Parsons PG, Sturm RA & Phillips DR (1996). Adriamycin-Induced DNA Adducts Inhibit the DNA Interactions of Transcription Factors and RNA Polymerase. *J Biol Chem* **271,** 5422–5429.

Cutts SM, Swift LP, Rephaeli A, Nudelman A & Phillips DR (2005). Recent Advances in Understanding and Exploiting the Activation of Anthracyclines by Formaldehyde. *Curr Med Chem Anticancer Agents* **5,** 431–447.

Cuzick J, Otto F, Baron JA, Brown PH, Burn J, Greenwald P, Jankowski J, La Vecchia C, Meyskens F, Senn HJ & Thun M (2009). Aspirin and Non-Steroidal Anti-Inflammatory Drugs for Cancer Prevention: An International Consensus Statement. *Lancet Oncol* **10,** 501–507.

Danska JS, Holland DP, Mariathasan S, Williams KM & Guidos CJ (1996). Biochemical and Genetic Defects in the DNA-Dependent Protein Kinase in Murine SCID. *Mol Cell Biol* **16,** 5507–5517.

Depew R, Liu L & Wang J (1978). Nteraction between DNA and Escherichia Coli Protein Omega. Formation of a Complex between Single-Stranded DNA and Omega Protein. *J Biol Chem* **253,** 511–518.

Deweese JE & Osheroff N (2009). The DNA Cleavage Reaction of Topoisomerase II: Wolf in Sheep's Clothing. *Nucleic Acids Res* **37,** 738–748.

DiDonato JA, Mercurio F & Karin M (2012). NF-κB and the Link Between Inflammation and Cancer. *Immunol Rev* **246,** 379–400.

Dikshit P, Chatterjee M, Goswami A, Mishra A & Jana NR (2006). Aspirin Induces Apoptosis through the Inhibition of Proteasome Function. *J Biol Chem* **281,** 29228–29235.

Di Leo A et al. (2011). HER2 and TOP2A as Predictive Markers for Anthracycline-Containing Chemotherapy Regimens as Adjuvant Treatment of Breast Cancer: A Meta-Analysis of Individual Patient Data. *Lancet Oncol* **12,** 1134–1142.

Di Renzo F, Cappelletti G, Broccia ML, Giavini E & Menegola E (2008). The Inhibition of Embryonic Histone Deacetylases as the Possible Mechanism Accounting for Axial Skeletal Malformations Induced by Sodium Salicylate. *Toxicol Sci* **104,** 397–404.

Doroshow JH & Kummar S (2014). Translational Research in Oncology—10 Years of Progress and Future Prospects. *Nat Rev Clin Oncol* **11,** 649–662.

Downes CS, Mullinger AM & Johnson RT (1991). Inhibitors of DNA Topoisomerase II Prevent Chromatid Separation in Mammalian Cells but Do Not Prevent Exit from Mitosis. *Proc Natl Acad Sci U S A* **88,** 8895–8899.

Drukker CA, Bueno-de-Mesquita JM, Retèl VP, van Harten WH, van Tinteren H, Wesseling J, Roumen RMH, Knauer M, van 't Veer LJ, Sonke GS, Rutgers EJT, van de Vijver MJ & Linn SC (2013). A Prospective Evaluation of a Breast Cancer Prognosis Signature in the Observational RASTER Study. *Int J Cancer* **133,** 929–936.

Duan Y, Chen F, Zhang A, Zhu B, Sun J, Xie Q & Chen Z (2014). Aspirin Inhibits Lipopolysaccharide-Induced COX-2 Expression and PGE(2) Production in Porcine Alveolar Macrophages by Modulating Protein Kinase C and Protein Tyrosine Phosphatase Activity. *BMB Rep* **47,** 45–50.

Dubois RN, Abramson SB, Crofford L, Gupta RA, Simon LS, Putte LBAVD & Lipsky PE (1998). Cyclooxygenase in Biology and Disease. *FASEB J* **12,** 1063–1073.

Du Q & Geller DA (2010). Cross-Regulation Between Wnt and NF-κB Signaling Pathways. *For Immunopathol Dis Therap* **1,** 155–181.

Du Y, Zhou Q, Yin W, Zhou L, Di G, Shen Z, Shao Z & Lu J (2011). The Role of Topoisomerase IIα in Predicting Sensitivity to Anthracyclines in Breast Cancer Patients: A Meta-Analysis of Published Literatures. *Breast Cancer Res Treat* **129,** 839–848.

Early Breast Cancer Trialists' Collaborative Group (2005). Effects of Chemotherapy and Hormonal Therapy for Early Breast Cancer on Recurrence and 15-Year Survival: An Overview of the Randomised Trials. *Lancet* **365,** 1687–1717.

Eckmann L, Stenson WF, Savidge TC, Lowe DC, Barrett KE, Fierer J, Smith JR & Kagnoff MF (1997). Role of Intestinal Epithelial Cells in the Host Secretory Response to Infection by Invasive Bacteria. Bacterial Entry Induces Epithelial Prostaglandin H Synthase-2 Expression and Prostaglandin E2 and F2α Production. *J Clin Invest* **100,** 296–309.

Eisen A, Fletcher GG, Gandhi S, Mates M, Freedman OC, Dent SF & Trudeau ME (2015). Optimal Systemic Therapy for Early Breast Cancer in Women: A Clinical Practice Guideline. *Curr Oncol* **22,** S67–S81.

Elston C w. & Ellis I o. (1991). Pathological Prognostic Factors in Breast Cancer. I. The Value of Histological Grade in Breast Cancer: Experience from a Large Study with Long-Term Follow-Up. *Histopathology* **19,** 403–410.

Feinberg H, Lima CD & Mondragón A (1999). Conformational Changes in E. Coli DNA Topoisomerase I. *Nat Struct Biol* **6,** 918–922.

Ferguson P, Fisher M, Stephenson J, Li D, Zhou B & Cheng Y (1988). Combined Modalities of Resistance in Etoposide-Resistant Human KB-Cell Lines. *Cancer Res* **48,** 5956–5964.

Ferlay J, Soerjomataram I, Dikshit R, Eser S, Mathers C, Rebelo M, Parkin DM, Forman D & Bray F (2015). Cancer Incidence and Mortality Worldwide: Sources, Methods and Major Patterns in GLOBOCAN 2012. *Int J Cancer* **136,** E359–E386.

Fisher ER, Costantino J, Fisher B & Redmond C (1993). Pathologic Findings From the National Surgical Adjuvant Breast Project (Protocol 4). Discriminants for 15-Year Survival. National Surgical Adjuvant Breast and Bowel Project Investigators. *Cancer* **71,** 2141–2150.

Flossmann E & Rothwell PM (2007). Effect of Aspirin on Long-Term Risk of Colorectal Cancer: Consistent Evidence from Randomised and Observational Studies. *Lancet* **369,** 1603–1613.

Forterre P & Gadelle D (2009). Phylogenomics of DNA Topoisomerases: Their Origin and Putative Roles in the Emergence of Modern Organisms. *Nucl Acids Res* **37,** 679–692.

Fortune JM & Osheroff N (1998). Merbarone Inhibits the Catalytic Activity of Human Topoisomerase IIα by Blocking DNA Cleavage. *J Biol Chem* **273,** 17643–17650.

Fry A, Chresta C, Davies S, Walker M, Harris A, Hartley J, Masters J & Hickson I (1991). Relationship Between Topoisomerase-II Level and Chemosensitivity in Human Tumor-Cell Lines. *Cancer Res* **51,** 6592–6595.

Fuster V & Sweeny JM (2011). Aspirin: A Historical and Contemporary Therapeutic Overview. *Circulation* **123,** 768–778.

Gadelle D, Filée J, Buhler C & Forterre P (2003). Phylogenomics of Type II DNA Topoisomerases. *BioEssays* **25,** 232–242.

Gala MK & Chan AT (2015). Molecular Pathways: Aspirin and Wnt Signaling—A Molecularly Targeted Approach to Cancer Prevention and Treatment. *Clin Cancer Res* **21,** 1543–1548.

Gandhi S, Fletcher GG, Eisen A, Mates M, Freedman OC, Dent SF & Trudeau ME (2014). Adjuvant Chemotherapy for Early Female Breast Cancer: A Systematic Review of the Evidence for the 2014 Cancer Care Ontario Systemic Therapy Guideline. *Curr Oncol* **22,** 82–94.

Gao R, Schellenberg MJ, Huang SN, Abdelmalak M, Marchand C, Nitiss KC, Nitiss JL, Williams RS & Pommier Y (2014). Proteolytic Degradation of Topoisomerase II (Top2) Enables the Processing of Top2·DNA and Top2·RNA Covalent Complexes by Tyrosyl-DNA-Phosphodiesterase 2 (TDP2). *J Biol Chem* **289,** 17960–17969.

Gasic GJ, Gasic TB & Murphy S (1972). Anti-Metastatic Effect of Aspirin. *Lancet* **2,** 932–933.

Gasic GJ, Gasic TB & Stewart CC (1968). Antimetastatic Effects Associated with Platelet Reduction. *Proc Natl Acad Sci U S A* **61,** 46–52.

Gewirtz DA (1999). A Critical Evaluation of the Mechanisms of Action Proposed for the Antitumor Effects of the Anthracycline Antibiotics Adriamycin and Daunorubicin. *Biochem Pharmacol* **57,** 727–741.

Gianni L, Salvatorelli E & Minotti G (2007). Anthracycline Cardiotoxicity in Breast Cancer Patients: Synergism with Trastuzumab and Taxanes. *Cardiovasc Toxicol* **7,** 67–71.

Goodman J & Hochstein P (1977). Generation of Free Radicals and Lipid Peroxidation by Redox Cycling of Adriamycin and Daunomycin. *Biochem Biophys Res Commun* **77,** 797–803.

Goto T & Wang J (1982). Yeast Dna Topoisomerase-II - an ATP-Dependent Type-II Topoisomerase that Catalyzes the Catenation, Decatenation, Unknotting, and Relaxation of Double-Stranded DNA Rings. *J Biol Chem* **257,** 5866–5872.

Gould SE, Junttila MR & Sauvage FJ de (2015). Translational Value of Mouse Models in Oncology Drug Development. *Nat Med* **21,** 431–439.

Grivennikov SI, Greten FR & Karin M (2010). Immunity, Inflammation, and Cancer. *Cell* **140,** 883–899.

Grosser T, Smyth E & FitzGerald GA (2011). Anti-inflammatory, Antipyretic, and Analgesic Agents; Pharmacotherapy of Gout. In *Goodman & Gilman's: The Pharmacological Basis of Therapeutics*, 12th edn., ed. Brunton LL, Chabner BA & Knollmann BC. McGraw-Hill Education, New York, NY.

Gurpinar E, Grizzle WE & Piazza GA (2013). COX-Independent Mechanisms of Cancer Chemoprevention by Anti-Inflammatory Drugs. *Front Oncol* **3,** 1–18.

Hainsworth JD & Greco FA (1995). Etoposide: Twenty Years Later. *Ann Oncol* **6,** 325–341.

Halligan BD, Liu LF, Rowe TC, Tewey KM & Yang L (1984). Adriamycin-Induced DNA Damage Mediated by Mammalian DNA Topoisomerase II. *Science* **226,** 466+.

Hanahan D & Weinberg RA (2000). The Hallmarks of Cancer. *Cell* **100,** 57–70.

Hanai R, Caron PR & Wang JC (1996). Human TOP3: A Single-Copy Gene Encoding DNA Topoisomerase III. *Proc Natl Acad Sci USA* **93,** 3653–3657.

Hande KR, Wedlund PJ, Noone RM, Wilkinson GR, Greco FA & Wolff SN (1984). Pharmacokinetics of High-Dose Etoposide (VP-16-213) Administered to Cancer Patients. *Cancer Res* **44,** 379–382.

Hass WK, Easton JD, Adams HPJ, Pryse-Phillips W, Molony BA, Anderson S, Kamm B & Group for the TASS (1989). A Randomized Trial Comparing Ticlopidine Hydrochloride with Aspirin for the Prevention of Stroke in High-Risk Patients. *N Engl J Med* **321,** 501–507.

Heck MM, Hittelman WN & Earnshaw WC (1988). Differential Expression of DNA Topoisomerases I and II During the Eukaryotic Cell Cycle. *Proc Natl Acad Sci USA* **85,** 1086–1090.

Hendrickson EA, Qin XQ, Bump EA, Schatz DG, Oettinger M & Weaver DT (1991). A Link Between Double-Strand Break-Related Repair and V(D)J Recombination: The Scid Mutation. *Proc Natl Acad Sci U S A* **88,** 4061–4065.

Herschkowitz JI et al. (2007). Identification of Conserved Gene Expression Features between Murine Mammary Carcinoma Models and Human Breast Tumors. *Genome Biol* **8,** R76.

Hoesel B & Schmid JA (2013). The Complexity of NF-κB Signaling in Inflammation and Cancer. *Mol Cancer* **12,** 86.

Howlader N, Altekruse SF, Li CI, Chen VW, Clarke CA, Ries LAG & Cronin KA (2014). US Incidence of Breast Cancer Subtypes Defined by Joint Hormone Receptor and HER2 Status. *J Natl Cancer Inst* **106,** dju055.

Huang S, Pettaway CA, Uehara H, Bucana CD & Fidler IJ (2001). Blockade of NF-kappaB Activity in Human Prostate Cancer Cells Is Associated with Suppression of Angiogenesis, Invasion, and Metastasis. *Oncogene* **20,** 4188–4197.

Huelsenbeck SC, Schorr A, Roos WP, Huelsenbeck J, Henninger C, Kaina B & Fritz G (2012). Rac1 Protein Signaling Is Required for DNA Damage Response Stimulated by Topoisomerase II Poisons. *J Biol Chem* **287,** 38590–38599.

Hugh J, Hanson J, Cheang MCU, Nielsen TO, Perou CM, Dumontet C, Reed J, Krajewska M, Treilleux I, Rupin M, Magherini E, Mackey J, Martin M & Vogel C (2009). Breast Cancer Subtypes and Response to Docetaxel in Node-Positive Breast Cancer: Use of an Immunohistochemical Definition in the BCIRG 001 Trial. *J Clin Oncol* **27,** 1168–1176.

Hynes NE & Lane HA (2005). ERBB Receptors and Cancer: The Complexity of Targeted Inhibitors. *Nat Rev Cancer* **5,** 341–354.

Jaffe BM (1974). Prostaglandins and Cancer: An Update. *Prostaglandins* **6,** 453–461.

Jhappan C, Morse HC, Fleischmann RD, Gottesman MM & Merlino G (1997). DNA-PKcs: a T-Cell Tumour Suppressor Encoded at the Mouse SCID Locus. *Nat Genet* **17,** 483–486.

Jiang Y & Kang YJ (2004). Metallothionein Gene Therapy for Chemical-Induced Liver Fibrosis in Mice. *Mol Ther* **10,** 1130–1139.

Joel SP, Clark PI & Slevin ML (1995). Stability of the I.V. And Oral Formulations of Etoposide in Solution. *Cancer Chemother Pharmacol* **37,** 117–124.

Joyce D, Albanese C, Steer J, Fu M, Bouzahzah B & Pestell RG (2001). NF-κB and Cell-Cycle Regulation: The Cyclin Connection. *Cytokine Growth Factor Rev* **12,** 73–90.

Ju B-G, Lunyak VV, Perissi V, Garcia-Bassets I, Rose DW, Glass CK & Rosenfeld MG (2006). A Topoisomerase IIß-Mediated dsDNA Break Required for Regulated Transcription. *Science* **312,** 1798–1802.

Kao J, Salari K, Bocanegra M, Choi Y-L, Girard L, Gandhi J, Kwei KA, Hernandez-Boussard T, Wang P, Gazdar AF, Minna JD & Pollack JR (2009). Molecular Profiling of Breast Cancer Cell Lines Defines Relevant Tumor Models and Provides a Resource for Cancer Gene Discovery ed. Blagosklonny MV. *PLoS ONE* **4,** e6146.

Kaufmann SH, McLaughlin SJ, Kastan MB, Liu LF, Karp JE & Burke PJ (1991). Topoisomerase II Levels During Granulocytic Maturation in Vitro and in Vivo. *Cancer Res* **51,** 3534–3543.

Kawachi K, Sasaki T, Murakami A, Ishikawa T, Kito A, Ota I, Shimizu D, Nozawa A, Nagashima Y, Machinami R & Aoki I (2010). The Topoisomerase II Alpha Gene Status in Primary Breast Cancer Is a Predictive Marker of the Response to Anthracycline-Based Neoadjuvant Chemotherapy. *Pathol Res Pract* **206,** 156–162.

Kennecke H, Yerushalmi R, Woods R, Cheang MCU, Voduc D, Speers CH, Nielsen TO & Gelmon K (2010). Metastatic Behavior of Breast Cancer Subtypes. *J Clin Oncol* **28,** 3271–3277.

Kessler DA, Austin RH & Levine H (2014). Resistance to Chemotherapy: Patient Variability and Cellular Heterogeneity. *Cancer Res* **74,** 4663–4670.

Knoop AS, Knudsen H, Balslev E, Rasmussen BB, Overgaard J, Nielsen KV, Schonau A, Gunnarsdottir K, Olsen KE, Mouridsen H & Ejlertsen B (2005). Retrospective Analysis of Topoisomerase IIa Amplifications and Deletions as Predictive Markers in Primary Breast Cancer Patients Randomly Assigned to Cyclophosphamide, Methotrexate, and Fluorouracil or Cyclophosphamide, Epirubicin, and Fluorouracil: Danish Breast Cancer Cooperative Group. *J Clin Oncol* **23,** 7483–7490.

Kohler BA, Sherman RL, Howlader N, Jemal A, Ryerson AB, Henry KA, Boscoe FP, Cronin KA, Lake A, Noone A-M, Henley SJ, Eheman CR, Anderson RN & Penberthy L (2015). Annual Report to the Nation on the Status of Cancer, 1975-2011, Featuring Incidence of Breast Cancer Subtypes by Race/Ethnicity, Poverty, and State. *J Natl Cancer Inst* **107,** djv048.

Kolber M, Sharif N, Marceau R & Szafran O (2013). Family Practice Patients' Use of Acetylsalicylic Acid for Cardiovascular Disease Prevention. *Can Fam Physician* **59,** 55–61.

Kopp E & Ghosh S (1994). Inhibition of NF-Kappa B by Sodium Salicylate and Aspirin. *Science* **265,** 956–959.

Kune GA, Kune S & Watson LF (1988). Colorectal Cancer Risk, Chronic Illnesses, Operations, and Medications: Case Control Results from the Melbourne Colorectal Cancer Study. *Cancer Res* **48,** 4399–4404.

Kurimasa A, Kumano S, Boubnov NV, Story MD, Tung CS, Peterson SR & Chen DJ (1999). Requirement for the Kinase Activity of Human DNA-Dependent Protein Kinase Catalytic Subunit in DNA Strand Break Rejoining. *Mol Cell Biol* **19,** 3877–3884.

Kurz EU & Lees-Miller SP (2004). DNA Damage-Induced Activation of ATM and ATM-Dependent Signaling Pathways. *DNA Repair (Amst)* **3,** 889–900.

Lawrence T & Fong C (2010). The Resolution of Inflammation: Anti-Inflammatory Roles for NF-κB. *Int J Biochem Cell Biol* **42,** 519–523.

Lee AV, Oesterreich S & Davidson NE (2015). MCF-7 Cells—Changing the Course of Breast Cancer Research and Care for 45 Years. *J Natl Cancer Inst* **107,** djv073.

Lee JS, Takahashi T, Hagiwara A, Yoneyama C, Itoh M, Sasabe T, Muranishi S & Tashima S (1995). Safety and Efficacy of Intraperitoneal Injection of Etoposide in Oil Suspension in Mice with Peritoneal Carcinomatosis. *Cancer Chemother Pharmacol* **36,** 211–216.

Leroux M (1930). Mémoir Relatif à L'analyse de L'écorce de Saule et à la Découverte d'un Principe Immediate Propre à Remplacer le Sulfate de Quinine. *J Chim Med Pharm Tox* **6,** 340–342.

Lévesque H & Lafont O (2000). L'aspirine à Travers les Siècles: Rappel Historique. *La Revue de Médecine Interne* **21,** S8–S17.

Lim E, Modi KD & Kim J (2009). In Vivo Bioluminescent Imaging of Mammary Tumors Using IVIS Spectrum. *J Vis Exp* **26,** 1210.

Lind MJ (2008). Principles of Cytotoxic Chemotherapy. *Medicine* **36,** 19–23.

Liu L & Wang J (1979). Interaction between DNA and Escherichia Coli DNA Topoisomerase I - Formation of Complexes between the Protein and Superhelical and Nonsuperhelical Duplex DNAs. *J Biol Chem* **254,** 1082–1088.

Liu ZG, Hsu H, Goeddel DV & Karin M (1996). Dissection of TNF Receptor 1 Effector Functions: JNK Activation Is Not Linked to Apoptosis While NF-κB Activation Prevents Cell Death. *Cell* **87,** 565–576.

Lowry OH, Rosebrough NJ, Farr AL & Randall RJ (1951). Protein Measurement with the Folin Phenol Reagent. *J Biol Chem* **193,** 265–275.

Mahdi JG, Mahdi AJ, Mahdi AJ & Bowen ID (2006). The Historical Analysis of Aspirin Discovery, its Relation to the Willow Tree and Antiproliferative and Anticancer Potential. *Cell Prolif* **39,** 147–155.

McCarty MF & Block KI (2006). Preadministration of High-Dose Salicylates, Suppressors of NF-KappaB Activation, May Increase the Chemosensitivity of Many Cancers: An Example of Proapoptotic Signal Modulation Therapy. *Integr Cancer Ther* **5,** 252–268.

Milano G, Raucci A, Scopece A, Daniele R, Guerrini U, Sironi L, Cardinale D, Capogrossi MC & Pompilio G (2014). Doxorubicin and Trastuzumab Regimen Induces Biventricular Failure in Mice. *J Am Soc Echocardiogr* **27,** 568–579.

Miner J & Hoffhines A (2007). The Discovery of Aspirin's Antithrombotic Effects. *Tex Heart Inst J* **34,** 179–186.

Molyneux G, Andrews M, Sones W, York M, Barnett A, Quirk E, Yeung W & Turton J (2011). Haemotoxicity of Busulphan, Doxorubicin, Cisplatin and Cyclophosphamide in the Female BALB/C Mouse Using a Brief Regimen of Drug Administration. *Cell Biol Toxicol* **27,** 13–40.

Morham SG, Kluckman KD, Voulomanos N & Smithies O (1996). Targeted Disruption of the Mouse Topoisomerase I Gene by Camptothecin Selection. *Mol Cell Biol* **16,** 6804–6809.

Morrison A & Cozzarelli NR (1979). Site-Specific Cleavage of DNA by E. coli DNA Gyrase. *Cell* **17,** 175–184.

Morton DB, Jennings M, Buckwell A, Ewbank R, Godfrey C, Holgate B, Inglis I, James R, Page C, Sharman I, Verschoyle R, Westall L & Wilson AB (2001). Refining Procedures for the Administration of Substances. *Lab Anim* **35,** 1–41.

Nagendran J, Kienesberger PC, Pulinilkunnil T, Zordoky BN, Sung MM, Kim T, Young ME & Dyck JRB (2013). Cardiomyocyte Specific Adipose Triglyceride Lipase Overexpression Prevents Doxorubicin Induced Cardiac Dysfunction in Female Mice. *Heart* **99,** 1041–1047.

Nakanishi M & Rosenberg DW (2013). Multifaceted Roles of PGE2 in Inflammation and Cancer. *Semin Immunopathol* **35,** 123–137.

Nan H et al. (2015). Association of Aspirin and NSAID Use with Risk of Colorectal Cancer According to Genetic Variants. *JAMA* **313,** 1133–1142.

Nitiss JL (2009). Targeting DNA Topoisomerase II in Cancer Chemotherapy. *Nat Rev Cancer* **9,** 338–350.

Oakman C, Moretti E, Galardi F, Santarpia L & Di Leo A (2009). The Role of Topoisomerase II alpha and HER-2 in Predicting Sensitivity to Anthracyclines in Breast Cancer Patients. *Cancer Treat Rev* **35,** 662–667.

O'Brien J, Wilson I, Orton T & Pognan F (2000). Investigation of the Alamar Blue (Resazurin) Fluorescent Dye for the Assessment of Mammalian Cell Cytotoxicity. *Eur J Biochem* **267,** 5421–5426.

Octavia Y, Tocchetti CG, Gabrielson KL, Janssens S, Crijns HJ & Moens AL (2012). Doxorubicin-Induced Cardiomyopathy: From Molecular Mechanisms to Therapeutic Strategies. *J Mol Cell Cardiol* **52,** 1213–1225.

Oeckinghaus A, Hayden MS & Ghosh S (2011). Crosstalk in NF-κB Signaling Pathways. *Nat Immunol* **12,** 695–708.

O'Malley FP, Chia S, Tu D, Shepherd LE, Levine MN, Huntsman D, Bramwell VH, Andrulis IL & Pritchard KI (2011). Topoisomerase II Alpha Protein and Responsiveness of Breast Cancer to Adjuvant Chemotherapy with CEF Compared to CMF in the NCIC CTG Randomized MA.5 Adjuvant Trial. *Breast Cancer Res Treat* **128,** 401–409.

Ottewell PD, Mönkkönen H, Jones M, Lefley DV, Coleman RE & Holen I (2008). Antitumor Effects of Doxorubicin Followed by Zoledronic Acid in a Mouse Model of Breast Cancer. *J Natl Cancer Inst* **100,** 1167–1178.

Patrono C, Coller B, FitzGerald GA, Hirsh J & Roth G (2004). Platelet-Active Drugs: The Relationships among Dose, Effectiveness, and Side Effects: The Seventh ACCP Conference on Antithrombotic and Thrombolytic Therapy. *Chest* **126,** 234S – 264S.

Perou CM, Sørlie T, Eisen MB, van de Rijn M, Jeffrey SS, Rees CA, Pollack JR, Ross DT, Johnsen H, Akslen LA, Fluge Ø, Pergamenschikov A, Williams C, Zhu SX, Lønning PE, Børresen-Dale A-L, Brown PO & Botstein D (2000). Molecular Portraits of Human Breast Tumours. *Nature* **406,** 747–752.

Perry K & Mondragón A (2003). Structure of a Complex Between E. Coli DNA Topoisomerase I and Single-Stranded DNA. *Structure* **11,** 1349–1358.

Polyak K (2011). Heterogeneity in Breast Cancer. *J Clin Invest* **121,** 3786–3788.

Pommier Y (2006). Topoisomerase I Inhibitors: Camptothecins and Beyond. *Nat Rev Cancer* **6,** 789–802.

Pommier Y (2013). Drugging Topoisomerases: Lessons and Challenges. *ACS Chem Biol* **8,** 82–95.

Pommier Y, Leo E, Zhang H & Marchand C (2010). DNA Topoisomerases and Their Poisoning by Anticancer and Antibacterial Drugs. *Chemistry & Biology* **17,** 421–433.

Prat A, Karginova O, Parker JS, Fan C, He X, Bixby L, Harrell JC, Roman E, Adamo B, Troester M & Perou CM (2013). Characterization of Cell Lines Derived from Breast Cancers and Normal Mammary Tissues for the Study of the Intrinsic Molecular Subtypes. *Breast Cancer Res Treat* **142,** 237–255.

Prat A, Parker JS, Karginova O, Fan C, Livasy C, Herschkowitz JI, He X & Perou CM (2010). Phenotypic and Molecular Characterization of the Claudin-Low Intrinsic Subtype of Breast Cancer. *Breast Cancer Res* **12,** R68.

Rainsford KD (2004). History and Development of the Salicylates. In *Aspirin and Related Drugs*, 1st edn., ed. Rainsford KD, pp. 1–19. Taylor & Francis Group, New York, NY.

Rampersad SN (2012). Multiple Applications of Alamar Blue as an Indicator of Metabolic Function and Cellular Health in Cell Viability Bioassays. *Sensors* **12,** 12347–12360.

Reagan-Shaw S, Nihal M & Ahmad N (2008). Dose Translation from Animal to Human Studies Revisited. *FASEB J* **22,** 659–661.

Redinbo MR, Champoux JJ & Hol WG (1999). Structural Insights into the Function of Type IB Topoisomerases. *Curr Opin Struct Biol* **9,** 29–36.

Reichman B, Markman M, Hakes T, Hoskins W, Rubin S, Jones W, Almadrones L, Ochoa M, Chapman D & Saigo P (1989). Intraperitoneal Cisplatin and Etoposide in the Treatment of Refractory/Recurrent Ovarian Carcinoma. *J Clin Oncol* **7,** 1327–1332.

Remichkova M, Yordanov M & Dimitrova P (2008). Etoposide Attenuates Zymosan-Induced Shock in Mice. *Inflammation* **31,** 57–64.

Rezaï K, Lokiec F, Grandjean I, Weill S, de Cremoux P, Bordier V, Ekue R, Garcia M, Poupon M-F & Decaudin D (2007). Impact of Imatinib on the Pharmacokinetics and In Vivo Efficacy of Etoposide and/or Ifosfamide. *BMC Pharmacol* **7,** 13.

Ricchi P, Palma AD, Matola TD, Apicella A, Fortunato R, Zarrilli R & Acquaviva AM (2003). Aspirin Protects Caco-2 Cells from Apoptosis after Serum Deprivation through the Activation of a Phosphatidylinositol 3-Kinase/AKT/p21Cip/WAF1Pathway. *Mol Pharmacol* **64,** 407–414.

Riddle JM (1999). Historical Data as an Aid in Pharmaceutical Prospecting and Drug Safety Determination. *J Altern Complement Med* **5,** 195–201.

Romero A, Martín M, Cheang MCU, López García-Asenjo JA, Oliva B, He X, de la Hoya M, García Sáenz JÁ, Arroyo Fernández M, Díaz Rubio E, Perou CM & Llopis TC (2011). Assessment of Topoisomerase IIα Status in Breast Cancer by Quantitative PCR, Gene Expression Microarrays, Immunohistochemistry, and Fluorescence in Situ Hybridization. *Am J Pathol* **178,** 1453–1460.

Roninson IB (2003). Tumor Cell Senescence in Cancer Treatment. *Cancer Res* **63,** 2705–2715.

Rossi R, Lidonnici MR, Soza S, Biamonti G & Montecucco A (2006). The Dispersal of Replication Proteins after Etoposide Treatment Requires the Cooperation of Nbs1 with the Ataxia Telangiectasia Rad3-Related/Chk1 Pathway. *Cancer Res* **66,** 1675–1683.

Roth GJ & Majerus PW (1975). The Mechanism of the Effect of Aspirin on Human Platelets. I. Acetylation of a Particulate Fraction Protein. *J Clin Invest* **56,** 624–632.

Roth GJ, Stanford N & Majerus PW (1975). Acetylation of Prostaglandin Synthase by Aspirin. *Proc Natl Acad Sci USA* **72,** 3073–3076.

Rothwell PM, Price JF, Fowkes FGR, Zanchetti A, Roncaglioni MC, Tognoni G, Lee R, Belch JF, Wilson M, Mehta Z & Meade TW (2012*a*). Short-Term Effects of Daily Aspirin on Cancer Incidence, Mortality, and Non-Vascular Death: Analysis of the Time Course of Risks and Benefits in 51 Randomised Controlled Trials. *Lancet* **379,** 1602–1612.

Rothwell PM, Wilson M, Elwin C-E, Norrving B, Algra A, Warlow CP & Meade TW (2010). Long-Term Effect of Aspirin on Colorectal Cancer Incidence and Mortality: 20-Year Follow-Up of Five Randomised Trials. *Lancet* **376,** 1741–1750.

Rothwell PM, Wilson M, Price JF, Belch JFF, Meade TW & Mehta Z (2012*b*). Effect of Daily Aspirin on Risk of Cancer Metastasis: A Study of Incident Cancers during Randomised Controlled Trials. *Lancet* **379,** 1591–1601.

Saleh-Gohari N, Bryant HE, Schultz N, Parker KM, Cassel TN & Helleday T (2005). Spontaneous Homologous Recombination Is Induced by Collapsed Replication Forks That Are Caused by Endogenous DNA Single-Strand Breaks. *Mol Cell Biol* **25,** 7158–7169.

Sander M & Hsieh T (1983). Double Strand DNA Cleavage by Type II DNA Topoisomerase from Drosophila Melanogaster. *J Biol Chem* **258,** 8421–8428.

Sausville EA & Burger AM (2006). Contributions of Human Tumor Xenografts to Anticancer Drug Development. *Cancer Res* **66,** 3351–3354.

Scheidereit C (2006). IκB Kinase Complexes: Gateways to NF-κB Activation and Transcription. *Oncogene* **25,** 6685–6705.

Schneider E, Horton J, Yang C, Nakagawa M & Cowan K (1994). Multidrug Resistance-Associated Protein Gene Overexpression and Reduced Drug-Sensitivity of Topoisomerase-II in a Human Breast-Carcinoma MCF7 Cell-Line Selected for Etoposide Resistance. *Cancer Res* **54,** 152–158.

Schwenger P, Alpert D, Skolnik EY & Vilcek J (1998). Activation of p38 Mitogen-Activated Protein Kinase by Sodium Salicylate Leads to Inhibition of Tumor Necrosis Factor-Induced IκB Alpha Phosphorylation and Degradation. *Mol Cell Biol* **18,** 78–84.

Senkus E, Kyriakides S, Ohno S, Penault-Llorca F, Poortmans P, Rutgers E, Zackrisson S & Cardoso F (2015). Primary Breast Cancer: ESMO Clinical Practice Guidelines for Diagnosis, Treatment and Follow-Up. *Ann Oncol* **26,** v8–v30.

Serizawa Y, Oshima R, Yoshida M, Sakon I, Kitani K, Goto A, Tsuda S & Hayashi T (2014). Salicylate Acutely Stimulates 5'-AMP-Activated Protein Kinase and Insulin-Independent Glucose Transport in Rat Skeletal Muscles. *Biochem Biophys Res Commun* **453,** 81–85.

Slamon DJ, Godolphin W, Jones LA, Holt JA, Wong SG, Keith DE, Levin WJ, Stuart SG, Udove J, Ullrich A & Et A (1989). Studies of the HER-2/Neu Proto-Oncogene in Human Breast and Ovarian Cancer. *Science* **244,** 707–712.

Slevin ML (1991). The Clinical Pharmacology of Etoposide. *Cancer* **67,** 319–329.

Sneader W (2000). The Discovery of Aspirin: A Reappraisal. *BMJ* **321,** 1591–1594.

Sørensen BS, Sinding J, Andersen AH, Alsner J, Jensen PB & Westergaard O (1992). Mode of Action of Topoisomerase II-Targeting Agents at a Specific DNA Sequence. Uncoupling the DNA Binding, Cleavage and Religation Events. *J Mol Biol* **228,** 778–786.

Sørlie T, Perou CM, Tibshirani R, Aas T, Geisler S, Johnsen H, Hastie T, Eisen MB, Rijn M van de, Jeffrey SS, Thorsen T, Quist H, Matese JC, Brown PO, Botstein D, Lønning PE & Børresen-Dale A-L (2001). Gene Expression Patterns of Breast Carcinomas Distinguish Tumor Subclasses with Clinical Implications. *PNAS* **98,** 10869–10874.

Sparmann A & Bar-Sagi D (2004). Ras-Induced Interleukin-8 Expression Plays a Critical Role in Tumor Growth and Angiogenesis. *Cancer Cell* **6,** 447–458.

Speyer JL, Green MD, Zeleniuch-Jacquotte A, Wernz JC, Rey M, Sanger J, Kramer E, Ferrans V, Hochster H, Meyers M, Blum RH, Feit F, Attubato M, Burrows W & Muggia FM (1992). ICRF-187 Permits Longer Treatment with Doxorubicin in Women with Breast Cancer. *J Clin Oncol* **10,** 117–127.

Spronck JC & Kirkland JB (2002). Niacin Deficiency Increases Spontaneous and Etoposide-Induced Chromosomal Instability in Rat Bone Marrow Cells In Vivo. *Mutat Res* **508,** 83–97.

Stark LA, Reid K, Sansom OJ, Din FV, Guichard S, Mayer I, Jodrell DI, Clarke AR & Dunlop MG (2007). Aspirin Activates the NF-κb Signalling Pathway and Induces Apoptosis in Intestinal Neoplasia in Two In Vivo Models of Human Colorectal Cancer. *Carcinogenesis* **28,** 968–976.

Staudt LM (2010). Oncogenic Activation of NF-κB. *Cold Spring Harb Perspect Biol* **2,** a000109.

Stingl J & Caldas C (2007). Molecular Heterogeneity of Breast Carcinomas and the Cancer Stem Cell Hypothesis. *Nat Rev Cancer* **7,** 791–799.

Sturman JA, Dawkins PD, McARTHUR N & Smith MJH (1968). The Distribution of Salicylate in Mouse Tissues after Intraperitoneal Injection. *J Pharm Pharmacol* **20,** 58–63.

Sugimoto K, Yamada K, Egashira M, Yazaki Y, Hirai H, Kikuchi A & Oshimi K (1998). Temporal and Spatial Distribution of DNA Topoisomerase II Alters During Proliferation, Differentiation, and Apoptosis in HL-60 Cells. *Blood* **91,** 1407–1417.

Swain A, Dutton S & Truswell A (1985). Salicylates in Foods. *J Am Diet Assoc* **85,** 950–960.

Takahashi S, Ushida M, Komine R, Shimodaira A, Uchida T, Ishihara H, Shibano T, Watanabe G, Ikeda Y & Murata M (2008). Platelet Responsiveness to in Vitro Aspirin Is Independent of COX-1 and COX-2 Protein Levels and Polymorphisms. *Thromb Res* **121,** 509–517.

Tak PP & Firestein GS (2001). NF-κB: A Key Role in Inflammatory Diseases. *J Clin Invest* **107,** 7–11.

Tewey KM, Chen GL, Nelson EM & Liu LF (1984). Intercalative Antitumor Drugs Interfere with the Breakage-Reunion Reaction of Mammalian DNA Topoisomerase II. *J Biol Chem* **259,** 9182–9187.

Thorn CF, Oshiro C, Marsh S, Hernandez-Boussard T, McLeod H, Klein TE & Altman RB (2011). Doxorubicin Pathways: Pharmacodynamics and Adverse Effects. *Pharmacogenet Genomics* **21,** 440–446.

Tiwari VK, Burger L, Nikoletopoulou V, Deogracias R, Thakurela S, Wirbelauer C, Kaut J, Terranova R, Hoerner L, Mielke C, Boege F, Murr R, Peters AHFM, Barde Y-A & Schübeler D (2012). Target Genes of Topoisomerase IIβ Regulate Neuronal Survival and Are Defined by Their Chromatin State. *PNAS* **109,** E934–E943.

Torregrosa D, Bolufer P, Lluch A, López JA, Barragán E, Ruiz A, Guillem V, Munárriz B & García Conde J (1997). Prognostic Significance of c-erbB-2/Neu

Amplification and Epidermal Growth Factor Receptor (EGFR) in Primary Breast Cancer and Their Relation to Estradiol Receptor (ER) Status. *Clin Chim Acta* **262,** 99–119.

Tse YC, Kirkegaard K & Wang JC (1980). Covalent Bonds Between Protein and DNA. Formation of Phosphotyrosine Linkage Between Certain DNA Topoisomerases and DNA. *J Biol Chem* **255,** 5560–5565.

Tsutsui K, Tsutsui K, Okada S, Watanabe M, Shohmori T, Seki S & Inoue Y (1993). Molecular Cloning of Partial cDNAs for Rat DNA Topoisomerase II Isoforms and Their Differential Expression in Brain Development. *J Biol Chem* **268,** 19076–19083.

Turley H, Comley M, Houlbrook S, Nozaki N, Kikuchi A, Hickson ID, Gatter K & Harris AL (1997). The Distribution and Expression of the Two Isoforms of DNA Topoisomerase II in Normal and Neoplastic Human Tissues. *Br J Cancer* **75,** 1340–1346.

Twelves CJ, Dobbs NA, Aldhous M, Harper PG, Rubens RD & Richards MA (1991). Comparative Pharmacokinetics of Doxorubicin given by Three Different Schedules with Equal Dose Intensity in Patients with Breast Cancer. *Cancer Chemother Pharmacol* **28,** 302–307.

Vainio H, Morgan G & Kleihues P (1997). An International Evaluation of the Cancer-Preventive Potential of Nonsteroidal Anti-Inflammatory Drugs. *Cancer Epidemiol Biomarkers Prev* **6,** 749–753.

Van Antwerp DJ, Martin SJ, Kafri T, Green DR & Verma IM (1996). Suppression of TNF-Alpha-Induced Apoptosis by NF-kappaB. *Science* **274,** 787–789.

Vane JR & Botting RM (2003). The Mechanism of Action of Aspirin. *Thromb Res* **110,** 255–258.

Vollenweider-Zerargui L, Barrelet L, Wong Y, Lemarchand-Béraud T & Gómez F (1986). The Predictive Value of Estrogen and Progesterone Receptors' Concentrations on the Clinical Behavior of Breast Cancer in Women. Clinical Correlation on 547 Patients. *Cancer* **57,** 1171–1180.

Wang CY, Mayo MW & Baldwin AS (1996). TNF- and Cancer Therapy-Induced Apoptosis: Potentiation by Inhibition of NF-Kappa B. *Science* **274,** 784–787.

Wang JC (2002). Cellular Roles of DNA Topoisomerases: A Molecular Perspective. *Nat Rev Mol Cell Biol* **3,** 430–440.

Wang Y, Huang J-W, Calses P, Kemp CJ & Taniguchi T (2012). MiR-96 Downregulates REV1 and RAD51 to Promote Cellular Sensitivity to Cisplatin and PARP Inhibition. *Cancer Res* **72,** 4037–4046.

Wheeler RH, Ensminger WD, Thrall JH & Anderson JL (1982). High-Dose Doxorubicin: An Exploration of the Dose-Response Curve in Human Neoplasia. *Cancer Treat Rep* **66,** 493–498.

Williams FM (1985). Clinical Significance of Esterases in Man. *Clin Pharmacokinet* **10,** 392–403.

Woessner RD, Mattern MR, Mirabelli CK, Johnson RK & Drake FH (1991). Proliferation- and Cell Cycle-Dependent Differences in Expression of the 170 Kilodalton and 180 Kilodalton Forms of Topoisomerase II in NIH-3T3 Cells. *Cell Growth Differ* **2,** 209–214.

Wood A, Baxter G, Thies F, Kyle J & Duthie G (2011). A Systematic Review of Salicylates in Foods: Estimated Daily Intake of a Scottish Population. *Mol Nutr Food Res* **55,** S7–S14.

Xu X-M, Sansores-Garcia L, Chen X-M, Matijevic-Aleksic N, Du M & Wu KK (1999). Suppression of Inducible Cyclooxygenase 2 Gene Transcription by Aspirin and Sodium Salicylate. *Proc Natl Acad Sci U S A* **96,** 5292–5297.

Yang X, Li W, Prescott ED, Burden SJ & Wang JC (2000). The Function of DNA Topoisomerase IIβ in Neuronal Development. *Science* **287,** 131–134.

Yap TA, Gerlinger M, Futreal PA, Pusztai L & Swanton C (2012). Intratumor Heterogeneity: Seeing the Wood for the Trees. *Sci Transl Med* **4,** 1–4.

Yin M-J, Yamamoto Y & Gaynor RB (1998). The Anti-Inflammatory Agents Aspirin and Salicylate Inhibit the Activity of IκB Kinase-β. *Nature* **396,** 77–80.

Yuan M, Konstantopoulos N, Lee J, Hansen L, Li ZW, Karin M & Shoelson SE (2001). Reversal of Obesity- and Diet-Induced Insulin Resistance with Salicylates or Targeted Disruption of Ikkβ. *Science* **293,** 1673–1677.

Yu H, Kortylewski M & Pardoll D (2007). Crosstalk between Cancer and Immune Cells: Role of STAT3 in the Tumour Microenvironment. *Nat Rev Immunol* **7,** 41–51.

Zhu Z, Chen L, Lu R, Jia J, Liang Y, Xu Q, Zhou C, Wang L, Wang S & Yao Z (2008). Tripeptide Tyroserleutide Plus Doxorubicin: Therapeutic Synergy and Side Effect Attenuation. *BMC Cancer* **8,** 342.